POLYENES BY REGIOSELECTIVE, LIVING POLYMERIZATION USING MOLYBDENUM ALKYLIDENE BIS(CARBOXYLATE) INITIATORS AND ZIEGLER-NATTA CATALYSIS EMPLOYING NEW ZIRCONIUM DIAMIDO COMPLEXES

by

FLORIAN JOHANNES SCHATTENMANN
Diplomchemiker
Technische Universität München
(1991)

Submitted to the Department of Chemistry
in Partial Fulfillment of the Requirements
for the Degree of

DOCTOR OF PHILOSOPHY
at the
MASSACHUSETTS INSTITUTE OF TECHNOLOGY
September 1997

Signature of Author_____
Department of Chemistry
July 10, 1997

Certified by_____
Richard R. Schrock
Thesis Supervisor

Accepted by_____
Dietmar Seyferth
Chairman, Departmental Committee on Graduate Students

This doctoral thesis has been examined by a Committee of the Department of Chemistry as follows:

Professor Dietmar Seyferth_____ Chairman

Professor Richard R. Schrock_____ Thesis Supervisor

Professor Timothy M. Swager_____

To my parents
and
Sheree

POLYENES BY REGIOSELECTIVE, LIVING POLYMERIZATION USING MOLYBDENUM ALKYLIDENE BIS(CARBOXYLATE) INITIATORS AND ZIEGLER-NATTA CATALYSIS EMPLOYING NEW ZIRCONIUM DIAMIDO COMPLEXES

by

FLORIAN JOHANNES SCHATTENMANN

Submitted to the Department of Chemistry, September 1997,
in Partial Fulfillment of the Requirements
for the Degree of Doctor of Philosophy in Chemistry

ABSTRACT

Chapter 1

The synthesis and reactivity of molybdenum imido alkylidene complexes containing carboxylates as ancillary ligands is presented. Addition of excess sodium triphenylacetate to Mo(N-1-adamantyl)(CHCMe$_2$Ph)(OTf)$_2$(DME) produced pale yellow crystalline Mo(N-1-adamantyl)(CHCMe$_2$Ph)(O$_2$CCPh$_3$)$_2$ (**1a**) in 76% yield. By similar methods a class of analogous complexes can be prepared as long as the carboxylate ligand is sufficiently large to prevent bimolecular decomposition and the formation of 'ate-complexes'. An X-ray structural study of Mo(NAr')(CHCMe$_3$)(O$_2$CCPh$_3$)$_2$ (Ar' = 2-*t*-Bu-C$_6$H$_4$) (**2b**) confirmed the *syn* configuration of the alkylidene ligand, suggested by the small alkylidene CH$_\alpha$ coupling constants (117-123 Hz) of these complexes. Both carboxylate ligands are bound to molybdenum in a bidentate (η^2), but unsymmetrical fashion. The *syn/anti* rotamer conversion behavior also suggests a coordination number higher than 4 in solution. Complexes containing the adamantylimido or the 2-*t*-butylphenylimido ligand are potent initiators for the polymerization of diethyldipropargylmalonate (DEDPM). An X-ray study of Mo(NAr)(CHCMe$_2$Ph)(O$_2$CCMePh$_2$)$_2$ (Ar = 2,6-*i*-Pr$_2$-C$_6$H$_3$) (**4**) suggests effective blocking of access to the metal center by the isopropyl substituents as an explanation for the lack of reactivity towards DEDPM of complexes containing the 2,6-diisopropylphenylimido ligand. This argument is supported by the inability of these complexes to form PMe$_3$ adducts in contrast to complexes containing the adamantylimido or the 2-*t*-butylphenylimido ligand.

Chapter 2

The living, regioselective cyclopolymerization of DEDPM is reported to give polyenes that contain only six-membered rings in the polymer backbone by using well-defined molybdenum imido bis(triphenylacetate) initiators. Complex **2b** initiates the cyclopolymerization of DEDPM yielding poly(DEDPM)$_n$ with a polydispersity ranging from 1.13 to 1.26. A linear dependence of the chain length on the amount of monomer added is consistent with living polymerization. Molecular weights and polydispersities of polymers prepared by using **1a** are found to be higher than expected. An explanation is offered by a large k_p/k_i value determined for the polymerization of DEDPM using **1a**. Polymerization in the presence of a base controls the rate of propagation and yields polymers with generally lower molecular weights and narrower polydispersities. MALDI TOF mass spectroscopy is introduced as an absolute method for the determination of molecular weights of polyenes. The polymer endgroups in poly(DEDPM)$_n$ prepared using

2b are identified by MALDI TOF MS. ^{13}C NMR revealed a regular structure of the polymer in which the backbone contains only six-membered rings. The formation of six-membered rings is ascribed to reaction of the first terminal triple bond with the *syn* alkylidene to give solely a β substituted molybdacyclobutene intermediate (β addition), followed by ring opening to a terminal alkylidene and intramolecular β addition of the second triple bond. Steric interactions between the crowded ligand sphere and DEDPM render α addition untenable. The steric argument is further supported by partial loss of selectivity upon polymerization of less substituted monomers. Treatment of poly(DEDPM)$_n$ with 2 equiv MOH (M = Na, K) provides regioregular, water soluble polymers. A reduced average conjugation length of regioregular poly(DEDPM)$_n$ compared to poly(DEDPM)$_n$ containing five- and six-membered rings in the polymer backbone is evidenced by lower values for λ_{max} in the UV/Vis and for γ in NLO measurements.

Chapter 3

Highly conjugated, completely soluble copolymers of DEDPM and acetylene were synthesized using bis(carboxylate) initiators Mo(N-1-adamantyl)($CHCMe_2Ph$)(O_2CCPh_3)$_2$ and Mo(NAr')($CHCMe_3$)(O_2CCPh_3)$_2$ (Ar' = 2-*t*-Bu-C_6H_4). Computer controlled acetylene addition permitted a high degree of control over the copolymer properties. The amount of acetylene incorporated into the polymers was found to be in very good agreement with the acetylene in the feed. ^{13}C NMR proved to be a sensitive tool to study the monomer sequence. The possible triads expected in a statistically random copolymer could be distinguished and assigned by varying the ratio of acetylene to DEDPM. Increasing this ratio leads to copolymers with an exceptional degree of conjugation as judged by λ_{max} values of up to 598 nm.

Chapter 4

The synthesis, characterization and polymerization behavior of zirconium complexes that contain tridentate bridged bisamide ligands is described. Reaction of $Zr(NMe_2)_4$ with $H_2[NSiN_2]$ where $[NSiN_2]^{2-}$ = [*t*-BuNSiMe_2N$CH_2CH_2NMe_2$]$^{2-}$ provides $[NSiN_2]Zr(NMe_2)_2$, which can easily be converted to $[NSiN_2]ZrCl_2$ by reaction with excess TMSCl. Several dialkyl complexes can be prepared from $[NSiN_2]ZrCl_2$ by reaction with 2 equiv of the corresponding Grignard reagent, most notably the β hydrogen containing $[NSiN_2]Zr(CH_2CHMe_2)_2$. An X-ray structural study of $MgCl_2$-bridged, dimeric $\{[NSiN_2]Zr(CH_2CHMe_2)_2MgCl_2\}_2$ proves the presence of β hydrogens, but also reveals the susceptibility of the ligand towards electrophilic attack. (2,6-*i*-Pr_2-$C_6H_3NHCH_2CH_2)_2O$ ($H_2[ArN_2O]$) and (2,6-Me_2-$C_6H_3NHCH_2CH_2)_2O$ ($H_2[Ar'N_2O]$) can conveniently be prepared from $(TsOCH_2CH_2)_2O$ and 2 equiv of the corresponding lithium anilide derivative. The use of protecting groups is required for the synthesis of unsubstituted $(PhNHCH_2CH_2)_2O$ ($H_2[PhN_2O]$). Reaction of ($H_2[ArN_2O]$) and ($H_2[Ar'N_2O]$) with $Zr(NMe_2)_4$ yields $[ArN_2O]Zr(NMe_2)_2$ and $[Ar'N_2O]Zr(NMe_2)_2$ respectively. Treatment with excess TMSCl results in the clean formation of $[ArN_2O]ZrCl_2$ and $[Ar'N_2O]ZrCl_2$. $[PhN_2O]Zr(NMe_2)_2(NHMe_2)$, obtained from the reaction of $H_2[PhN_2O]$ and $Zr(NMe_2)_4$, reacts with TMSCl by loss of ligand. Alkylation of $[ArN_2O]ZrCl_2$ with 2 equiv BrMgR provides $[ArN_2O]ZrR_2$ (R = Me, CH_2CHMe_2). All complexes containing the $[ArN_2O]$ ligand exhibit hindered rotation of the aryl group around the N-C_{ipso} bond. Similarly $[Ar'N_2O]ZrMe_2$ can be prepared by reaction of $[Ar'N_2O]ZrCl_2$ with 2 equiv of BrMgMe. Reaction of $[Ar'N_2O]ZrCl_2$ with 2 equiv of $BrMgCH_2CMe_3$ produces $[Ar'N_2O]Zr(CH_2CMe_3)Cl$, but with 2 equiv of $LiCH_2CMe_3$ the desired bisalkyl complex $[Ar'N_2O]Zr(CH_2CMe_3)_2$. An X-ray study of $[Ar'N_2O]ZrMe_2$ revealed a coordination environment reminiscent of Cp_2ZrMe_2. The activation of dialkyl

complexes containing the $[ArN_2O]^{2-}$ and $[Ar'N_2O]^{2-}$ ligand using $[PhNMe_2H][B(C_6F_5)_4]$ was investigated by NMR. $\{[ArN_2O]ZrMe(PhNMe_2\}[B(C_6F_5)_4]$ and $\{[Ar'N_2O]ZrMe(PhNMe_2\}[B(C_6F_5)_4]$ form cleanly in chlorobenzene-d_5 solution. $[ArN_2O]ZrMe_2$ can be activated with $[PhNMe_2H][B(C_6F_5)_4]$ and $[Ph_3C][B(C_6F_5)_4]$ to completely polymerize 200 equiv of 1-hexene in chlorobenzene at 0 °C. Low molecular weights (M_n = 1000 - 2600 g/mol, PDI = 1.3 to 1.7) of the polymers and polymer carbon NMR spectroscopy indicate loss of olefin by β hydride elimination. Analogous activation of $[Ar'N_2O]ZrMe_2$ and polymerization of 1-hexene produces polymers with higher M_ns (9000 - 11700 g/mol, PDI = 1.4 to 1.5), but only 65 to 70% conversion. A regioregular structure was found for poly(1-hexene)$_n$ prepared using activated $[Ar'N_2O]ZrMe_2$.

Thesis Supervisor: Dr. Richard R. Schrock
Title: Frederick G. Keyes Professor of Chemistry

TABLE OF CONTENTS

List of Figures

List of Tables

Chapter 4 page

List of Schemes

Abbreviations Used in Text

$[ArN_2O]^{2-}$	$[(2,6\text{-}i\text{-}Pr_2\text{-}C_6H_3NCH_2CH_2)_2O]^{2-}$
$[Ar'N_2O]^{2-}$	$[(2,6\text{-}Me_2\text{-}C_6H_3NCH_2CH_2)_2O]^{2-}$
$[BDEP]^{2-}$	$[(2,6\text{-}Et_2\text{-}C_6H_3NCH_2)_2NC_5H_3]^{2-}$
BEDPM	*t*-butylethyldipropargylmalonate
br	broad
C_α	carbon bound to metal
C_{ipso}	carbon in aromatic ring bound to nitrogen
C_m	carbon in the meta position of an aromatic ring
C_o	carbon in the ortho position of an aromatic ring
C_p	carbon in the para position of an aromatic ring
Cp	C_5H_5
d	doublet
DBDPM	di-*t*-butyldipropargylmalonate
DEDPM	diethyldipropargylmalonate
DMDPM	dimethyldipropargylmalonate
DME	1,2-dimethoxyethane
DPBCA	dipropargyl-*t*-butylacetate
DPBCA	dipropargyl-*t*-butylcyanoacetate
DPEA	dipropargylethylacetate
DPMCA	dipropargylmethylcyanoacetate
DPNpA	dipropargylneopentylacetate
Bu	butyl
eq	equation
equiv	equivalent(s)
Et	ethyl
h	hours
H_α	hydrogen (proton) bound to C_α
H_m	hydrogen (proton) bound to C_m
H_o	hydrogen (proton) bound to C_o
H_p	hydrogen (proton) bound to C_p
Hz	Hertz
GPC	gel permeation chromatography
J	coupling constant in Hertz
m	multiplet

MALDI	matrix-assisted laser desorption ionisation
Me	methyl
min	minutes
M_n	number average molecular weight
M_w	weight average molecular weight
MS	mass spectroscopy
NLO	nonlinear optics
NMR	nuclear magnetic resonance
$[NON]^{2-}$	$[(t\text{-Bu-}d_6\text{-N-}o\text{-}C_6H_4)_2O]^{2-}$
Np	neopentyl
$[NSiN_2]^{2-}$	$[t\text{-BuNSiMe}_2\text{NCH}_2\text{CH}_2\text{NMe}_2]^{2-}$
OTf	O_3SCF_3, triflate, trifluoromethanesulfonate
PDI	polydispersity index (M_w/M_n)
Ph	phenyl
$[PhN_2O]^{2-}$	$[(PhNCH_2CH_2)_2O]^{2-}$
ppm	parts per million
Pr	propyl
py	pyridine
q	quartet
ROMP	ring-opening metathesis polymerization
s	singlet
sep	septet
t	triplet
THF	tetrahydrofuran
THG	third harmonic generation
tol	toluene
TMS	trimethylsilyl
TOF	time-of-flight
Ts	tosyl
UV/Vis	ultraviolet/visible
δ	chemical shift downfield from tetramethylsilane
ε	extinction coefficient at wavelength of maximum optical absorption
λ_{max}	wavelength of maximum optical absorption

CHAPTER 1

Carboxylates as Ancillary Ligands for Molybdenum(VI) Imido Alkylidene Complexes

Much of the material covered in this chapter has appeared in print:

Schattenmann F. S.; Schrock, R. R.; Davis, W. M. *J. Am. Chem. Soc.* **1996**, *118*, 3295.

INTRODUCTION

Tungsten and molybdenum are among the most active metals for the metathesis of ordinary olefins in classical metathesis catalyst systems.[1,2] The development of well-defined metathesis catalysts has culminated in the preparation of complexes of the general type $M(NR)(CHR')(OR'')_2$ (M = Mo or W).[3-6] Such catalysts have been successfully employed for the metathesis of ordinary olefins,[3,7,8] the living ring-opening metathesis polymerization (ROMP)[7,9-13] of strained olefins and the synthesis of polyenes.[14-19] In ROMP control over the nature of the groups at both ends of the polymer has been demonstrated. The initial alkylidene group is introduced to the originating end of the polymer.[11,20,21] The termination reaction in these polymerizations is a Wittig-like capping reaction with an aldehyde such as benzaldehyde.[22,23] Molybdenum catalysts have emerged as the catalysts of choice for most purposes because they tolerate a greater number of functionalities, are easier to synthesize than the corresponding tungsten catalysts, and molybdenum starting materials are less expensive.

Perhaps the most valuable asset of this class of catalysts is their versatility. Many studies demonstrated control over activity,[8] cis/trans selectivity[20,24-26] and tacticity[9,25,27] in ROMP by steric and electronic "fine-tuning" of the ligand sphere. Effects of the electronic and steric properties of the alkylidene, imido and alkoxide ligands on catalytic activity and selectivity could be established. The steric and electronic nature of the alkylidene ligand strongly affects the rate of initiation (k_i). The ratio of the rate of propagation to the rate of initiation (k_p/k_i) directly influences the polydispersity and degree of polymerization of the resulting polymer.[20,21,28,29] Ideally alkylidene ligands on the initiator that closely resemble the propagating species yield polymers with narrow polydispersities. The influence of steric and electronic variation of the imido ligand on the polymerization behavior is less apparent. However in this and the following chapter examples will be presented that show dramatic changes of reactivity upon variation of the imido ligand. The alkoxide ligands have been extensively studied with regard to their effect

on catalyst reactivity[30] as they are facilely introduced in the final step of the catalyst synthesis. Complexes with a wide variety of alkoxide and phenoxide ligands have been prepared.[5] Activity of the catalysts can systematically be varied by altering the electron withdrawing ability of the alkoxides.[30] The pK_a of the corresponding alcohol provides some indication for the σ donor ability of an alkoxide.

Despite the high level of control over polymerization behavior and polymer properties by using such "tailored" catalysts, a wide variety of challenges regarding selectivity still remain. One example is the living cyclopolymerization of heptadiynes such as diethyldipropargylmalonate (DEDPM) using catalysts of the type Mo(CH-*t*-Bu)(NAr)[OCMe$(CF_3)_2]_2$ (Ar = 2,6-*i*-$Pr_2C_6H_3$).[15] The polymer backbone was found to contain a mixture of five- and six-membered rings as a consequence of head to head and head to tail polymerization.[31] Extensive variation of the alkoxide-based catalysts did not show satisfactory selectivity towards the exclusive formation of one ring size.[31]

Aiming to address this particular regioselectivity issue, catalyst systems that contain monoanionic ancillary ligands electronically and sterically very different from the extensively studied alkoxides were considered. A possible choice is the carboxylate ligand. Weaker σ donor ability indicated by lower pK_a values of carboxylic acids compared to alcohols, two possible bonding modes for monomeric complexes, η^1 and η^2, and enhanced bridging tendency of the bidentate carboxylato ligand are among the most prominent differences. This chapter is concerned with the synthesis, characterization and reactivity of molybdenum(VI) imido alkylidene complexes containing carboxylate ligands.

RESULTS AND DISCUSSION

Synthesis of Molybdenum(VI) Imido Alkylidene Bis(carboxylate) Complexes.

In analogy to the synthesis of alkoxide complexes of the type $Mo(NR)(CHR')(OR'')_2$, reaction of 2 equiv of a sodium carboxylate with an appropriate molybdenum alkylidene bis(triflate) complex was employed as a general approach. Initial focus was directed towards the preparation of molybdenum bis(carboxylate) complexes containing the adamantylimido ligand since a noticeable preference towards the formation of six-membered rings in the polymerization of DEDPM using Mo(N-1-adamantyl)($CHCMe_2Ph$)[$OCMe(CF_3)_2$]$_2$ had been reported.[31] Carboxylates with different electronic and steric properties were explored as possible ancillary ligands.

Preliminary studies involved benzoates, since a wide variety of sterically and electronically different derivatives are commercially available. No pure product, however, could be obtained by the reaction of Mo(N-1-adamantyl)($CHCMe_2Ph$)$(OTf)_2$(DME) with 2 equiv of KO_2CPh. Sterically more demanding, substituted benzoates as Na(O_2C-3,5-*t*-Bu_2-C_6H_3) and Na(O_2C-2,6-Me_2-C_6H_3) yielded white crystalline products in moderate yield. In both cases NMR spectroscopy indicated the formation of 'ate-complexes', Na[Mo(N-1-adamantyl)($CHCMe_2Ph$)(O_2C-3,5-*t*-Bu_2-C_6H_3)$_3$]•$(THF)_{0.5}$ and Na[Mo(N-1-adamantyl)($CHCMe_2Ph$)(O_2C-2,6-Me_2-C_6H_3)$_3$], with one carboxylate ligand exhibiting different resonances than the other two. These findings suggested that sterically significantly more demanding carboxylate ligands were required to stabilize neutral bis(carboxylate) complexes.

Addition of excess sodium triphenylacetate to Mo(N-1-adamantyl)($CHCMe_2Ph$)$(OTf)_2$(DME) produced pale yellow crystalline Mo(N-1-adamantyl)($CHCMe_2Ph$)(O_2CCPh_3)$_2$ (**1a**) in 72% isolated yield (eq 1). The proton and carbon NMR spectra of **1a** show that only one rotamer[32,33] is present which has an

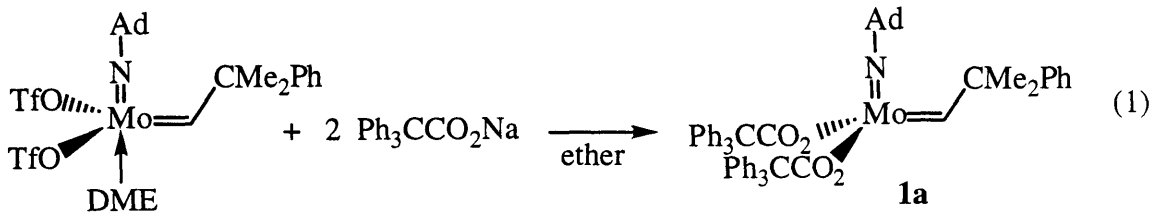

(1)

Ad = N-1-adamantyl

alkylidene H_α resonance at 13.89 ppm and an alkylidene C_α resonance at 305.5 ppm. Other carboxylate complexes that have been prepared by similar methods are listed in Table 1.1, along with NMR data that suggest that all are analogous. The relatively small alkylidene CH_α coupling constants (between 117 and 123 Hz) suggest that the alkylidene ligand has the *syn* orientation. In solution the compounds exhibit a plane of symmetry as only one set of resonances for the two carboxylate ligands is observed in the proton and

Table 1.1. NMR and Yield Data for Carboxylato Complexes, $Mo(CHR')(NR)(O_2CR'')_2$.

R		R'	R''	δH_α	δC_α (J_{CH})	yield (%)
1-adamantyl	**1a**	CMe_2Ph	CPh_3	13.89	305.5 (117)	72
1-adamantyl	**1b**	CMe_3	CPh_3	13.84		45
2-*t*-BuC_6H_4	**2a**	CMe_2Ph	CPh_3	13.92	309.4 (123)	55
2-*t*-BuC_6H_4	**2b**	CMe_3	CPh_3	13.76	313.4	60
2,6-*i*-Pr_2-C_6H_3	**3**	CMe_2Ph	CPh_3	13.91	308.9 (122)	88
2,6-*i*-Pr_2-C_6H_3	**4**	CMe_2Ph	$CMePh_2$	13.96	308.5 (121)	64

carbon NMR. Compounds containing the 2,6-dimethylphenylimido ligand retained one equivalent of loosely bound THF, but decomposed to form insoluble materials when the THF was removed under vacuum in the solid state or when the THF adduct was dissolved

in solvents such as toluene. The only complex isolated with the smaller diphenylmethylacetate ligand utilizes the bulky 2,6-diisopropylphenylimido ligand. Mo(N-2,6-*i*-Pr_2-C_6H_3)(CHCMe$_2$Ph)(O_2CCMePh$_2$)$_2$ (**4**) was obtained from the reaction of 2 equiv of Ph$_2$MeCO$_2$Na with Mo(N-2,6-*i*-Pr_2-C_6H_3)(CHCMe$_2$Ph)(OTf)$_2$(DME), addition of 3 equiv of Ph$_2$MeCO$_2$Na yields predominantly the 'ate-complex'. All attempts to isolate bis(diphenylmethylacetate) complexes containing the adamantylimido or the 2-*t*-butylphenylimido ligand failed.

Complexes with alkylidene ligands substantially smaller than the neopentylidene or neophylidene ligand are not sufficiently stabilized by the triphenylacetate ligands. For example, metathesis reactions of **1a** with ethylene and styrene,[7] which were expected to generate smaller alkylidenes, ultimately led to decomposition. Synthesis of the benzylidene biscarboxylate complex starting from Mo(NAr')$_2$Cl$_2$(DME) (Ar' = 2-*t*-Bu-C_6H_4) was attempted as outlined in Scheme 1.1. Dibenzyl complex **5** and bis(triflate) complex **6** can be obtained by standard methodology[5] in 53% and 37% yield, respectively. Reaction of **6** with sodium triphenylacetate did not lead to the expected Mo(NAr')(CHPh)(O_2CCPh$_3$)$_2$.

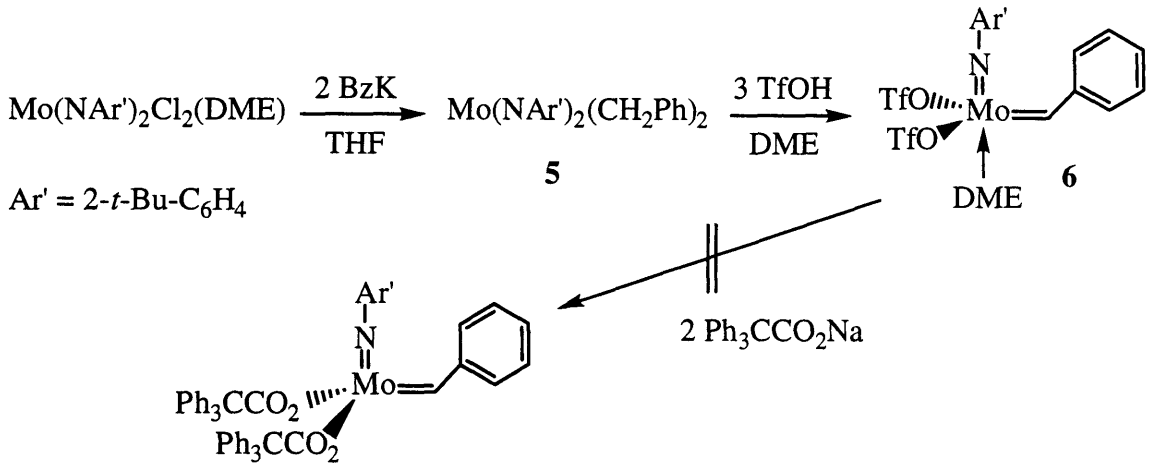

Scheme 1.1. Attempted Synthesis of a Molybdenum Benzylidene Bis(triphenylacetate) Complex.

Instead a highly crystalline compound was isolated that did not show an alkylidene resonance in the proton NMR.

Neutral bis(carboxylate) complexes based on the $(Me_3Si)_3SiCO_2$ ligand can similarly be prepared by reaction of bis(triflate) complexes with 2 equiv of $(Me_3Si)_3SiCO_2Na$. Although all three complexes formed cleanly by proton NMR, only Mo(N-2,6-*i*-Pr_2-C_6H_3)($CHCMe_2Ph$)($O_2CSi(SiMe_3)_3)_2$ (**7**) and Mo(N-2-*t*-Bu-C_6H_4)($CHCMe_2Ph$)($O_2CSi(SiMe_3)_3)_2$ (**8**) could be obtained as crystalline solids; Mo(N-1-adamantyl)($CHCMe_2Ph$)($O_2CSi(SiMe_3)_3)_2$ was isolated as an oil. This carboxylate, although electronically and sterically distinctively different from triphenylacetate, is also sterically very demanding demonstrating the importance of size of the carboxylato ligand for the stabilization of such complexes.

X-ray Structural Studies.

An X-ray structural study of **2b** (Figure 1.1, Figure 1.2, Table 1.2) showed it to be a monomeric species. The steric bulk provided by the carboxylates is likely to prevent bimolecular decomposition of **2b**. The bulky carboxylate and imido ligands form a "shield-like" arrangement with the alkylidene group protruding perpendicularly (sideview in Figure 1.2). The alkylidene ligand is *syn*, as suspected on the basis of the magnitude of $J_{CH\alpha}$. Neither the Mo-C(7) distance (1.884(9) Å) nor the Mo-C(7)-C(9) angle (145.9(7)°) is unusual (relevant bond lengths and angles are listed in Table 1.3). The imido ligand is bent slightly (Mo-N(6)-C(12) = 164.5(6)°), and the plane of the phenyl ring is oriented approximately perpendicular to the C(7)-Mo-N(6) plane. The carboxylate ligands are both bound to the molybdenum in a bidentate (η^2) fashion, although unsymmetrically; the longer Mo-O bonds (2.261(5) and 2.336(6) Å) are those that are in positions more transoid to the imido or alkylidene ligand, respectively (N(6)-Mo-O(4) = 155.4(3)°; C(7)-Mo-O(5) = 151.9(3)°). The other two Mo-O bonds are relatively short (2.136 and 2.090 Å). The distinctively unsymmetric η^2 bonding mode in the solid state and a plane of symmetry in

Table 1.2. Crystallographic Data, Collection Parameters, and Refinement Parameters for $Mo(NAr')(CHCMe_3)(O_2CCPh_3)_2$ (**2b**).[a]

Empirical Formula	$C_{56.50}H_{55.50}Cl_3NO_4Mo$[a]
Formula Weight	1014.81
Crystal Color	yellow
Crystal Dimensions (mm)	0.22 x 0.13 x 0.13
Crystal System	Triclinic
a	12.2272(11) Å
b	14.2111(12) Å
c	17.474(2) Å
α	97.2310(10)°
β	110.2270(10)°
γ	106.178(2)°
V	2651.8(4) $Å^3$
Space Group	$P\bar{1}$
Z	2
D_{calc}	1.271 g/cm^3
F_{000}	1053
Diffractometer	Siemens SMART/CCD
$\lambda(MoK_\alpha)$	0.71073 Å
Scan Type	ω scans
Temperature	188(2) K
Total No. Unique Reflections	5527
No. Variables	602
R	0.0728
R_w	0.1806
GoF	1.094

[a] The molecule contains a severely disordered, partial methylenechloride molecule in the lattice.

Figure 1.1. X-ray Crystal Structure of $Mo(NAr')(CHCMe_3)(O_2CCPh_3)_2$ (**2b**).

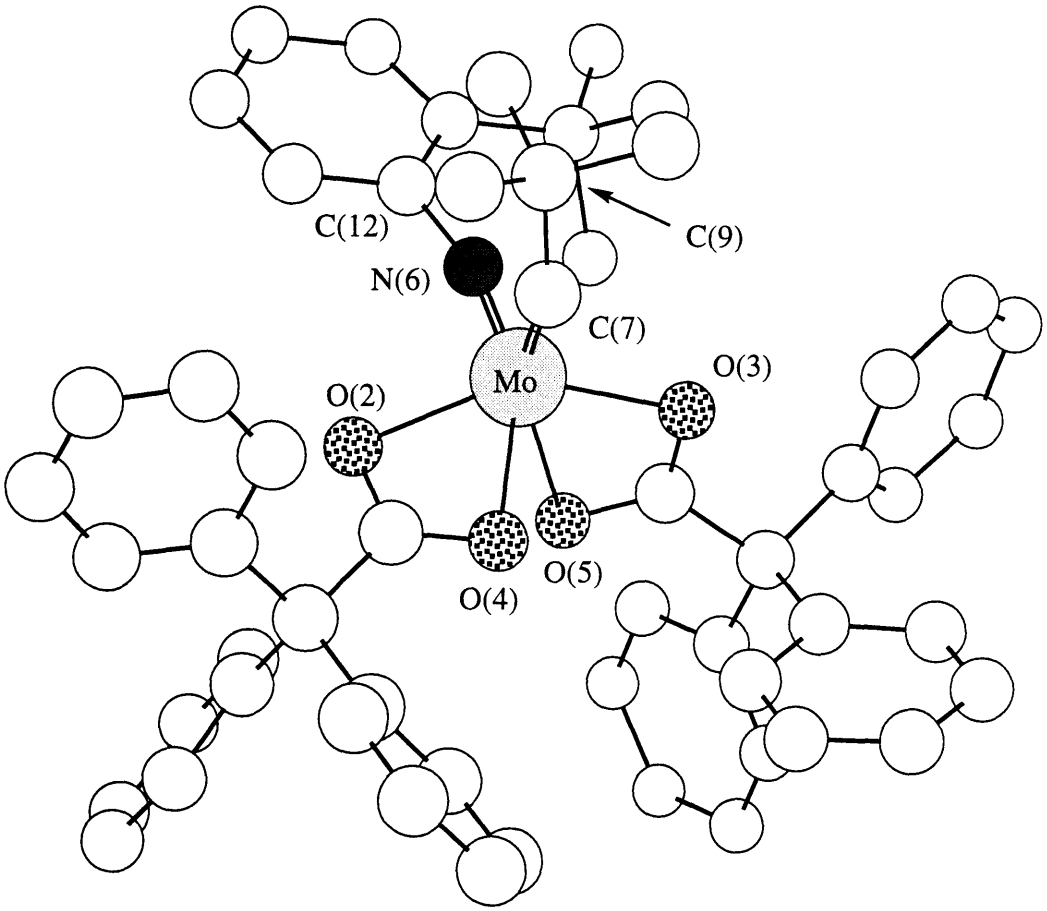

Figure 1.2. X-ray Crystal Structure of Mo(NAr')($CHCMe_3$)(O_2CCPh_3)$_2$ (**2b**), viewed with the Mo-C(7) double bond approximately in the paper plane.

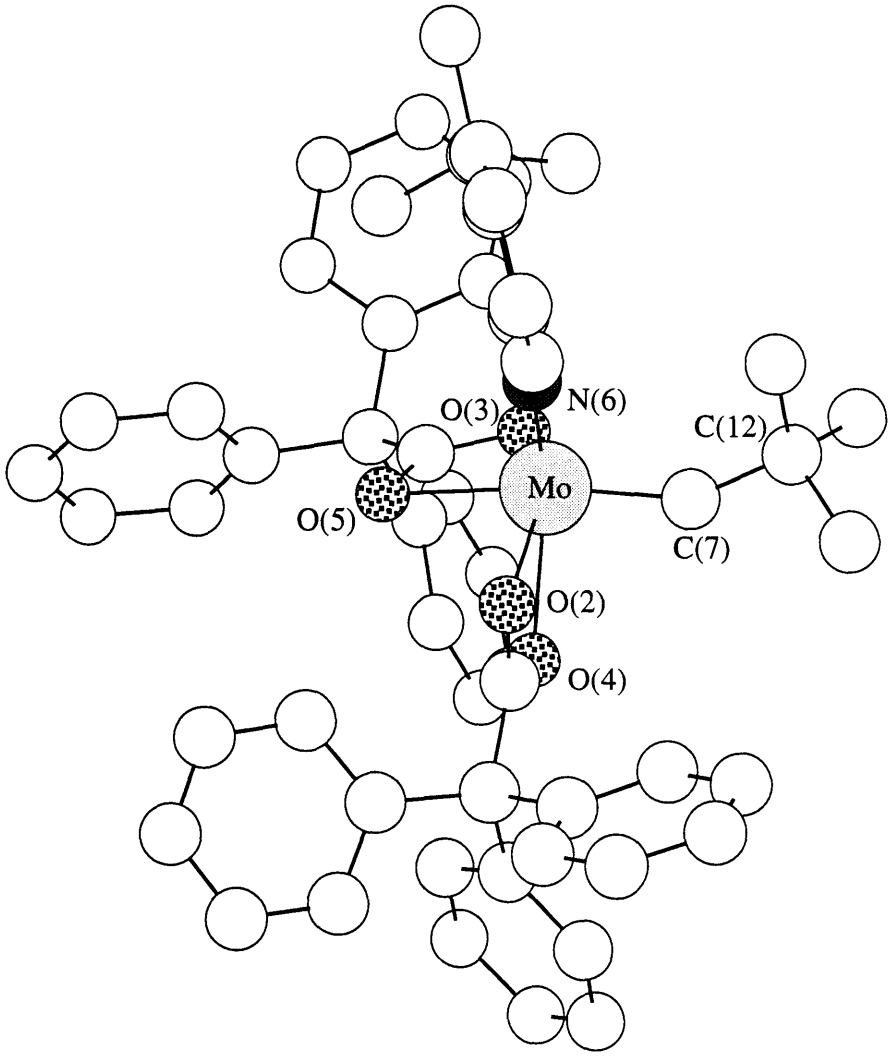

Table 1.3. Selected Interatomic Distances (Å) and Angles (deg) for the Non-Hydrogen Atoms of Mo(NAr')($CHCMe_3$)(O_2CCPh_3)$_2$ (**2b**).

Bond Lengths

Mo-C(7)	1.884(9)	Mo-O(4)	2.261(5)
Mo-O(2)	2.136(5)	Mo-O(5)	2.336(6)
Mo-O(3)	2.090(6)	Mo-N(6)	1.709(7)

Bond Angles

Mo-N(6)-C(12)	164.5(6)	C(7)-Mo-O(3)	98.1(3)
Mo-C(7)-C(9)	145.9(7)	C(7)-Mo-O(4)	89.8(3)
N(6)-Mo-C(7)	99.7(4)	C(7)-Mo-O(5)	151.9(3)
N(6)-Mo-O(2)	96.6(3)	O(2)-Mo-O(3)	147.5(2)
N(6)-Mo-O(3)	105.6(3)	O(4)-Mo-O(5)	77.9(2)
N(6)-Mo-O(4)	155.4(3)	O(2)-Mo-O(4)	59.2(2)
N(6)-Mo-O(5)	101.8(3)	O(3)-Mo-O(5)	58.8(2)
C(7)-Mo-O(2)	101.2(3)		

Table 1.4. Crystallographic Data, Collection Parameters, and Refinement Parameters for $Mo(NAr)(CHCMe_2Ph)(O_2CMePh_2)_2$ (**4**).

Empirical Formula	$C_{52}H_{55}NO_4Mo$
Formula Weight	853.95
Diffractometer	Enraf-Nonius CAD-4
Crystal Color, Habit	yellow, prismatic
Crystal Dimensions (mm)	0.300 x 0.280 x 0.280
Crystal System	Triclinic
No. Reflections Used for Unit Cell Determination (2θ range)	19 (26.1 - 37.1°)
a	13.844(5) Å
b	14.395(6) Å
c	11.676(5) Å
α	95.81(4)°
β	102.80(3)°
γ	95.32(3)°
V	2241(2) $Å^3$
Space Group	$P\bar{1}$ (#2)
Z	2
D_{calc}	1.265 g/cm^3
F_{000}	896
$\mu(MoK_\alpha)$	3.27 cm^{-1}
Scan Type	ω-2θ
Temperature	188 K
Total No. Unique Reflections	7900
No. Observations with $I > 3.00\sigma(I)$	5858
No. Variables	523
R	0.043
R_w	0.052
GoF	1.52

Figure 1.3. X-ray Crystal Structure of $Mo(NAr)(CHCMe_2Ph)(O_2CMePh_2)_2$ (**4**).

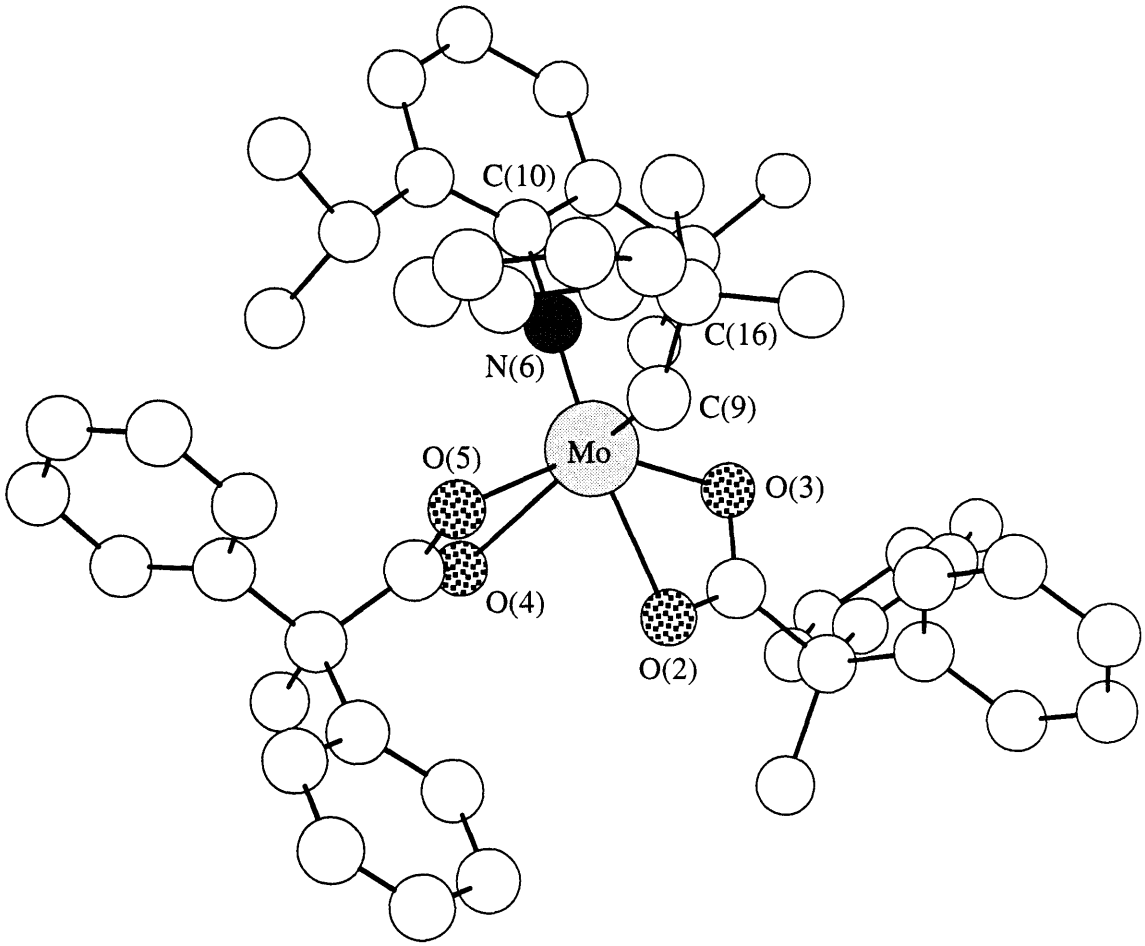

Table 1.5. Selected Interatomic Distances (Å) and Angles (deg) for the Non-Hydrogen Atoms of $Mo(NAr)(CHCMe_2Ph)(O_2CMePh_2)_2$ (**4**).

Bond Lengths

Mo-C(9)	1.889(4)	Mo-O(4)	2.401(3)
Mo-O(2)	2.254(3)	Mo-O(5)	2.074(3)
Mo-O(3)	2.111(3)	Mo-N(6)	1.732(3)

Bond Angles

Mo-C(9)-C(16)	143.5(3)	O(5)-Mo-C(9)	93.1(1)
Mo-N(6)-C(10)	175.8(3)	O(4)-Mo-C(9)	149.0(1)
N(6)-Mo-C(9)	101.3(2)	O(2)-Mo-N(6)	157.0(1)
O(2)-Mo-O(3)	59.5(1)	O(4)-Mo-N(6)	98.1(1)
O(4)-Mo-O(5)	57.9(1)		

solution suggest the accessibility of η^1 binding. The electron count in **2b** is 18 if the carboxylato ligands are counted as bidentate ligands and π electron donation from the imido ligand is included. Bending of the imido ligand as well as η^2 to η^1 conversion of the carboxylato ligands may be important features of **2b** as a catalyst.

Similar structural features were found in an X-ray structural study of complex **4** (Figure 1.3). (See Table 1.4 for crystallographic details and Table 1.5 for selected intramolecular distances and angles.) As in **2b** the alkylidene ligand is also *syn* consistent with the C-H_α coupling constant. The Mo-C(9) distance (1.896(3) Å), the Mo-C(9)-C(16) angle (143.5(3)°) and the Mo-N(6) distance (1.732(3) Å) are in the expected range, the Mo-N(6)-C(10) angle (175.8(3)°) is virtually linear in contrast to the slightly bent orientation

found for **2b**. The linear Mo-imido arrangement and the approximately perpendicular orientation of the aryl ring to the C(9)-Mo-N(6) plane provide comparable crowding by the isopropyl substituents at both sides of the C(9)-Mo-N(6) plane. This structural feature may be responsible for the significantly different reactivity of **4** in comparison to **2b** as will be discussed later in this chapter. Similar to the structure of **2b**, both carboxylate ligands are bound to molybdenum in a bidentate, but unsymmetrical fashion (Mo-O distances between 2.076 and 2.412 Å) resulting in a distorted octahedral coordination environment around the metal center.

Interconversion of Alkylidene Rotamers.

The interconversion of the two alkylidene rotational isomers, *syn* and *anti*, and their reactivities have been studied in great detail for many alkylidene complexes.[34-38] In particular complexes of the type $M(NR)(CHR')(OR'')_2$ (M = Mo or W)[32,33] favor the *syn* orientation; however up to 35% of the *anti* rotamer can be generated by low temperature photolysis, which reverts to the thermodynamically generally favored *syn* rotamer. The interconversion rates were found to strongly depend on the nature of the alkoxide ligand.

The observed dependence on the ancillary ligand motivated us to explore the effect of carboxylates on the interconversion rates. Photolysis of **1a** for 6 to 16 h at -85 °C at 366 nm produced up to 36% *anti* rotamer depending on the nature of the solvent (eq 2). The

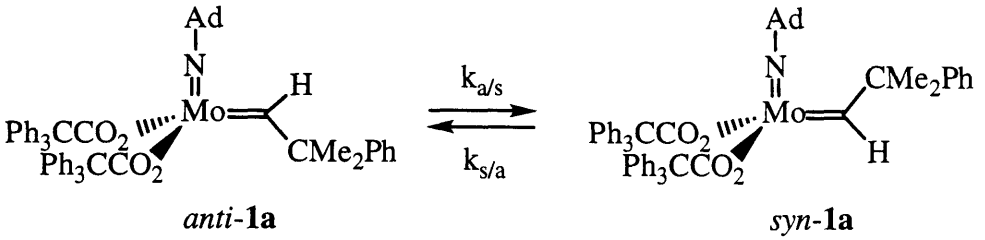

anti-**1a** *syn*-**1a** (2)

$K_{eq} = k_{a/s}/k_{s/a}$

chemical shifts for H_α of the *syn* and *anti* rotamer are only 0.2 ppm apart. In the tetrahedral bisalkoxide complexes the difference in chemical shift for the two rotamers is typically approximately 1 ppm.[33] The conversion of the *anti* to the *syn* rotamer was followed by monitoring the decrease in the intensity of the H_α resonance for the *anti* rotamer in d_8-toluene. In contrast to the bis(alkoxide) systems the conversion of the *anti* to the *syn* rotamer was found to be unmeasurable slow at lower temperatures. Even at room temperature the half life still amounted to approximately 7 h. Since K_{eq} is relatively large (K_{eq} = 49), conversion of the *anti* to the *syn* rotamer could be assumed to be irreversible and a rough estimate of $k_{a/s}$ (~ 3 x 10^{-5} s^{-1}) was obtained by applying first-order kinetics.

The much decreased rate of rotamer rotation can be explained if the η^2 bonding of the carboxylato ligands is compared to the interactions between a coordinating solvent such as THF and a sufficiently electrophilic metal center in Mo(NR)(CHR')(OR'')$_2$ complexes. If evidence for binding of THF to the metal center was observed,[33] the rotamer rotation was inhibited to a significant degree. Dissociation of THF prior to alkylidene rotation was proposed based on activation parameters. Direct analogy suggests η^1 bonding mode during rotamer interconversion. These studies further manifest the different coordination environment provided by the Ph_3CCO_2 ligand compared to the alkoxide ligands.

Reactivity of Bis(carboxylate) Complexes.

As described in the introduction, intention for the development of this new class of bis(carboxylate) alkylidene complexes was their potential use as catalysts for the regioselective polymerization of heptadiynes such as diethyldipropargylmalonate (DEDPM). Addition of DEDPM to **2b** in toluene yields poly(DEDPM)$_n$ with a polydispersity that ranges from 1.13 to 1.26. Indeed all complexes of the type Mo(NR)(CHR')(O_2CCPh_3)$_2$ with NR = N-1-adamantyl (**1a** and **1b**) and N-2-*t*-Bu-C_6H_4 (**2a** and **2b**) are potent catalysts for the polymerization of DEDPM. A detailed study of this reaction and the properties of such polymers will be presented in Chapter 2. Surprisingly

compounds containing the N-2,6-*i*-Pr_2-C_6H_3 ligand (**3** and **4**) are impractically slow initiators for the polymerization of DEDPM. Even after 24 h only approximately 50% of the monomer had been consumed. This can best be explained on steric grounds since electronically complexes **3** and **4** are expected to be similar to **2a** and **2b**. The first triple bond of the monomer has to attack one of the two CNO faces. X-ray structural data showed that in **2b** one CNO face is blocked by the *t*-butyl group, while the other side is accessible. In **4**, however, both faces are blocked by the isopropyl substituents.

To substantiate this suggestion, the accessibility to the metal center was probed by reaction of the bis(carboxylato) complexes with PMe_3. **1a** forms a white PMe_3 adduct quantitatively. Only one isomer can be detected in the proton NMR (δ 13.28 ppm, H_α). **2a** and **2b** also form the corresponding PMe_3 adduct (**10a** and **10b**), but two isomers are observed in solution (δ 14.00 ppm and 13.30 ppm for **10a**; 13.70 ppm and 13.13 ppm for **10b**). Interestingly recrystallization of **10b** from CH_2Cl_2/ether gave yellow microcrystals that initially exhibited only one isomer in the proton NMR (δ 13.13); the other isomer slowly grew in and remained the minor isomer after equilibrium had been reached within approximately 2 h. In contrast **3** did not react with 1 equiv of PMe_3 at all, the starting material was recovered in good yield. Reaction of **4** (containing the smaller Ph_2MeCO_2 ligand) with 1 equiv of PMe_3 led to an equilibrium between the PMe_3 adduct and **4** in solution. All PMe_3 adducts do not polymerize DEDPM effectively.

A similar dependence on the imido ligand was found for the reactivity behavior towards DEDPM using initiators **7** and **8** with bulky $(Me_3Si)_3SiCO_2$ ligands. **7** containing the N-2,6-*i*-Pr_2-C_6H_3 ligand did not initiate the polymerization of DEDPM while **8** proved to be an active catalyst for the cyclopolymerization of DEDPM.

All bis(triphenylacetate) complexes are unsuccessful ROMP initiators. Typical ROMP monomers such as 2,3-dicarbomethoxynorbornadiene, methyltetracyclododecene (MTD) and even norbornene are not readily polymerized by **1a** or **2b**. Presumably a disubstituted olefin, even one as reactive as norbornene cannot coordinate to the metal

center for steric reasons. In addition, **1a** does not react with *ortho*-((trimethylsilyl)-phenyl)acetylene or even phenylacetylene itself.

CONCLUSIONS

A new family of molybdenum imido alkylidene initiators containing bulky carboxylates such as triphenylacetate as ancillary ligands has been developed. The steric bulk of such carboxylate ligands with respect to the smaller benzoate based ligands is necessary to prevent the formation of 'ate-complexes' as well as bimolecular decomposition. X-ray structural analysis shows an unsymmetric η^2 bonding mode of the carboxylate ligands. A higher coordination number around the metal center is further evidenced by distinctive differences of *syn/anti* rotamer interconversion behavior in comparison to the tetrahedral bis(alkoxide) complexes. Despite the formal electron count of 18, assuming a bidentate bonding mode of each carboxylato ligand and π electron donation from the imido ligand, such compounds are potent initiators for the polymerization of diethyldipropargylmalonate suggesting the accessibility of η^1 bonding. Exceptions are complexes containing the N-2,6-*i*-Pr_2-C_6H_3 ligand, where the isopropyl substituents presumably block access to the metal center at both coordination positions. All complexes are poor initiators for typical ROMP monomers.

EXPERIMENTAL

General details. All experiments were performed under a nitrogen atmosphere in a Vacuum Atmospheres dry box or by standard Schlenk techniques under an argon atmosphere unless specified otherwise. Celite and alumina were dried at ~130 °C for at least a week. Pentane was washed with sulfuric/nitric acid (95/5 v/v), sodium bicarbonate and water, stored over calcium chloride, and distilled from sodium benzophenone ketyl

under nitrogen. Reagent grade diethyl ether, tetrahydrofuran, toluene, benzene and 1,2-dimethoxyethane were distilled from sodium benzophenone ketyl under nitrogen. Reagent grade dichloromethane was distilled from calcium hydride under nitrogen. Toluene used for polymerizations was stored over 4Å molecular sieves prior to use. Benzene-d_6 and dichloromethane-d_2 were sparged with argon and stored over 4Å molecular sieves.

NMR data were obtained either at 300 MHz (^{1}H) and 75.43 MHz (^{13}C) on a Varian XL 300 NMR spectrometer or a Varian Unity 300 NMR spectrometer or at 500 MHz (^{1}H) and 125 MHz (^{13}C) on a Varian 500 NMR spectrometer and are listed in parts per million downfield from tetramethylsilane for proton and carbon. Spectra were obtained at room temperature unless noted otherwise. X-ray data were collected on an Enraf-Nonius CAD-4 diffractometer or a Siemens platform goniometer with a CCD detector. Elemental analyses (C, H, N) were performed on a Perkin-Elmer 2400 CHN analyzer in our laboratories

All chemicals used were reagent grade (Aldrich) and used without further purification unless specified otherwise. Mo(N-1-adamantyl)(CHCMe$_2$Ph)(OTf)$_2$(DME),[5] Mo(N-1-adamantyl)(CHCMe$_3$)(OTf)$_2$(DME),[5] Mo(N-2,6-*i*-Pr$_2$-C$_6$H$_3$)(CHCMe$_2$Ph)(OTf)$_2$(DME),[5] Mo(N-2-*t*-Bu-C$_6$H$_4$)(CHCMe$_2$Ph)(OTf)$_2$(DME),[5] Mo(N-2-*t*-Bu-C$_6$H$_4$)(CHCMe$_3$)(OTf)$_2$(DME),[5] Mo(N-2-*t*-Bu-C$_6$H$_4$)$_2$Cl$_2$(DME),[5] (Me$_3$Si)$_3$SiCO$_2$H,[39] and diethyldipropargylmalonate[40] were prepared as reported in the literature.

General synthesis of Na or K carboxylates. A THF solution of the carboxylic acid (1 equiv) was slowly treated with one equiv of metal hydride. In cases where the metal carboxylate was soluble in THF, a slight excess of metal hydride was added and after stirring overnight the solution was filtered through Celite and all volatiles removed under vacuum. When the resulting metal carboxylate precipitated, a slight excess of the acid was added and after stirring overnight, the product was collected on a frit and dried under vacuum. Isolated yields were 90% or higher.

Na[Mo(N-1-adamantyl)(CHCMe$_2$Ph)(O$_2$C-3,5-*t*-Bu$_2$-C$_6$H$_2$)$_3$]•(THF)$_{0.5}$. A chilled (-30 °C) solution of 3,5-*t*-Bu$_2$-C$_6$H$_3$CO$_2$Na (161 mg, 0.63 mmol) was added to a chilled (-30 °C) solution of Mo(N-1-adamantyl)(CHCMe$_2$Ph)(OTf)$_2$(DME) (200 mg, 0.26 mmol). After stirring for 1.5 h, the solvents were removed under vacuum and the yellow solid extracted with pentane. The sodium triflate was removed by filtration through Celite, all volatiles were removed under vacuum and the product was recrystallized from pentane yielding white crystals (103 mg, 36%): ^{1}H NMR (C$_6$D$_6$) δ 14.97 (s, 1H, MoCHR), 8.42 (s, 2H, H$_o$), 8.26 (s, 4H, H$_o$), 7.94 (d, 2H, H$_o$), 7.60 (s, 1H, H$_p$), 7.49 (s, 2H, H$_p$), 7.47 (t, 2H, H$_m$), 7.21 (t, 1H, H$_p$), 3.55 (t, 2H, OCH$_2$), 1.86 (d, 6H, CH$_2$), 2.03 (br, 12H, CH$_2$ and CHC(C*H*$_3$)$_2$Ph), 1.74 (br, 3H, CH), 1.35 (m, 2H, OCH$_2$C*H*$_2$), 1.32 (s, 24H, CH$_2$ and CMe$_3$), 1.12 (s, 36H, CMe$_3$); ^{13}C NMR (C$_6$D$_6$) δ 310.0 (MoCHR), 178.4, 175.6 (CO$_2$), 153.2, 151.1, 150.9, 136.3, 134.6, 128.8, 128.7, 128.3, 126.23, 126.15, 125.1, 124.9 (C$_{aryl}$), 73.0 (NC), 53.2 (CH*C*Me$_2$Ph), 43.2 (CH$_2$), 36.4 (CH$_2$), 35.3, 35.2 (*C*Me$_3$), 33.1 (CH), 32.0, 31.8 (C*Me*$_3$), 29.9 (CHC*Me*$_2$Ph).

Na[Mo(N-1-adamantyl)(CHCMe$_2$Ph)(O$_2$C-2,6-Me$_2$-C$_6$H$_3$)$_3$]. Solid 2,6-Me$_2$-C$_6$H$_3$CO$_2$Na (138 mg, 0.80 mmol) was added to a chilled (-30 °C) solution of Mo(N-1-adamantyl)(CHCMe$_2$Ph)(OTf)$_2$(DME) (200 mg, 0.26 mmol) in THF. Within seconds a clear solution formed and after stirring for 45 min all volatiles were removed under vacuum. The solid was extracted with pentane, the sodium triflate was filtered off using Celite and all volatiles were removed under vacuum. Recrystallisation of the crude product from pentane at -30 °C gave white crystals (124 mg, 56%): ^{1}H NMR (CD$_2$Cl$_2$) δ 13.98 (s, 1H, MoCHR), 7.35 (d, 2H, H$_o$), 7.25-6.83 (m, 12H, H$_{aryl}$), 2.23 (s, 12H, *o*-CH$_3$), 2.10 (s, 6H, *o*-CH$_3$), 1.97 (s, 9H, CH$_2$ and CH), 1.62 (s, 6H, CHC(C*H*$_3$)$_2$Ph), 1.52 (s, 6H, CH$_2$).

Mo(N-1-adamantyl)(CHCMe$_2$Ph)(O$_2$CPh$_3$)$_2$ (1a). Sodium triphenylacetate (446 mg, 1.437 mmol) was added over a period of 10 minutes to a solution

of Mo(N-1-adamantyl))(CHCMe$_2$Ph)(OTf)$_2$(DME) (500 mg, 0.635 mmol) in 20 mL of chilled (-30 °C) THF. After stirring the mixture for 1 h, all solvents were removed under vacuum and the yellow residue was extracted with a mixture of pentane and toluene (5/1 v/v) and the extract was filtered through Celite. The solvents were removed from the filtrate under vacuum and the resulting yellow solid was recrystallized from ether by adding pentane and cooling to -30 °C; white crystals with a yield of 450 mg in two crops (0.47 mmol, 72%) were obtained: ^{1}H NMR (C_6D_6) δ 13.89 (s, 1H, MoCHR), 7.51-7.47 (m, 12H, H_{aryl}), 7.27-7.24 (dd, 2H, H_{aryl}), 7.13-7.00 (m, 21H, H_{aryl}), 1.86 (d, 6H, CH_2), 1.71 (br, 3H, CH), 1.59 (s, 6H, CHC(CH_3)$_2$Ph), 1.29 (t, 6H, CH_2); ^{13}C NMR (C_6D_6) δ 305.5 (d, J_{CH} = 116.5, MoCHR), 191.7 (CO_2), 150.8 (C_{ipso}), 143.5 (C_o), 141.4, 131.1 (C_m), 127.1 (C_p), 126.0, 75.4 (NC), 69.6 (CCO_2), 51.8 (CHCMe$_2$Ph), 43.5 (CH_2), 35.8 (CH_2), 31.6 (CH), 29.5 (CHCMe_2Ph). Anal. Calcd. for $MoC_{60}H_{57}NO_4$: C, 75.69; H, 6.03; N, 1.47. Found: C, 75.92; H, 6.28; N, 1.35.

Mo(N-1-adamantyl)(CH-*t*-Bu)(O$_2$CPh$_3$)$_2$ (1b). To a chilled (-30 °C) solution of Mo(N-1-adamantyl))(CHCMe$_3$)(OTf)$_2$(DME) (300 mg, 0.426 mmol) in 15 mL THF was added a chilled (-30 °C) solution of sodium triphenylacetate (292 mg, 0.94 mmol) in 15 mL THF over 2 min. After stirring for 25 min all volatiles were removed under vacuum. The yellow solid was extracted with a mixture of pentane and toluene (4/1 v/v) and the solution was filtered through Celite. The solvents were removed under vacuum and the resulting yellow solid was recrystallized from a small amount of ether to yield pale yellow needles (172 mg, 0.194 mmol, 45%): ^{1}H NMR (C_6D_6) δ 13.84 (s, 1H, MoCHR), 7.53-6.99 (m, 30H, H_{aryl}), 2.00 (m, 6H, CH_2), 1.75 (br, 3H, CH), 1.33 (m, 6H, CH_2), 1.21 (s, 9H, CHC(CH_3)$_3$). Anal. Calcd. for $MoC_{55}H_{55}NO_4$: C, 74.23; H, 6.23; N, 1.57. Found: C, 73.85; H, 6.38; N, 1.44.

Mo(N-2-*t*-BuC$_6$H$_4$)(CHCMe$_2$Ph)(O$_2$CPh$_3$)$_2$ (2a). Solid sodium triphenylacetate (268 mg, 0.864 mmol) was added to a chilled (-30 °C) solution of Mo(N-2-*t*-BuC$_6$H$_4$)(CHCMe$_2$Ph)(OTf)$_2$(DME) (300 mg, 0.393 mmol) in 18 mL of diethyl ether.

While warming up to room temperature the suspension was stirred for 45 min. After removal of all volatiles under vacuum, the yellow solid was extracted with a mixture of pentane and CH_2Cl_2 (30/1; v/v). The sodium triflate was removed by filtration through Celite and the solvents were removed under vacuum. Yellow crystals were isolated from pentane at room temperature (225 mg, 0.236 mmol, 60 %): ^{1}H NMR (C_6D_6) δ 13.92 (s, 1H, MoCHR), 7.73-6.74 (m, 39H, H_{aryl}), 1.55 (s, 6H, CHC*Me*$_2$Ph), 1.29 (s, 9H, CMe_3); ^{13}C NMR (C_6D_6) δ 309.4 (d, J_{CH} = 123, MoCHR), 192.4 (CO_2), 154.5, 150.0, 145.2, 143.1, 135.6, 131.2, 128.5, 128.0, 127.9, 127.2, 126.9, 126.4, 126.1, 126.0 (C_{aryl}), 69.4 (*C*CO_2), 56.7 (CH*C*Me$_2$Ph), 35.6 (CMe_3), 31.1 (CHC*Me*$_2$Ph), 24.0 (CMe_3). Anal. Calcd. for $MoC_{60}H_{55}NO_4$: C, 75.86; H, 5.83; N, 1.47. Found: C, 75.89; H, 5.68; N, 1.59.

Mo(N-2-*t*-BuC$_6$H$_4$)(CHCMe$_3$)(O$_2$CPh$_3$)$_2$ (2b). To a chilled (-30 °C) solution of Mo(N-2-*t*-BuC$_6$H$_4$)(CHCMe$_3$)(OTf)$_2$(DME) (400 mg, 0.570 mmol) in 20 mL diethyl ether was added solid sodium triphenylacetate (389 mg, 1.25 mmol). After stirring for 1 h all volatiles were removed under vacuum. The remaining yellow solid was extracted with a mixture of pentane and toluene (1/1; v/v) and then with a small amount of toluene. After filtering off the sodium triflate, the solvents were removed under vacuum and the resulting yellow solid was recrystallized from CH_2Cl_2/pentane to yield yellow crystals (280 mg, 0.315 mmol, 55%). Crystals suitable for X-ray crystallography could be obtained by recrystallization from a mixture of pentane and dichloromethane at -30 °C: ^{1}H NMR (CD_2Cl_2) δ 13.76 (s, 1H, MoCHR), 7.58 (m, 1H, H_{aryl}), 7.35-7.17 (m, 33H, H_{aryl}), 1.33 (s, 9H, CMe_3), 1.17 (s, 9H, MoCHC(*C*H$_3$)$_3$); ^{13}C NMR (CD_2Cl_2) δ 313.4 (MoCHR), 191.9 (CO_2), 154.6, 145.6, 143.0, 135.6, 131.0, 128.5, 128.2, 127.5, 127.1, 126.4 (C_{aryl}), 69.4 (*C*CO_2), 50.9 (MoCH*C*(CH$_3$)$_3$), 36.0 (*C*Me$_3$), 31.5 (MoCHC(*C*H$_3$)$_3$), 30.7 (C*Me*$_3$). Anal. Calcd. for $MoC_{55}H_{53}NO_4$: C, 74.40; H, 6.02; N, 1.58. Found: C, 74.67; H, 5.86; N, 1.36.

Mo(N-2,6-*i*-$Pr_2C_6H_3$)(CHCMe$_2$Ph)(O_2CPh_3)$_2$ (3). A solution of sodium triphenylacetate (862 mg, 2.78 mmol) in 15 mL of THF was added to a stirred solution of Mo(NAr)(CHCMe$_2$Ph)(OTf)$_2$(DME) (1.00 g, 1.26 mmol) in 15 mL THF at -30 °C. After 20 min all volatiles were removed under vacuum and the yellow solid was extracted with a mixture of pentane and CH_2Cl_2 (10/1 v/v). The mixture was filtered through Celite and the filtrate was concentrated under vacuum. Yellow crystals were isolated (1.08 g, 1.104 mmol, 88%) upon cooling the filtrate to -30 °C: ^{1}H NMR (C_6D_6) δ 13.91 (s, 1H, MoCHR), 7.49-6.89 (m, 38H, H_{aryl}), 3.78 (sep, 2, C*H*Me$_2$), 1.50 (s, 6H, CHC*Me*$_2$Ph), 1.03 (d, 12H, CH*Me*$_2$); ^{13}C NMR (C_6D_6) δ 308.9 (d, J_{CH} = 122.3, MoCHR), 192.5 (CO_2), 153.1, 150.4, 149.6, 143.5, 131.5, 129.1, 128.8, 128.4, 127.6, 126.7, 126.5, 123.6 (C_{aryl}), 69.7 (*C*CO_2), 56.8 (CH*C*Me$_2$Ph), 31.2 (*C*HMe$_2$), 29.4 (CHC*Me*$_2$Ph), 24.0 (CH*Me*$_2$).

Mo(N-2,6-*i*-$Pr_2C_6H_3$)(CHCMe$_2$Ph)(O_2CMePh$_2$)$_2$ (4). Sodium diphenylmethylacetate (552 mg, 2.22 mmol) was added to a stirred solution of Mo(NAr)(CHCMe$_2$Ph)(OTf)$_2$(DME) (800 mg, 1.01 mmol) in 30 mL THF at -30 °C. After 20 min all volatiles were removed under vacuum and the yellow solid was extracted with 60 mL pentane. The sodium triflate was removed by filtration through Celite. The solution was concentrated under vacuum and allowed to stand at room temperature to yield yellow cubes (553 mg, 0.648 mmol, 64%). Crystals suitable for X-ray crystallography were obtained by recrystallization from a mixture of pentane and dichloromethane at -30 °C: ^{1}H NMR (C_6D_6) δ 13.96 (s, 1H, MoCHR), 7.49-6.90 (m, 28H, H_{aryl}), 3.73 (sep, 2H, C*H*Me$_2$), 2.04 (s, 6H, CH_3CCO_2), 1.51 (s, 6H, CHC(C*H*$_3$)$_2$Ph), 1.05 (d, 12H, CH(C*H*$_3$)$_2$); ^{13}C NMR (C_6D_6) δ 308.5 (d, J_{CH} = 120.6, MoCHR), 193.9 (CO_2), 153.0, 150.5, 149.4, 145.3, 145.1, 129.3, 129.0, 128.8, 127.4, 126.6, 126.5, 123.5 (C_{aryl}), 58.6 (*C*CO_2), 56.6 (CH*C*Me$_2$Ph), 31.2 (*C*HMe$_2$), 29.5 (CHC(*C*H$_3$)$_2$Ph), 27.0 (*C*H$_3$CCO$_2$), 23.9 (*C*HMe$_2$).

Mo(N-2-*t*-Bu-C_6H_4)$_2$(CH_2Ph)$_2$ (5). Solid benzylpotassium (2.08 g, 16.0 mmol) was added to a chilled (-30 °C) solution of Mo(N-2-*t*-Bu-C_6H_4)$_2$$Cl_2$(DME) (4.0 g, 7.25 mmol) in THF (75 mL) over 2 min. The suspension was stirred for 7 h allowing the suspension to warm to room temperature. After removal of all volatiles under vacuum, followed by the addition of ether, the suspension was filtered through Celite and the filtrate was concentrated. Crystallization at -30 °C afforded orange cubes (2.2 g, 53%): ^{1}H NMR (CD_2Cl_2) δ 7.22-6.90 (m, 18H, H_{aryl}), 2.47 (s, 4H, CH_2), 1.59 (s, 18H, CH_3); ^{13}C NMR (CD_2Cl_2) δ 155.7, 141.5, 136.5, 132.4, 130.6, 130.4, 126.9, 126.7, 125.9, 125.3 (C_{aryl}), 48.2 ($C(CH_3)_3$), 36.1 (CH_2), 30.5 ($C(CH_3)_3$). Anal. Calcd. for $MoC_{34}H_{40}N_2$: C, 71.31; H, 7.04; N, 4.89. Found: C, 71.33; H, 6.68; N, 4.86.

Mo(N-2-*t*-Bu-C_6H_4)(CHPh)(OTf)$_2$(DME) (6). A chilled (-30 °C) solution of triflic acid (1.433 g, 9.61 mmol) in DME (5 mL) was added to a chilled (-30 °C) solution of **5** (1.835 g, 3.20 mmol) in DME (50 mL) over 5 min resulting in significant darkening of the reaction mixture. After stirring at room temperature for 1.5 h, all volatiles were removed under vacuum and the residue was extracted with toluene. After filtration through Celite, the solvent was removed and the product recrystallized from ether at -30 °C to yield greenish-yellow microcrystals (770 mg, 1.19 mmol, 37%): ^{1}H NMR (C_6D_6) δ (major isomer: 90%) 14.61 (s, 1H, Mo=CH), 8.39 (d, 1H, H_{aryl}), 7.56 (d, 2H, H_{aryl}), 7.05-6.72 (m, 6H, H_{aryl}), 3.83 (br, 3H, CH_3O), 3.20 (br, 2H, CH_2O), 2.81 (br, 5H, CH_3O and CH_2O), 1.34 (s, 9H, $C(CH_3)_3$); δ 308.5 (MoCHR), 164.3, 153.8, 148.4, 147.1, 135.5, 131.4, 130.9, 130.1, 128.1, 126.9 (C_{aryl}), 120.5 (CF_3), 73.6, 70.7, 66.3, 62.3 (CH_3O and CH_2O), 36.3 (CMe_3), 30.9 (CMe_3).

Mo(N-2,6-*i*-Pr_2-C_6H_3)($CHCMe_2Ph$)[$O_2CSi(SiMe_3)_3$]$_2$ (7). Solid $(Me_3Si)_3SiCO_2Na$ (155 mg, 0.49 mmol) was added to a chilled solution (-30 °C) of Mo(N-2,6-*i*-Pr_2-C_6H_3)($CHCMe_2Ph$)(OTf)$_2$(DME) (190 mg, 0.24 mmol) in 4 mL THF. After stirring for 40 min all volatiles were removed under vacuum and the yellow solid was extracted with 3 mL pentane. The sodium triflate was removed by filtration through Celite.

The solution was then concentrated under vacuum to approximately half the volume and allowed to crystallize at room temperature yielding yellow crystals (170 mg, 0.17 mmol, 72%): ^{1}H NMR (C_6D_6) δ 13.82 (s, 1H, MoCHR), 7.36 (d, 1H, H_{aryl}), 7.25 (t, 2H, H_{aryl}), 7.09 (t, 1H, H_{aryl}), 6.99 (br, 3H, H_{aryl}), 3.98 (sep, 2H, C*H*Me$_2$), 1.61 (s, 6H, CHC(C*H*$_3$)$_2$Ph), 1.30 (d, 12H, CH(C*H*$_3$)$_2$), 0.39 (s, 54H, SiCH$_3$); ^{13}C NMR (C_6D_6) δ 304.0 (MoCHR), 211.4 (CO_2), 153.3, 151.5, 149.2, 128.9, 128.7, 126.8, 126.4, 123.6 (C_{aryl}), 56.7 (CHC*M*e$_2$Ph), 31.9 (*C*HMe$_2$), 29.0 (CHC*Me*$_2$Ph), 24.6 (CH*Me*$_2$), 1.7 (SiCH$_3$). Anal. Calcd. for $MoC_{42}H_{83}O_4Si_8$: C, 51.12; H, 8.48; N, 1.42. Found: C, 50.98; H, 8.69 N, 1.32.

Mo(N-2-*t*-Bu-C$_6$H$_4$)(CHCMe$_2$Ph)[O$_2$CSi(SiMe$_3$)$_3$]$_2$ (8). Solid (Me$_3$Si)$_3$SiCO$_2$Na (69 mg, 0.22 mmol) was added to a chilled (-30 °C) solution of Mo(N-2-*t*-Bu-C$_6$H$_4$)(CHCMe$_2$Ph)(OTf)$_2$(DME) (80 mg, 0.105 mmol) in 4 mL THF. After stirring for 40 min all volatiles were removed under vacuum and the yellow solid was extracted with 3 mL pentane. The sodium triflate was removed by filtration through Celite. The solution was concentrated under vacuum to approximately half its original volume and allowed to crystallize at room temperature yielding yellow crystals (85 mg, 0.087 mmol, 83%): ^{1}H NMR (C_6D_6) δ 13.78 (s, 1H, MoCHR), 8.00 (d, 1H, H_{aryl}), 7.37 (d, 2H, H_{aryl}), 7.26 (t, 2H, H_{aryl}), 7.12-6.99 (m, 3H, H_{aryl}), 6.86 (t, 1H, H_{aryl}), 1.70 (s, 6H, CHC(C*H*$_3$)$_2$Ph), 1.51 (s, 9H, C(C*H*$_3$)$_3$), 0.39 (s, 54H, SiCH$_3$).

Mo(N-1-adamantyl)(CHCMe$_2$Ph)[O$_2$C(C$_6$H$_5$)$_3$]$_2$(PMe$_3$) (9). Neat PMe$_3$ (12 μL, 0.116 mmol) was added to a chilled (-30 °C) solution of **1a** (100 mg, 0.105 mmol) in toluene. After 2 h stirring at room temperature all volatiles were removed under vacuum and the remaining solid was washed with cold pentane to yield white microcrystals in quantitative yield: ^{1}H NMR (C_6D_6) δ 13.28 (d, 1H, MoCHR), 7.75-6.96 (m, 35H, H_{aryl}), 2.20 (s, 3H, C(C*H*$_3$)MePh), 1.97 (d, 6H, CH$_2$), 1.78 (br, 3H, CH), 1.49 (s, 3H, CMe(C*H*$_3$)Ph), 1.35 (br, 6H, CH$_2$), 0.39 (d, 9H, PCH$_3$).

Mo(N-2-*t*-Bu-C_6H_4)(CHCMe$_2$Ph)[$O_2C(C_6H_5)_3$]$_2$(PMe$_3$) (10a). Neat PMe_3 (12 μL, 0.116 mmol) was added to a chilled (-30 °C) solution of **2a** (100 mg, 0.105 mmol) in CH_2Cl_2 (5 mL). After 4 h of stirring at room temperature all volatiles were removed under vacuum. The remaining solid was found to be clean by ^1H NMR. There are two isomers in solution: ^1H NMR (C_6D_6) δ 14.00, 13.30 (d, 1H, MoCHR), 8.23-6.62 (m, 39H, H_{aryl}), 2.07, 1.70 (s, 6H, C(CH_3)$_2$Ph), 1.59, 1.39 (s, 9H, C(CH_3)$_3$), 0.38, 0.35 (d, 9H, PCH_3).

Mo(N-2-*t*-Bu-C_6H_4)(CHCMe$_3$)[$O_2C(C_6H_5)_3$]$_2$(PMe$_3$) (10b). Neat PMe_3 (19 μL, 0.116 mmol) was added to a chilled (-30 °C) solution of **2b** (147 mg, 0.165 mmol) in CH_2Cl_2 (5 mL). After standing at room temperature for 2 h, all volatiles were removed under vacuum. Yellow microcrystals were obtained by recrystallization from CH_2Cl_2/ether at -30 °C (85 mg, 53%). ^1H NMR of a freshly prepared solution showed only one isomer. A second isomer slowly grew in and remained the minor isomer after equilibrium had been reached after approximately 2 h (major/minor isomer = 60%/40%): ^1H NMR (C_6D_6) δ (major isomer) 13.13 (d, 1H, J_{HP} = 4.9, MoCHR), 7.92 (dd, 1H, H_o), 7.62-7.57 (m, 12H, H_o), 7.16 (dd, 1H, H_m), 7.08-6.98 (m, 18H, H_m and H_p), 6.91, 6.84 (dt, 2H, H_m and H_p) 1.38 (s, 6H, MoCHC(CH_3)$_3$), 1.27 (s, 9H, C(CH_3)$_3$), 0.63 (d, 9H, PCH_3); (minor isomer) 13.70 (d, 1H, J_{HP} = 6.6, MoCHR), 8.26 (dd, 1H, H_o), 7.66-7.54 (m, 12H, H_o), 7.09-6.98 (m, 19H, H_m and H_p), 6.77, 6.73 (dt, 2H, H_m and H_p), 1.58 (s, 6H, MoCHC(CH_3)$_3$), 1.32 (s, 9H, C(CH_3)$_3$), 0.59 (d, 9H, PCH_3); ^{13}C NMR (C_6D_6) δ (major isomer, partially assigned) 314.9 (d, J_{CP} = 19.5, MoCHR), 146.0 (C_{ipso}), 132.2, 127.9 (C_o and C_m), 126.7 (C_p), 69.8 (CCO_2), 49.7 (MoCHC(CH_3)$_3$), 36.3 (C(CH_3)$_3$), 32.7 (MoCHC(CH_3)$_3$), 31.6 (C(CH_3)$_3$), 16.2 (PMe_3).

General procedure for the generation of *anti* rotamers by photolysis. Photolysis was performed on solutions of the initiator in sealed high resolution NMR tubes (535-PP). NMR tubes with a lower grade quality of glass gave smaller percentages of the

anti isomer. Concentrations were usually about 0.1 M. The apparatus employed for photolysis consisted of the NMR sample tube supported in a quartz dewar containing hexane as coolant and a cold finger of a low temperature refrigeration unit with temperature control thermocouple. The dewar was further supported and insolated in a borosilicate glass jar. Originally the temperature employed was -85 °C, however for initiators with a slow back reaction ($k_{a/s}$), photolysis was performed at room temperature employing water or hexane as coolant. Photolysis times were usually 8 to 12 h at -85 °C and 2 to 6 h at room temperature. The lamp used was a medium-pressure mercury vapor lamp that is supported in a box with a small rectangular opening at one end. In front of the opening a filter only allowing light with a wavelength of 366 nm to transmit, was attached .

Polymerization of DEDPM. A representative polymerization is described in the experimental section of Chapter 2.

ROMP of norbornene, 2,3-dicarbomethoxynorbornadiene and MTD. A procedure similar to the polymerization of DEDPM was employed as described in Chapter 2. A solution of the monomer (0.63 mmol) was added in one shot to a solution of **1a** (6 mg, 6.3 μmol) in 5 mL toluene. After stirring for 5 h, benzaldehyde was added. The reaction mixture was stirred for additional 3 h, passed through alumina and all volatiles were removed under vacuum.

CHAPTER 2

Regioselective Cyclopolymerization Using Molybdenum(VI) Imido Alkylidene Bis(carboxylate) Complexes

Much of the material covered in this chapter has appeared in print:

Schattenmann F. S.; Schrock, R. R.; Davis, W. M. *J. Am. Chem. Soc.* **1996**, *118*, 3295.

INTRODUCTION

Soluble, conjugated organic polymers have potentially useful optical and electronic properties.[41-45] Polyacetylene is the most fundamental of such polymers and its properties have been the subject of an enormous amount of theoretical and experimental studies. It exhibits high electrical conductivity when doped,[46] especially when oriented[47] and possesses a high third-order hyperpolarizability (γ).[48,49] The correlation of these properties to chain length or average conjugation length, however, is extremely difficult since polyacetylene is an insoluble and intractable material. Substituted polyacetylene derivatives, although often soluble, usually suffer from a strongly diminished degree of conjugation. A comprehensive review of the synthesis and properties of acetylenic polymers has appeared recently.[50] Therefore soluble polyacetylene derivatives with a high degree of conjugation have been of great interest. The cyclopolymerization of dipropargyl compounds is one approach to such polymers. Previous preparations of substituted polyacetylenes by cyclopolymerization methods employed Ziegler-Natta type catalysts,[51-53] Pd(II) catalysts[54-57] and classical metathesis catalytic systems[58-69] as 1:1 mixtures of $MoCl_5$ and tetraalkyltin compounds and proceed by unknown mechanisms. A wide variety of diynes were polymerized, however, insoluble materials were obtained in most cases; typically alkyl and ester substituted monomers provide polymers with the highest solubilities.

An important ultimate goal is to prepare polymers with a narrow molecular weight distribution, known chain length and endgroup identity, and a regular structure, to correlate these attributes with an NLO property such as γ, and to use this information to prepare polymers with optimal properties of some specific type. As mentioned in Chapter 1, Fox and Schrock recently reported that 1,6-heptadiynes such as diethyldipropargylmalonate (DEDPM) could be cyclopolymerized in a living manner by initiators of the type Mo(CH-*t*-Bu)(NAr)[OCMe$(CF_3)_2]_2$ (Ar = 2,6-*i*-$Pr_2C_6H_3$).[15,31] However, the polyene backbone was found to contain a mixture of five- and six-membered rings as a consequence of the

first terminal triple bond adding to an alkylidene to give either an α-substituted or a β-substituted metallacyclobutene intermediate (α or β addition, respectively; eq 1). The research efforts in this chapter were targeted towards the development of catalytic systems to yield polymers with a regular structure that contain only one ring size in the polymer backbone.

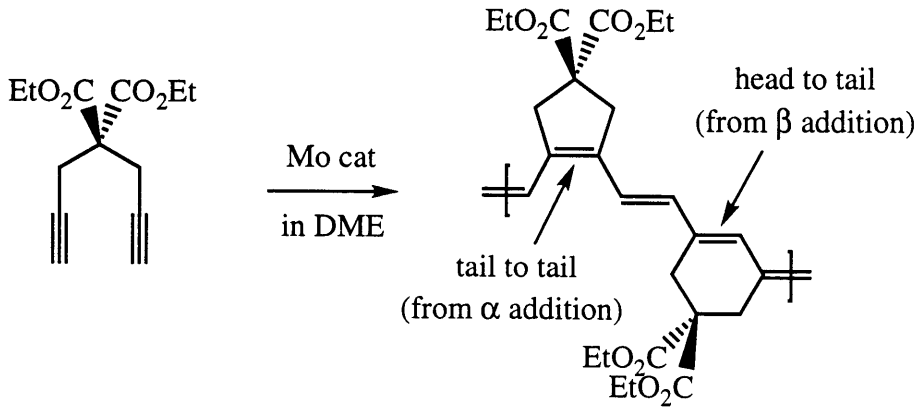

(1)

A new family of molybdenum(VI) alkylidene catalysts containing bulky carboxylate ligands was introduced in the previous chapter. Complexes of the type $Mo(NR)(CHR')(O_2CCPh_3)_2$,[70] where NR = N-1-adamantyl (**1a** and **1b**) and N-2-*t*-Bu-C_6H_4 (**2a** and **2b**), were identified as catalysts for the polymerization of DEDPM. The living, regioselective polymerization of DEDPM and related monomers using such initiators is the subject of this chapter. Carbon NMR analysis of the polymers exhibited a regular structure with only six-membered rings in the polymer backbone. Differences in the properties of these polymers compared to those containing a mixture of five- and six-membered rings in the polymer backbone are addressed as well as limitations in the choice of catalyst and monomer.

RESULTS AND DISCUSSION

Living Cyclopolymerization of DEDPM.

The bulk polymerization of DEDPM was investigated using well-defined alkylidene initiators containing the triphenylacetate ligand. A series of homopolymers of DEDPM was prepared using initiator **1a** in toluene. The polymerizations were terminated with benzaldehyde. Molecular weights of the polymers were determined by GPC on-line light scattering in THF. The results are summarized in Table 2.1. The polymers are soluble in

Table 2.1. GPC and Yield Data for Poly(DEDPM)$_n$ Using **1a** as Initiator in Toluene.

sample	M_n(theory)	M_n(g/mol)[a]	M_w(g/mol)[a]	M_w/M_n[a]	yield (%)
poly(DEDPM)$_3$	931	16360	19750	1.21[b]	85
poly(DEDPM)$_5$	1404	14030	18320	1.31[b]	97
poly(DEDPM)$_7$	1876	19370	28430	1.47	92
poly(DEDPM)$_9$	2349	18450	30080	1.63	[d]
poly(DEDPM)$_{11}$	2821	21010	35870	1.71	74
poly(DEDPM)$_{14}$	2530	24630	41730	1.69	[d]
poly(DEDPM)$_{20}$	4948	43060	69970	1.63	91
poly(DEDPM)$_{30}$	7311	65070	98340	1.51	90
poly(DEDPM)$_{45}$	10856	58000	121100	2.09[c]	92
poly(DEDPM)$_{65}$	15582	103900	168200	1.62	91
poly(DEDPM)$_{90}$	21489	109600	190700	1.74	82
poly(DEDPM)$_{125}$	29760	122700	221100	1.80	75
poly(DEDPM)$_{200}$	47482	140500	247900	1.77	68

[a] Determined by GPC on-line light scattering (Wyatt Technology). [b] Some high molecular weight; not included in peak analysis. [c] High molecular weight shoulder was included in molecular weight determination. [d] Not available.

most organic solvents (THF, benzene, toluene, CH_2Cl_2, $CHCl_3$, DME, MeCN), but insoluble in pentane and diethyl ether. Yields between 85% and 97% were obtained except for the polymers with the highest molecular weights (75% and 68%).

The molecular weights of the polymers, determined by GPC on-line light scattering were found to be higher than expected, in particular for the polymers with shorter chain lengths (up to 17 times the expected molecular weight). Also the molecular weight distributions are considerably broader than typical for a living system. A plot of the number molecular weight (M_n) as a function of the number of equivalents DEDPM employed in the polymerization shows a significant deviation from linearity, further supporting the argument that this system can not be considered strictly living (Figure 2.1).

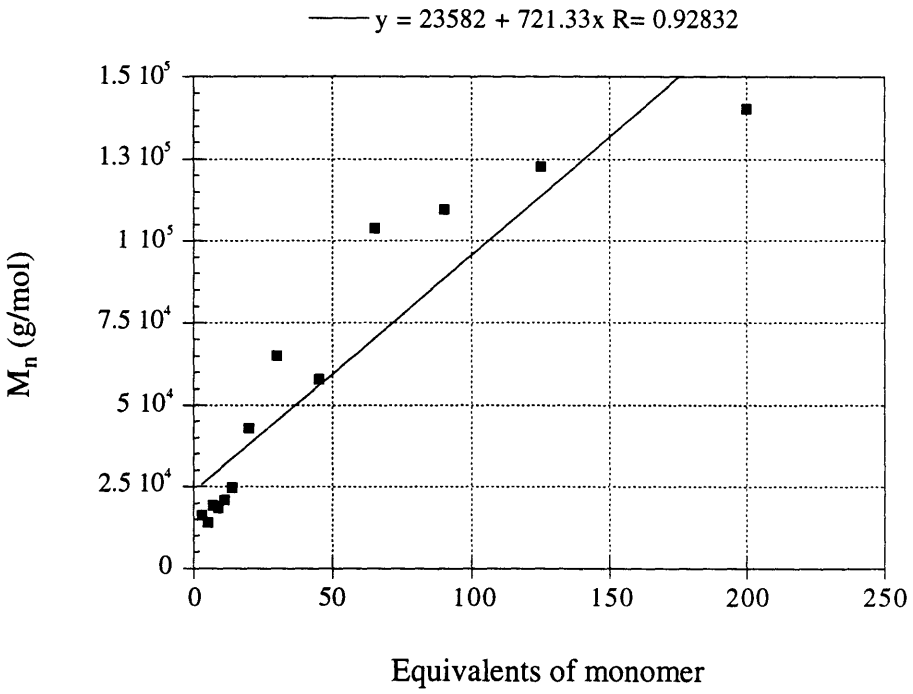

Figure 2.1. Number Average Molecular Weight (M_n) of Poly(DEDPM)$_n$ versus Number of Equivalents of Monomer Added to Initiator **1a** in Toluene.

The fact that the molecular weights are especially high for lower molecular weight polymers suggests a significant k_p/k_i problem. The large value found for the ratio of the rate of propagation to the rate of initiation[20] (k_p/k_i = 207) for the reaction of **1a** with DEDPM confirms this presumption. **1b** containing the smaller neopentylidene ligand yielded poly(DEDPM)$_n$ with slightly narrower polydispersity (1.50) and smaller molecular weight (M_n = 26500) than poly(DEDPM)$_n$ prepared using **1a**, consistent with an enhanced rate of initiation for the initiator with the smaller alkylidene ligand (compare also entries 1 and 6 in Table 2.4).

Table 2.2. GPC, Visible, and Yield Data for Poly(DEDPM)$_n$ Prepared Using **2b** in Toluene.

Sample	M_n(theory)	M_n[a]	M_w/M_n[a]	λ_{max} (nm)[b]	yield (%)
poly(DEDPM)$_5$	1403	6847	1.18	470	96
poly(DEDPM)$_8$	2112	7105	1.22	488	90
poly(DEDPM)$_{11}$	2821	9452	1.26	494	97
poly(DEDPM)$_{15}$	3766	11500	1.26	502	97
poly(DEDPM)$_{20}$	4947	13590	1.26	500	91
poly(DEDPM)$_{40}$	9673	40280	1.13	518	92
poly(DEDPM)$_{60}$	14398	45690	1.13	526	91
poly(DEDPM)$_{80}$	19124	72440	1.15	530	89
poly(DEDPM)$_{120}$	28574	99470	1.15	534	92

[a] Determined by GPC on-line viscometry versus a polystyrene universal calibration curve (Viscotek). [b] In CH_2Cl_2.

Bis(carboxylate) initiators containing the N-2-*t*-Bu-C_6H_4 ligand are better behaved catalysts for the polymerization of DEDPM than those containing the adamantylimido ligand. Initiator **2a** reacted with 20 equiv of DEDPM to give a polymer with smaller M_n (14900) and narrower PDI (1.30) than polymers prepared by using **1a**. The narrowest polydispersities were achieved employing initiator **2b** (M_w/M_n = 1.17; M_n = 14900; see also Table 2.4, entries 13 and 18). A series of homopolymers of DEDPM was prepared using **2b** as catalyst in toluene. GPC, visible and yield data can be found in Table 2.2.

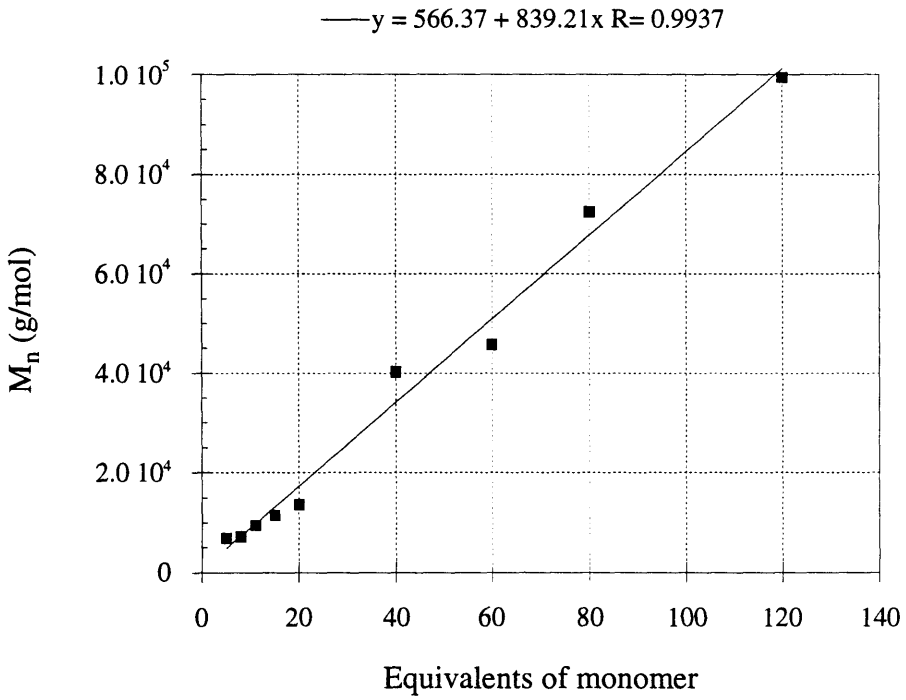

Figure 2.2. Number Average Molecular Weight (M_n) of Poly(DEDPM)$_n$ versus Number of Equivalents of Monomer Added to Initiator **2b** in Toluene.

The plot of M_n as a function of the number of equivalents employed in the polymerization (Figure 2.2) shows good linear dependence in contrast to the data obtained for initiator **1a** (Figure 2.1). The results are consistent with living behavior of the polymerization, although the M_n determined by GPC (on-line viscometry versus a polystyrene universal

calibration curve) were found to deviate from the expected molecular weights (M_{calc}) by a factor of 3 to 4 (Table 2.2). The GPC on-line light scattering setup could not be used due to a permanent change of solvent from THF to methylenechloride. The solvatochromic shift for poly(DEDPM)$_n$ in CH_2Cl_2 versus THF was sufficient to render the molecular weight analysis impossible due to absorption of the polymers at the detector wave length.

A comparably small k_p/k_i value[20] of 12 was determined for the reaction of **2b** with DEDPM. A second series of polymers was prepared using **2b** yielding essentially identical GPC results.

Table 2.3. UV/Vis[a] Data for Poly(DEDPM)$_n$ using **1a** as Initiator in Toluene.

polymer	λ_{max} (nm)	ε_{max} ($M^{-1}cm^{-1}$)[b]
poly(DEDPM)$_3$	506 (480)	3886
poly(DEDPM)$_5$	508 (488)	4397
poly(DEDPM)$_7$	512 (492)	4899
poly(DEDPM)$_9$	516 (497)	5387
poly(DEDPM)$_{11}$	516 (493)	4742
poly(DEDPM)$_{14}$	516 (500)	3871
poly(DEDPM)$_{20}$	522 (498)	5660
poly(DEDPM)$_{30}$	522 (506)	5786
poly(DEDPM)$_{45}$	526 (497)	5930
poly(DEDPM)$_{65}$	528 (507)	5802
poly(DEDPM)$_{90}$	528 (510)	6046
poly(DEDPM)$_{125}$	530 (511)	6143
poly(DEDPM)$_{200}$	534 (510)	5968

[a] In CH_2Cl_2 and THF (in parenthesis). [b] Per conjugated double bond based on GPC data (see Table 2.1).

UV/Vis spectra reveal that the optical absorption maximum (λ_{max}) increases with increasing chain length (Table 2.2). Surprisingly however, these λ_{max} values are lower by 20-30 nm for a given apparent chain length than those for the previously reported cyclopolymers that contain both five- and six-membered rings in the polymer backbone.[15,31] A similar situation was found for polymers prepared by using initiator **1a**. Although much longer chain lengths were determined in this case, the values for λ_{max} do not exceed 534 nm (Table 2.3), consistent with a lower average degree of conjugation in these polymers.

Polymerizations in the Presence of a Base.

The influence of bases in the synthesis of polyenes involving alkylidene initiators has been demonstrated before.[16,17] In particular in systems with a large k_p/k_i ratio polymerization in the presence of a base often leads to improved polymerization behavior.

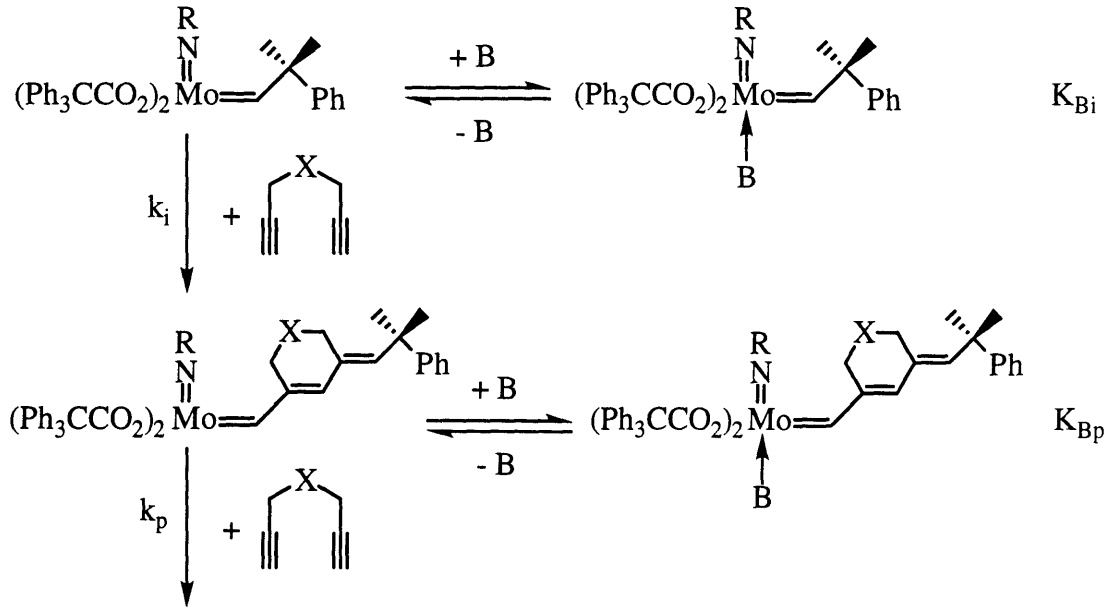

Scheme 2.1. Base-on and Base-off Equilibria for Initiator (K_{Bi}) and Propagating Species (K_{Bp}).

Table 2.4. GPC Data for Poly(DEDPM)$_{20}$ Using **1a**, **1b**, **2a** and **2b** as Initiators in Toluene in the Presence of a Base.

entry	initiator	base	M_n[a]	M_w[a]	M_w/M_n[a]
1	**1a**	-	35160	50360	1.43
2	**1a**	PMe_2Ph	14520	17740	1.22
3	**1a**	pyridine	31140	40320	1.30
4	**1a**	2-picoline	33440	45460	1.36
5	**1a**	3,5-lutidine	28220	35410	1.25
6	**1b**	-	20510	27300	1.33
7	**1b**	PMe_2Ph	22330	23770	1.07[b]
8	**1b**	pyridine	17470	20460	1.17
9	**1b**	3,5-lutidine	15830	18500	1.17
10	**1b**	2 equiv 3,5-lutidine	16770	20080	1.20
11	**1b**	4 equiv 3,5-lutidine	15770	18370	1.16
12	**1b**	10 equiv 3,5-lutidine	14420	17310	1.20
13	**2a**	-	25490	32380	1.27
14	**2a**	PMe_2Ph	19540	24940	1.28
15	**2a**	$PMePh_2$	32670	39900	1.22
16	**2a**	pyridine	26230	31360	1.20
17	**2a**	3,5-lutidine	22960	27620	1.20
18	**2b**	-	14940	17530	1.17
19	**2b**	PMe_2Ph	16220	21030	1.30
20	**2b**	pyridine	15580	18490	1.19
21	**2b**	3,5-lutidine	17060	20300	1.19

[a] Determined by GPC on-line viscometry versus a polystyrene universal calibration curve (Viscotek). [b] Isolated yield was 18 %.

The most straightforward explanation for such improvement of polymerization behavior is that the base interacts stronger with the less crowded propagating species.[16] As a result the rate of propagation is decreased to a larger extent than the rate of initiation. A schematic representation is pictured in Scheme 2.1. The choice of base is crucial since a too strong interaction leads to an impractically slow polymerization system.

A series of polymers was prepared by using initiators **1a**, **1b**, **2a** and **2b** and a variety of bases. One equiv of the respective base was added to the initiator solution before addition of 20 equiv of DEDPM. The dependence on the base concentration was determined by variation of the amount of base added. The GPC data (viscometry versus a polystyrene calibration curve) are summarized in Table 2.4. Isolated yields ranged from 85 to 95% with the exception of entry 8 (18%).

Compared to the base-free polymerizations, considerably smaller molecular weights and narrower polydispersities of the polymers were observed with most of the bases in polymerizations employing **1a**, **1b** and to a lesser extent **2a**. However no improvement could be obtained in polymerizations involving initiator **2b**. 2-picoline did not show any detectable influence on the polymerization using **1a,** as did $PMePh_2$ on the polymerization using **2a**. Both bases simply cannot access the metal center sufficiently. The influence of PMe_2Ph on the polymerization behavior varies with the nature of the initiator. Overall the best results were achieved with pyridine and 3,5-lutidine. Especially with initiator **1b** polymers were obtained with polydispersities and molecular weights that match the values of polymers prepared by using **2b**. Both bases exhibit very similar behavior in the regulation of molecular weights and polymer distributions. The enhanced electron donating ability of 3,5-lutidine compared to pyridine is presumably counterbalanced by increased steric interaction with the ligand sphere. No significant differences in the molecular weights and polydispersities could be observed upon variation of the base concentration within the experimental error.

Molecular Weight Determination by MALDI TOF MS.

The living nature of the cyclopolymerization of DEDPM using initiator **2b** was established earlier in this chapter. The number average molecular weights (M_n) determined by GPC on-line viscometry versus a polystyrene calibration curve were found to be 3 to 4 times higher than expected contradictory to the evidence for living polymerization behavior. The almost constant factor between the determined and the expected molecular weights suggested a possible systematic error in the molecular weight determination. Matrix-Assisted Laser Desorption Ionization (MALDI) time-of-flight (TOF) mass spectrometry, a technique developed in the late 1980s and used for the molecular weight determination of biological macromolecules, has only recently been employed for the characterization of synthetic polymers.[71-73] Soft ionization allows the detection of individual mass signals for the different chains within a polymer distribution without fragmentation. Ideally molecular weights and polymer distributions can be determined from a spectrum.

MALDI TOF mass spectra were obtained from all samples in Table 2.2. The spectrum of sample poly(DEDPM)$_5$ is shown in Figure 2.3. The mass difference between the individual signals is 236 representing the molecular mass of a single monomer unit. We conclude that only single ionization had occurred which could not automatically be assumed considering the high degree of conjugation in the polymer backbone. M_n, M_w and PDI of the polymers up to poly(DEDPM)$_{20}$ were determined using the corresponding formulas (eq 2) and a spread sheet program (Table 2.5). The peak height instead of the peak area was used as a an approximate measure for n_i. The peak widths of the most significant peaks are almost identical keeping the error presumably reasonably small. MALDI TOF MS spectra of the higher molecular weight polymers (poly(DEDPM)$_{40}$ and up) exhibited lower signal to noise ratios and a reliable determination of molecular weights and polydispersities was impossible.

$$M_n = \frac{\sum n_i M_i}{\sum n_i} \qquad M_w = \frac{\sum n_i M_i^2}{\sum n_i M_i} \qquad PDI = \frac{M_w}{M_n} \qquad (2)$$

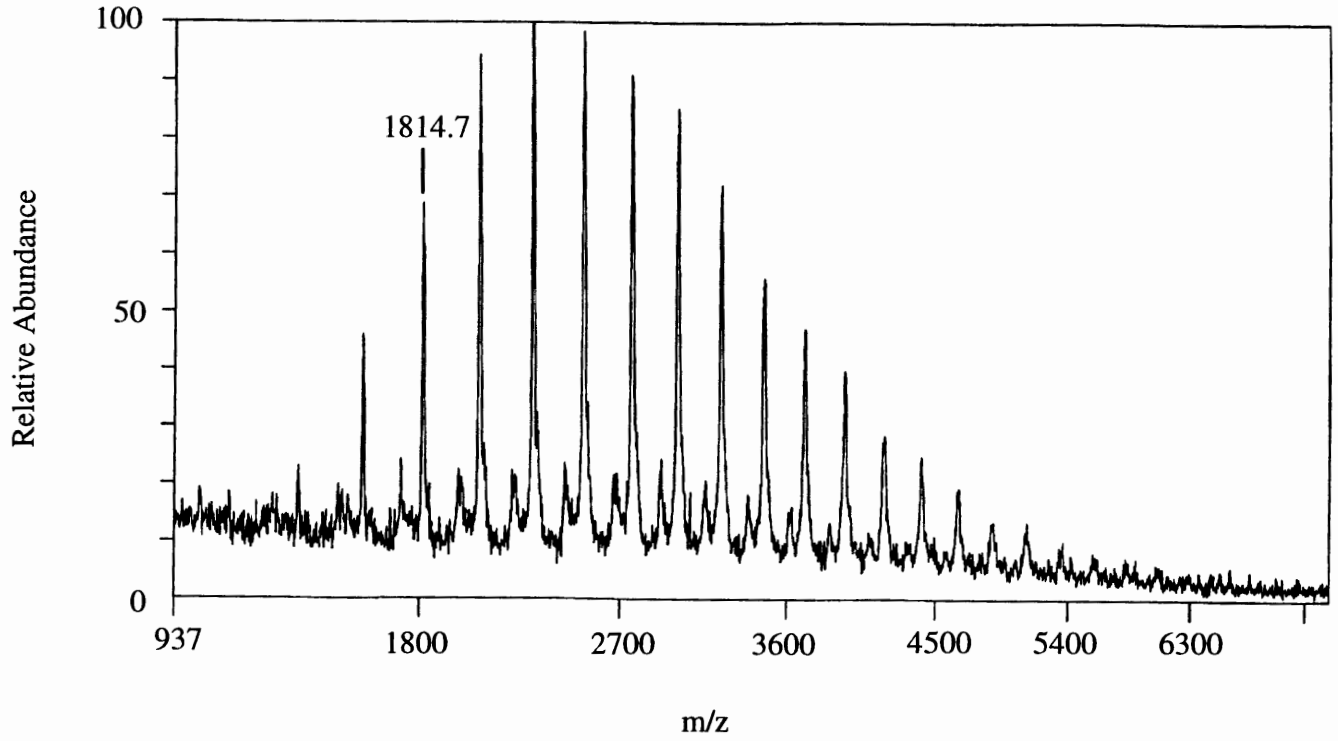

Figure 2.3. MALDI TOF Mass Spectrum of Poly(DEDPM)$_5$.

The molecular weights determined from the MALDI mass spectra were found to be higher than expected in particular for shorter chain length polymers, however much closer to the expected values compared to the GPC data further supporting the living nature of the polymerization. Also slightly smaller polydispersities were calculated from the MALDI mass spectra in comparison to the GPC data. The discrepancy between the expected molecular weights and the number average molecular weights determined by MALDI diminishes towards higher molecular weights consistent with any polymerization with a k_p/k_i value larger than 1. A relatively constant factor ($F_{GPC/MALDI}$ = 2.4; average value from Table 2.5) between the molecular weights determined by GPC and the ones determined by MALDI MS was established. This fact can best be explained by a different solution behavior of these presumably more rigid polymers and the polystyrene standards in the relative molecular weight determination by GPC.

Table 2.5. GPC and MALDI TOF MS Data for Poly(DEDPM)$_n$ Prepared Using **2b** in Toluene.

		GPC		MALDI		
Sample	M_n(theory)	M_n[a]	M_w/M_n[a]	M_n[b]	M_w/M_n[b]	$F_{GPC/MALDI}$[c]
poly(DEDPM)$_5$	1342	6850	1.18	2810	1.09	2.4
poly(DEDPM)$_8$	2050	7110	1.22	3270	1.11	2.2
poly(DEDPM)$_{11}$	2759	9450	1.26	3730	1.14	2.5
poly(DEDPM)$_{15}$	3704	11500	1.26	4960	1.13	2.3
poly(DEDPM)$_{20}$	4886	13590	1.26	5470	1.15	2.5

[a] Determined by GPC on-line viscometry versus a polystyrene universal calibration curve (Viscotek). [b] Determined by MALDI TOF mass spectroscopy. [c] $F_{GPC/MALDI} = M_{n(GPC)}/M_{n(MALDI)}$.

MALDI TOF mass spectra also provide proof about the identity of the polymer endgroups. Each signal corresponds to a polymer with a certain chain length and represents therefore the sum of the masses of a particular number of repeating units and both endgroups. In this case the endgroups are the neopentylidene ligand from initiator **2b** and the benzylidene group from the termination reaction with benzaldehyde. A polymer with seven repeating units serves as an example. Adding the masses of the endgroups and of seven DEDPM molecules gives $M_{n(calc)}$ = 1814.2. A signal at 1814.7 can be found in the MALDI spectrum in Figure 2.3.

The optical data can now be correlated to the real molecular weights. λ_{max} of each polymer is inversely proportional to the number of double bonds in the polymer (Figure 2.4), as reported for the unsubstituted polyene series.[14]

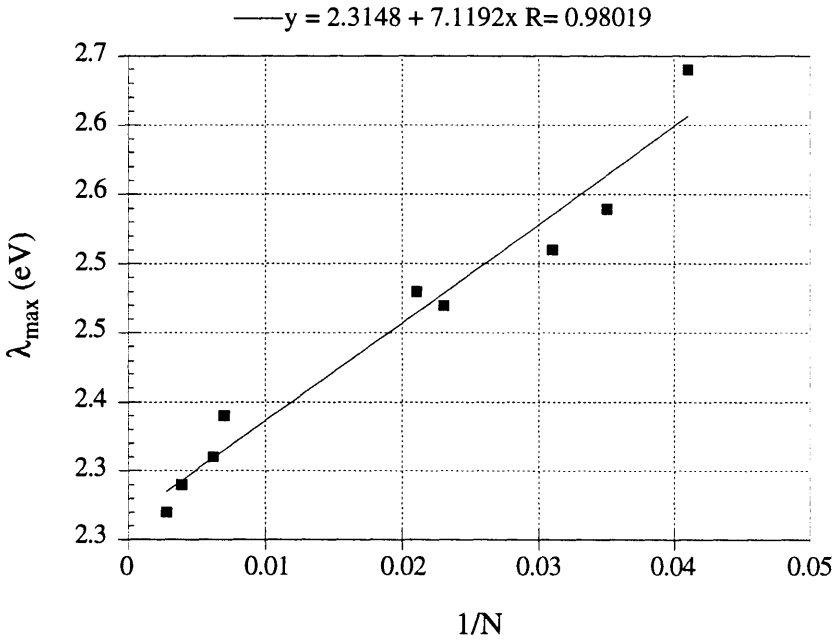

Figure 2.4. Dependence of λ_{max} in CH_2Cl_2 on the Reciprocal of the Number of Double Bonds (N; Based on M_n Determined by MALDI TOF MS) in Poly(DEDPM)$_n$ Prepared Using Initiator **2b**.

Regular Polymer Structure.

The polymers of DEDPM obtained by using the alkylidene bis(triphenylacetate) initiators **1a**, **1b**, **2a** and **2b** exhibit physical properties similar to those prepared using bis(alkoxide) initiators with one significant exception, the average degree of conjugation. Only structural differences can sufficiently explain this fact. The structure of these polymers can be determined by ^{13}C NMR, since the carbonyl carbon and the quaternary carbon are especially sensitive to the ring size. In Figure 2.5a the carbon NMR of the quaternary carbon in the polymers containing a mixture of five- and six-membered rings is shown.[31] Carbon resonances for the quaternary carbon at 57-58 ppm are characteristic of five-membered rings, while resonances at 54 ppm are characteristic of six-membered rings. The large number of resonances is due to the fact that the chemical shift of the resonance is not only sensitive to the ringsize but also depends on the immediate neighbors (e.g. a five-membered ring between a five- and a six-membered ring). In Figure 2.5b the same region in the ^{13}C NMR spectrum for poly(DEDPM)$_n$ is shown prepared using initiator **1a**. No resonances in the 57-58 ppm region indicative of five-membered rings are observed. In the region characteristic of six-membered rings only one major peak at 54.5 ppm is found as expected for a six-membered ring with only six-membered rings as neighbors.

Two resonances in the ^{13}C NMR were reported for the carbonyl carbon in poly(DEDPM)$_n$ containing five- and six-membered rings.[31] A signal at 172.0 ppm is typical for a five-membered ring, at 170.8 ppm for a six-membered ring (see Figure 2.6a).[31] The carbonyl carbon resonance is not sensitive to the local environment. Only one resonance can be detected in the carbon NMR of poly(DEDPM)$_n$ prepared using **1a** at 170.7 ppm (Figure 2.6b) characteristic for six-membered rings consistent with the findings for the quaternary carbon resonance. Four resonances between 131.7 and 134.3 ppm for the four sp^2 carbons and two resonances for the ring CH_2 groups make a complete assignment of resonances possible (Figure 2.6b) in contrast to the complicated carbon

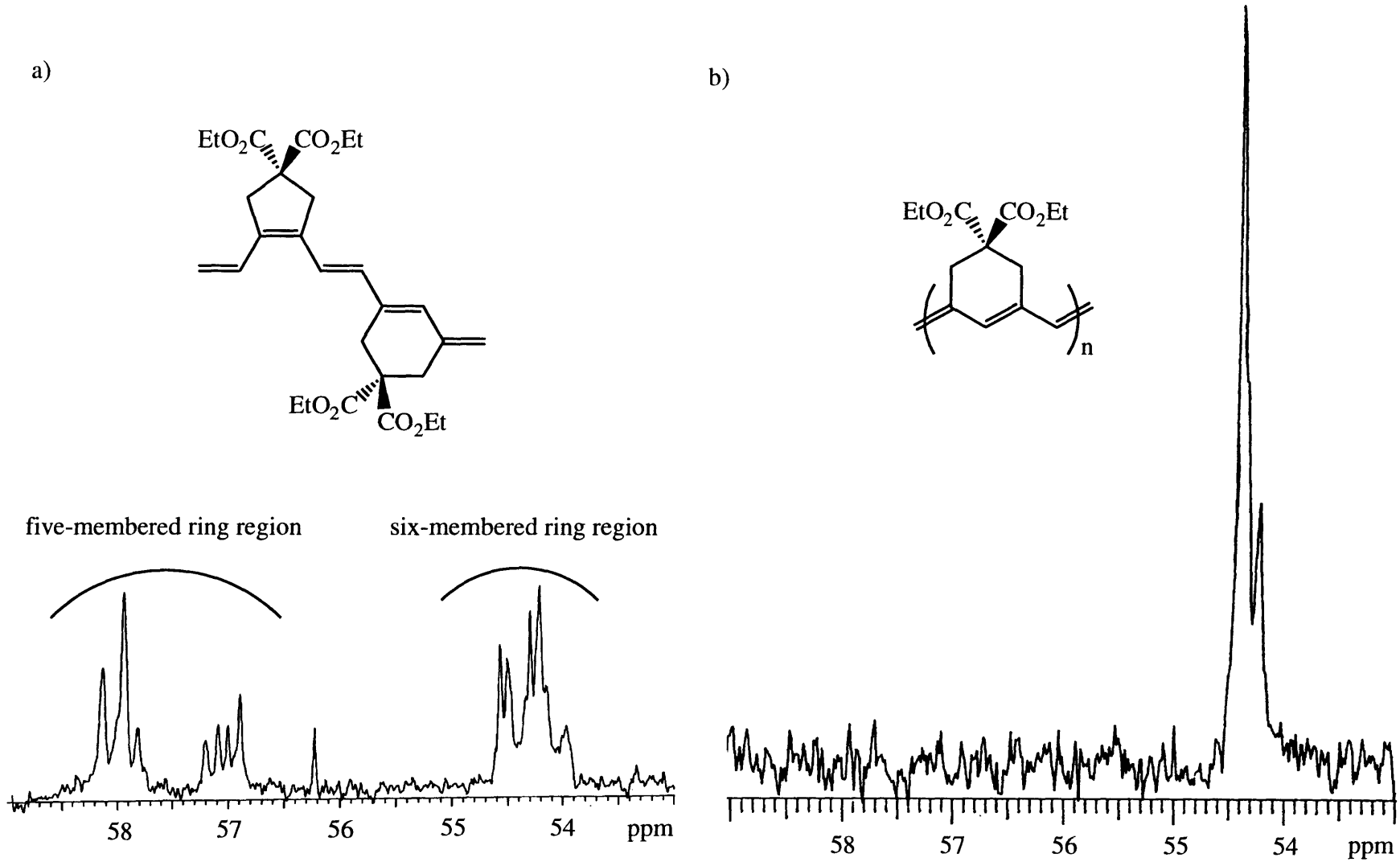

Figure 2.5. ^{13}C NMR Spectra of the Quaternary Carbons in Poly(DEDPM)$_n$ Prepared Using (a) Mo(N-2,6-*i*-$Pr_2C_6H_3$)($CHCMe_2Ph$) [$OC(CF_3)_2CF_2CF_2CF_3]_2$ and (b) **1a**.

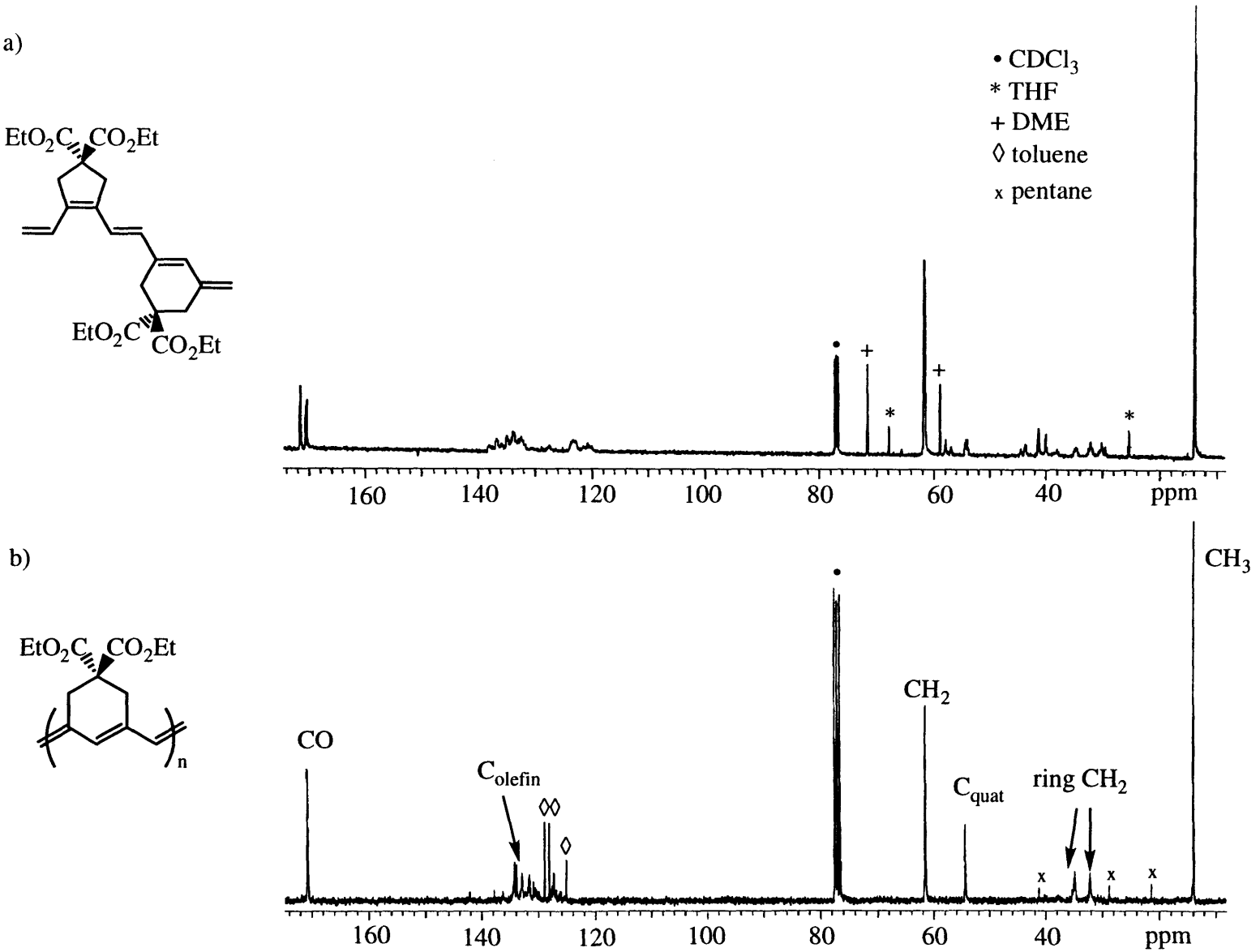

Figure 2.6. ^{13}C NMR Spectra of Poly(DEDPM)$_n$ Prepared Using (a) Mo(N-2,6-*i*-$Pr_2C_6H_3$)(CHCMe$_2$Ph)[OC(CF$_3$)$_2$CF$_2$CF$_2$CF$_3$]$_2$ and (b) **1a**.

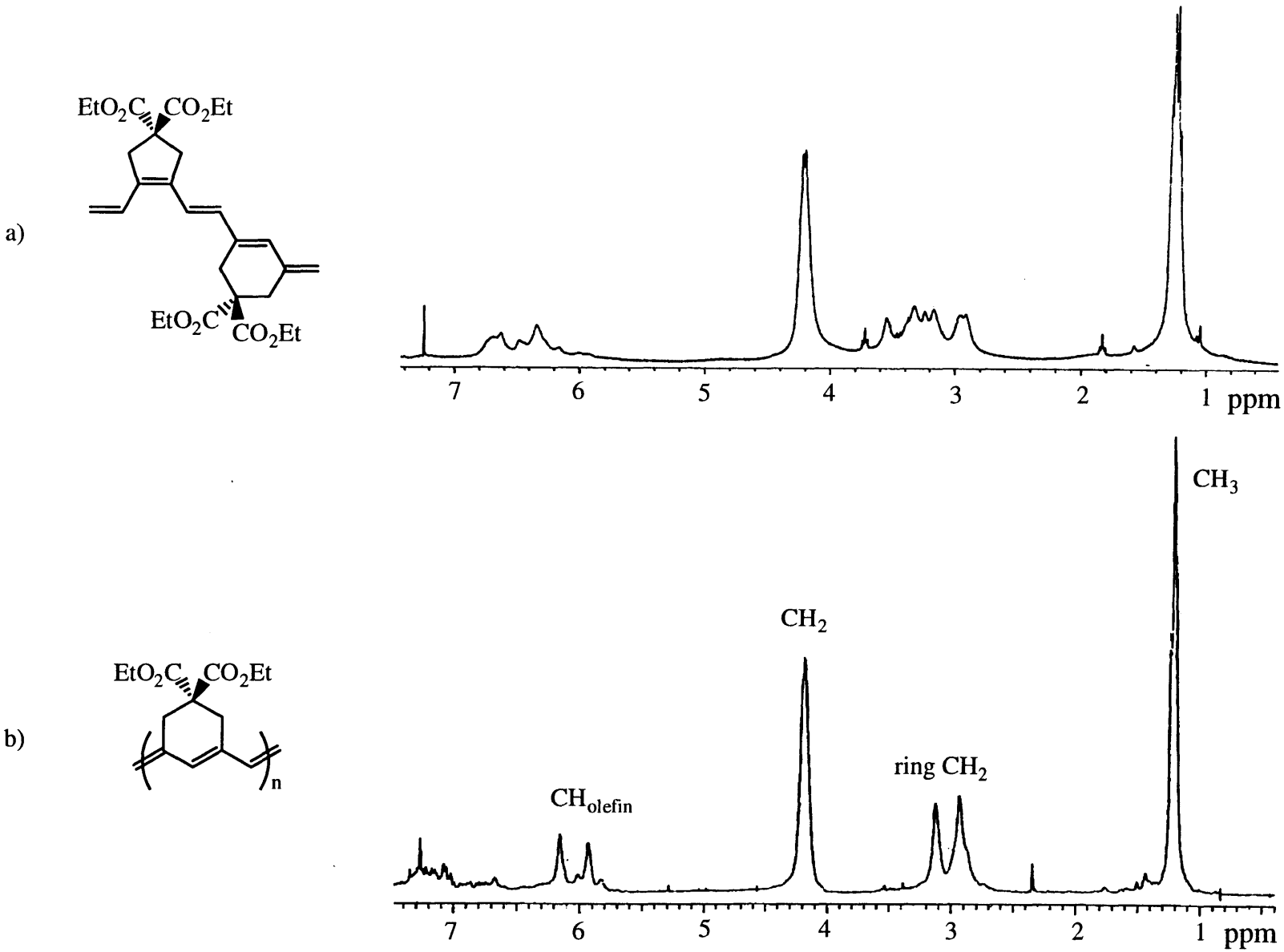

Figure 2.7. ^{1}H NMR Spectra of Poly(DEDPM)$_n$ Prepared Using (a) Mo(N-2,6-*i*-$Pr_2C_6H_3$)($CHCMe_2Ph$)[$OC(CF_3)_2CF_2CF_2CF_3$]$_2$ and (b) **1a**.

NMR for poly(DEDPM)$_n$ containing a mixture of five- and six-membered rings. Two different resonances are observed for the ring CH_2 carbons as a result of the asymmetry of the six-membered ring.

It is important to note that all the initiators containing the triphenylacetate ligand (**1a**, **1b**, **2a** and **2b**) exhibit the same selectivity towards the exclusive formation of six-membered rings. Also no dependence of the regioregularity of the polymers on the solvent was observed. Polymerizations in toluene, DME, THF and CH_2Cl_2 all gave polymers only containing six-membered rings. ^{13}C labelling of the quaternary carbon of DEDPM allowed to more precisely quantify the relative contents of five- and six-membered rings (97.8% six-membered rings in poly(DEDPM)$_n$ prepared using initiator **2b**).

The ^1H NMR spectrum of poly(DEDPM)$_{80}$ prepared using Mo(N-2,6-*i*-Pr_2-C_6H_3)(CHCMe$_3$)[OC(CF$_3$)$_2$Me]$_2$ exhibits only broad resonances and contains only very little information (Figure 2.7a). The proton NMR spectra of the polymers containing only six-membered rings in contrast are relatively simple and can be assigned completely (Figure 2.7b). Two signals at 6 ppm for the olefinic protons on the ring and on the bridging sp^2 carbons, the peaks for the ethyl ester substituents (4.2 and 1.2 ppm) and two resonances at 3 ppm for the ring CH_2 groups can be identified. The cis/trans configuration of the exocyclic double bond or the s-cis/s-trans configuration of the backbone single bond cannot be determined. However the minor peak at 54.2 ppm in the carbon NMR (Figure 2.5.b) can best be explained by cis/trans isomerism of the exocyclic double bond since no coalescense of the two resonances was observed at temperatures up to 120 °C. Two possible idealized planar conformational isomers (**A** and **B**; R = CO_2Et) are drawn below.

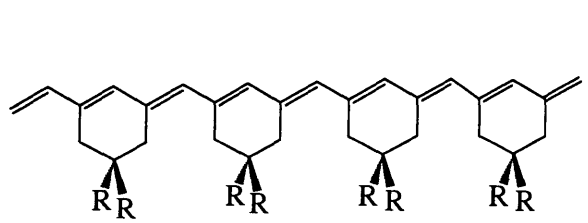

A

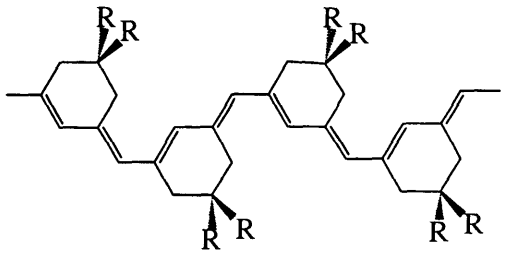

B

The reduced degree of conjugation of the regular polymers in comparison to the polymers containing five- and six-membered rings in the backbone can best be explained by stronger steric interactions between the repeating units forcing them out of the plane of conjugation. No evidence for a possible break of conjugation due to a 1,3-tautomeric shift within the six-membered ring could be found. Such a tautomeric shift would change the chemical shift of the quaternary carbon drastically since one adjacent CH_2-sp^3 carbon would be replaced by a CH-sp^2 carbon at C_{quat}. Additionally this break of conjugation has to occur at least in about 5% of the rings in order to affect the average conjugation length noticeably. In the ^{13}C labelled carbon NMR spectrum only the resonances for the five- (58.0 ppm) and six-membered (54.5 ppm) rings were observed.

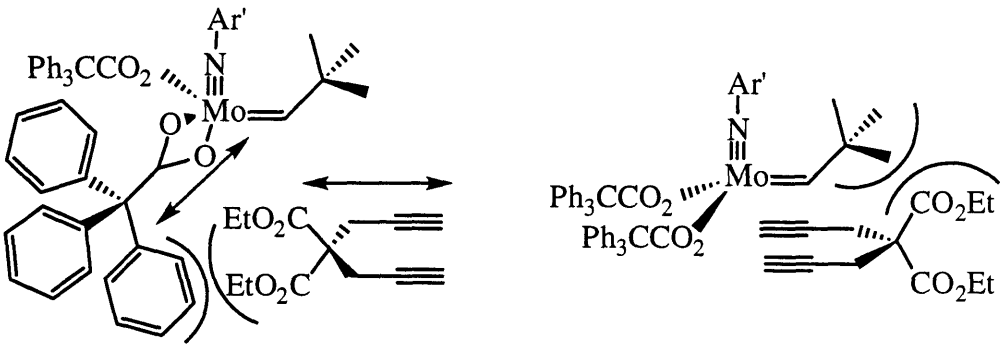

α addition β addition

Figure 2.8. Schematic Representation of the Bulk of Steric Interaction in α and β Addition. Severe Interactions Between the Ligand Sphere and the Substituents on C_{quat} of DEDPM during α Addition.

The mechanism of polymerization presumably consists of addition of the first triple bond to an alkylidene to give exclusively a β-substituted metallacyclobutene intermediate which upon intramolecular cyclization forms the six-membered ring structure. But why are these bis(triphenylacetate) initiators so selective towards the formation of six-membered rings? Steric interaction during the addition of the first triple bond and formation of the metallacyclobutene ring offers the most plausible explanation. In α addition the monomer

sterically interacts mainly with the ligand sphere of the metal center, while in β addition mainly with the substituent on the alkylidene carbon C_α (Figure 2.8). A sterically demanding ligand sphere, as provided by the bulky triphenylacetate ligands, is more likely to enforce β addition than α addition, but steric bulk of the ancillary ligands alone does not make a catalyst selective. Some of the bis(alkoxide) catalysts also contain a sterically demanding ligand sphere, but show no selectivity towards the formation of six-membered rings. Also loss of selectivity is observed employing the sterically demanding bis(carboxylato) complex $Mo(N\text{-}2\text{-}t\text{-}Bu\text{-}C_6H_4)(CHCMe_2Ph)(O_2CSi(SiMe_3)_3)_2$. Surprisingly a slight tendency towards the formation of five-membered rings was found in this case (62:38; five- to six-membered rings).

The distance of the steric bulk from the metal center is crucial to enforce most effective interaction between the ligand sphere and the substituents on C_{quat} in DEDPM during the metallacyclobutene formation step. The X-ray structure of **2b** (Chapter 1, Figure 1.1 and Figure 1.2) shows that all *ortho* carbons of the triphenylacetate ligands are positioned 4.5 to 6 Å remote from the metal center. This range approximately corresponds to the range of expected distances between the terminal sp-carbon and atoms of the substituents on C_{quat} in DEDPM. The triphenylacetate ligands can be viewed as umbrellas providing severe interactions with the substituents on the monomer upon coordination during α addition. As a result α addition is simply sterically untenable.

Variation of Monomer.

The argument for the selectivity towards the formation of six-membered rings was based on steric grounds. Variation of monomers, in particular with emphasis on different steric environments, should provide more evidence on this matter. Three sterically different groups of monomers (Scheme 2.2) were investigated in the bulk polymerization using the bis(triphenylacetate) initiator **2b**. All compounds of type **I** can be synthesized in

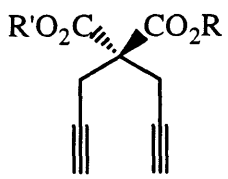

I

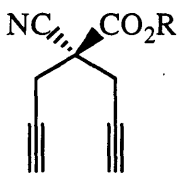

II

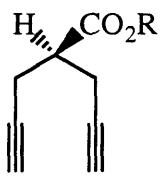

III

DMDPM	R = Me;	R' = Me	DPMCA	R = Me		DPEA	R = Et
DEDPM	R = Et;	R' = Et	DPBCA	R = *t*-Bu		DPNpA	R = Np
BEDPM	R = Et;	R' = *t*-Bu				DPBA	R = *t*-Bu
DBDPM	R = *t*-Bu;	R' = *t*-Bu					

Scheme 2.2. List of All Monomers Used in this Chapter.

one simple step from the corresponding malonic acid diester. Similarly double deprotonation of the cyano acetate derivative with sodium hydride and treatment with two equiv of propargylbromide yields monomers of type **II** in good yield as crystalline solids (DPMCA was reported to be an oil; we isolated the pure material as crystals). The compounds of group **III** can be obtained as colorless oils in one step from the acidchloride[74] as pictured in eq 3.

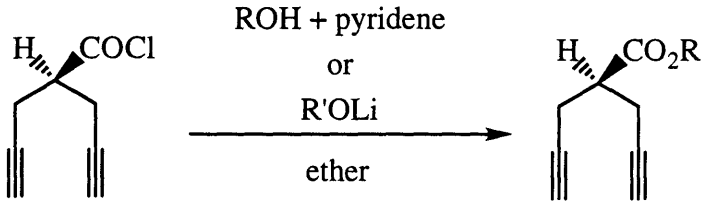

(3)

R = neopentyl
R' = *t*-butyl

All malonate based monomers (type **I**) are cyclopolymerized in toluene by initiator **2b** in very good isolated yields (>90%). The relative content of five- and six-membered rings was determined by ^{13}C NMR and the results are listed in Table 2.6.

Table 2.6. Relative Portions of Five- and Six-membered Rings in Cyclopolymers Prepared Using Initiator **2b** in Toluene.[a]

	CO-region[b]		$C_{quaternary}$[c]	
sample	5-rings	6-rings	5-rings	6-rings
poly(DMDPM)$_{30}$	9	91	d	d
poly(DEDPM)$_{30}$	1.2	98.8	2.2[e]	97.8[e]
poly(BEDPM)$_{30}$	3.3	96.7	2.2	97.8
poly(DBDPM)$_{30}$	4.2	95.8	3.3	96.7

[a] All spectra were obtained at 25 °C in $CDCl_3$ at 125 MHz. [b] Resonances in the carbonyl region of 165-172 ppm were used. [c] Signals of the quaternary carbon in the region of 40-60 ppm were used. [d] Not determinable. [e] ^{13}C labelled quaternary carbon.

DMDPM exhibited less selectivity than the monomers with bigger substituents. DMDPM is probably already too small and the steric interactions that determine the energy difference of the transition states of the two addition modes are diminished resulting in reduced selectivity. A slight decrease in selectivity compared to DEDPM in decending order is also observed in poly(BEDPM)$_n$ and poly(DBDPM)$_n$ consistent with findings by H. H. Fox.[31] Presumably large ester groups thermodynamically favor five-membered rings. Poly(BEDPM)$_n$ containing only six-membered rings in the polymer backbone represents an interesting type of polymer since it possesses asymmetric carbons in the polymer backbone. The quaternary carbon has four different substituents due to the asymmetry of the six-membered ring. If all the asymmetric carbons have the same

configuration, the polymer is intrinsically chiral. Polymerization of a prochiral monomer such as BEDPM with a chiral catalyst or with the use of a chiral auxillary could potentially give intrinsically chiral polymers. These considerations were further incentive to explore the regioselective polymerization of prochiral monomers of type **II** and **III**.

The homopolymerization of dipropargyl cyanoacetates (type **II**) and dipropargyl acetates (type **III**) using **2b** was investigated. Toluene was used as the solvent for all polymerizations except for the preparation of poly(DPMCA)$_{30}$. In this case CH_2Cl_2 was used as solvent since the polymer precipitated from toluene during the reaction. The asymmetry of C_{quat} implied some difficulty in the determination of five- and six-membered rings since extra resonances had to be expected due to tacticity. The preparation of a model polymer provided the solution. Diethylmalonate derivatives are known to undergo decarboxoethylation under appropriate conditions.[75] This reaction applied on poly(DEDPM)$_n$ containing only six-membered rings should yield an atactic polymer also containing only six-membered rings. The ^{13}C NMR spectrum of the obtained polymer served as the reference to determine the content of five- and six-membered rings in polymers of type **III** monomers. For these polymers the carbonyl carbon is a better reference than the quaternary carbon, since no other resonances interfere in this region. The all six-membered ring polymer shows only one peak at 174.5 ppm. Comparison with the carbon NMR spectra of poly(DPEA)$_n$ indicates that a resonance at 175.5 ppm corresponds to five-membered ring structures. The contents of five- and six-membered rings for polymers prepared by reacting **2b** with monomers of type **II** and **III** are listed in Table 2.7.

The results in Table 2.7 indicate that the selectivity is significantly reduced by replacing an ester with a smaller cyano group on the monomer. Selectivity towards formation of six-membered rings is almost completely lost in the polymerization of the less substituted group **III** monomers. Presumably the monomer can now add in an α addition

Table 2.7. Relative Portions of Five- and Six-membered Rings in Cyclopolymers Prepared Using Initiator **2b**.[a]

	CO-region[b]		$C_{quaternary}$[c]	
sample	5-rings	6-rings	5-rings	6-rings
poly(DPEA)$_n$	31	69	31	69
poly(DPNpA)$_n$	37	63	d	d
poly(DPBA)$_n$	37	63	d	d
poly(DPMCA)$_n$	13	87	d	d
poly(DPBCA)$_n$	17	83	d	d

[a] All spectra were obtained at 25 °C in $CDCl_3$ at 125 MHz. [b] Resonances in the carbonyl region of 165-172 ppm were used. [c] Signals of the quaternary carbon in the region of 40-60 ppm were used. [d] Not determinable.

mode with a small proton pointing towards the ligand sphere instead of a large ester group. These findings strongly support the steric argument established earlier in this chapter for the selectivity towards the formation of six-membered rings in cyclopolymerizations involving the bis(triphenylacetate) initiators.

Water Soluble, Conjugated Polymers.

Water soluble, highly conjugated polymers are desirable materials in view of the abundance and versatility of water as solvent. Poly(DEDPM)$_n$ containing a mixture of five- and six-membered rings reacts with 2 equiv of NaOH to afford highly conjugated, completely water-soluble polymers. However no further characterization of these polymers was reported. Water soluble polymers prepared from all six-membered ring poly(DEDPM)$_n$ could exhibit interesting properties and their structure determination was expected to be greatly facilitated.

Reaction under reflux of a solution of regioregular poly(DEDPM)$_n$ in THF with two equiv of KOH per repeating unit under dinitrogen precipitates the hydrolyzed polymer in quantitative yield as shown in eq 4. The polymers were found to be soluble only in water to form intensely colored, purple solutions.

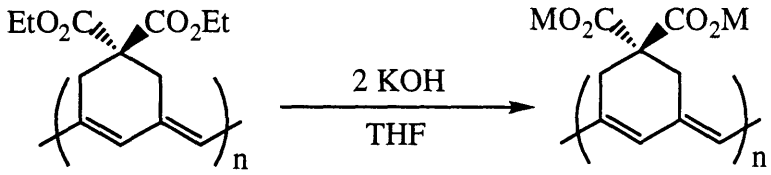

(4)

^{1}H and ^{13}C NMR spectra in D_2O are consistent with the depicted structure. No evidence for ethyl groups could be found. Traces of THF could not completely be removed under vacuum. The polymers are stable in degassed water, but decolorize in the presence of oxygen.

The *tert*-butyl group in *t*-butylethylmalonate can selectively be cleaved off with acid, and the ethyl group with base. Several attempts to selectively remove the *t*-butyl group with trifluoroacetic acid, the most common reagent for this reaction, lead to decomposition of the polymer. However with one equivalent of KOH or NaOH, analogous to the reaction described above, the ethyl group can selectively be cleaved off (eq 5). The polymer is still water soluble, but to a lesser extent than the polymer with higher metal content (eq 4).

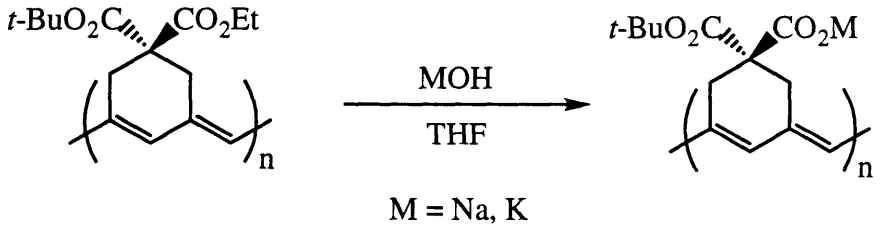

(5)

^1H and ^{13}C NMR spectra exhibit only resonances for the *t*-butyl group, but not for the ethyl substituent and suggest a regular structure of the polymer backbone. Again instability towards air was observed.

Nonlinear Optical Properties.

Polyenes and their oligomers are very important candidates for the study of nonlinear optics since these materials possess large third-order nonlinearities and serve as excellent model conjugated systems. When light interacts with a bulk material it induces a polarization (P) according to eq 6.[76] The first term represents the linear portion of the

$$P = \chi^{(1)} E + \chi^{(2)} E^2 + \chi^{(3)} E^3 + ... \quad (6)$$

response with the linear susceptibility $\chi^{(1)}$ related to the refraction of the material. Macroscopic polar asymmetry is the requirement for second order response ($\chi^{(2)}$). Third-order nonlinear optical effects arise universally and have no special requirements on structural symmetry. However $\chi^{(3)}$ is often unmeasurable small. On a molecular level γ represents the molecular third-order hyperpolarizabilty. For small numbers of double bonds (N), a power-law dependence $\gamma = kN^{\alpha}$ is found to approximate the theoretical results in all models (α between 3 and 6). For large N a linear dependence of γ on N is found.

A study of γ was performed on the series of homopolymers of DEDPM prepared using **1a** (see Table 2.1 and Table 2.3) in collaboration with Dr. Ifor D. W. Samuel at the Centre National d'Etudes des Telecommunications (Table 2.8). γ was measured in solution (THF) by third harmonic generation (THG) at 1.9 μm. The graph of γ as a function of N (Figure 2.9) suggests that γ is proportional to N (the graph of γ versus N does not pass exactly through the origin, but the difference is within the experimental error).

Table 2.8. Nonlinear Optical Data for Poly(DEDPM)$_n$ Using **1a** as Initiator in Toluene.

polymer	N[a]	γ (10^{-34} esu)[b]	γ/N
poly(DEDPM)$_3$	136.6	326.8	2.393
poly(DEDPM)$_5$	116.9	235.2	2.013
poly(DEDPM)$_7$	162.1	249.3	1.538
poly(DEDPM)$_9$	154.3	438.8	2.844
poly(DEDPM)$_{11}$	175.9	355.1	2.018
poly(DEDPM)$_{14}$	206.6	443.5	2.147
poly(DEDPM)$_{20}$	362.6	955.7	2.636
poly(DEDPM)$_{30}$	548.9	1650.9	3.008
poly(DEDPM)$_{45}$	489.0	1234.3	2.524
poly(DEDPM)$_{65}$	877.5	2771.8	3.159
poly(DEDPM)$_{90}$	925.8	2245.0	2.425
poly(DEDPM)$_{125}$	1036.6	3423.7	3.303
poly(DEDPM)$_{200}$	1187.3	3758.3	3.165

[a] Number of double bonds based on M_n determined by GPC (Table 2.1). [b] Determined by THG at 1.9 μm in THF.

These results are consistent with data reported for the homopolymers of DEDPM containig a mixture of five- and six-membered rings for polymers with larger chain length.[77] There is, however, a very important difference between the two series of polymers: the values of γ/N in the series of the all six-membered ring polymers are less than one fifth of the values reported for the polymers with a mixture of five- and six-membered rings. This finding can best be explained by a reduced extent of electron delocalization as suspected based on the UV/Vis absorption spectra. Possibly the

crossover from short chain behavior ($\gamma = kN^{\alpha}$) to long-chain saturation ($\gamma \approx N$) occurs at a different chain length for the polymers with a regular structure.

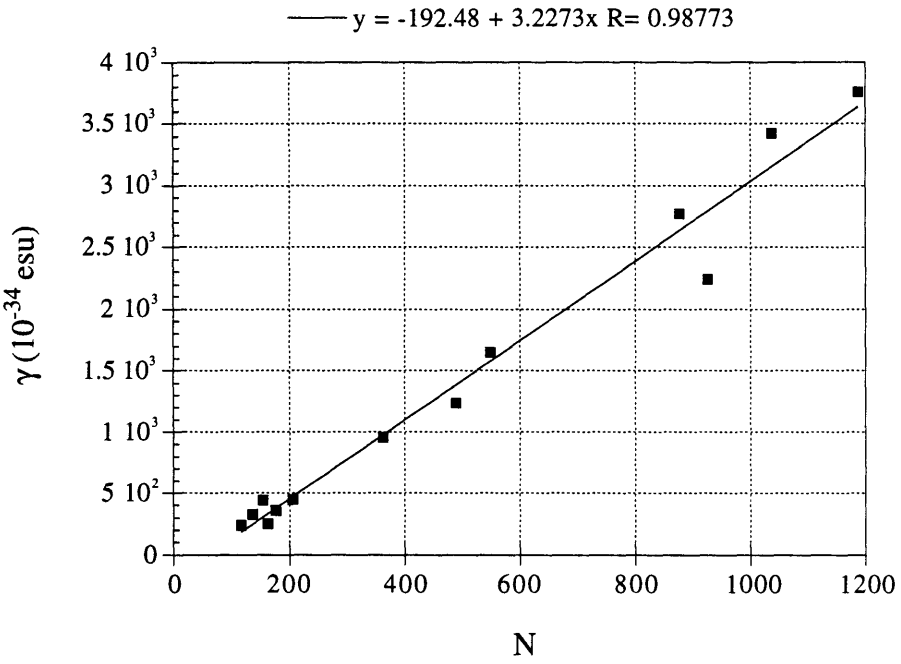

Figure 2.9. Plot Showing the Third-order Hyperpolarizability γ versus the Average Number of Double Bonds in Poly(DEDPM)$_n$ Prepared Using **1a** in Toluene.

CONCLUSIONS

The cyclopolymerization of diethyldipropargylmalonate was investigated using the molybdenum(VI) alkylidene initiators containing bulky carboxylate ligands introduced in Chapter 1. The living nature of the polymerization employing Mo(N-2-*t*-Bu-C_6H_4)(CHCMe$_3$)(O_2CCPh$_3$)$_2$ was established by the synthesis of series of polyenes with low polydispersities. Polymerizations involving adamantylimido complexes suffer from a large ratio of the rate of propagation to the rate of initiation and cannot considered to be strictly living. However improvements in the regulation of molecular weights and polymer distributions can be achived in those cases by polymerization in the presence of a base.

MALDI TOF MS was introduced as an absolut method for the molecular weight determination of conjugated polymers. The results not only revealed a systematic error of the molecular weight determination by GPC with an on-line viscometer, but also proved the identity of the polymer endgroups.

Poly(DEDPM)$_n$ prepared using bis(triphenylacetate) initiators exhibited reduced average conjugation compared to poly(DEDPM)$_n$ containing five- and six-membered rings in the polymer backbone. ^{13}C NMR analysis revealed a regular polymer structure containing only six-membered rings. The bulky triphenylacetate ligands encourage regioselective addition of the first triple bond to give exclusively (>98%) a β-substituted metallacyclobutene intermediate. The partial loss of selectivity upon polymerization of less substituted heptadiyne derivatives substantiates an explanation of the "β selectivity" on steric grounds. The cyclopolymerization of DEDPM employing Mo(N-2-*t*-Bu-C_6H_4)(CHCMe$_3$)(O_2CCPh$_3$)$_2$ represents a rare example of full control over chain length, endgroups and regularity of structure by living, regioselective polymerization in the field of conjugated polymers.

EXPERIMENTAL

General details. All experiments were performed under a nitrogen atmosphere in a Vacuum Atmospheres dry box or by standard Schlenk techniques under an argon atmosphere unless specified otherwise. Celite and alumina were dried at ~130 °C for at least a week. Pentane was washed with sulfuric/nitric acid (95/5 v/v), sodium bicarbonate and water, stored over calcium chloride, and distilled from sodium benzophenone ketyl under nitrogen. Reagent grade diethyl ether, tetrahydrofuran, toluene, benzene and 1,2-dimethoxyethane were distilled from sodium benzophenone ketyl under nitrogen. Reagent grade dichloromethane was distilled from calcium hydride under nitrogen. Toluene, THF CH_2Cl_2 and DME used for polymerizations were stored over 4Å molecular sieves.

Benzene-d_6 and dichloromethane-d_2 were sparged with argon and stored over 4Å molecular sieves. Benzaldehyde was distilled and passed through alumina prior to use.

Two different GPC setups were employed for polymer samples presented in this Chapter. The GPC on-line light scattering setup consisted of two Jordi-Gel DVB Mixed Bed columns in series, a Wyatt Mini Dawn light scattering detector (Wyatt Technology) and a Knauer Refractometer using samples 0.5-0.6% w/v in THF, which were filtered through a Millex-SR 0.5 μm filter in order to remove particulates. The GPC data were analyzed using Astrette 1.2 (Wyatt Technology). The GPC on-line viscometry setup consisted of two Jordi-Gel DVB Mixed Bed columns in series and a Viscotek Differential Refractometer/Viscometer H-500 using samples 0.1-0.2% w/v in THF, which were filtered through a Millex-SR 0.5 μm filter. GPC columns were calibrated versus polystyrene standards (Polymer Laboratories Ltd.) which ranged from 1206 to 1.03x106 MW. The GPC data were analyzed using Unical 4.03 (Viscothek). UV/Vis spectra were obtained using a Hewlett Packard 8452 A Diode Array Spectrometer.

NMR data were obtained either at 300 MHz (^{1}H) and 75.43 MHz (^{13}C) on a Varian XL 300 NMR spectrometer or a Varian Unity 300 NMR spectrometer or at 500 MHz (^{1}H) and 125 MHz (^{13}C) on a Varian 500 NMR spectrometer and are listed in parts per million downfield from tetramethylsilane for proton and carbon. Spectra were obtained at room temperature unless noted otherwise.

All chemicals used were reagent grade (Aldrich) and used without further purification unless noted otherwise. Diethyldipropargylmalonate,[40] dipropargyldi-*tert*-butylmalonate,[31] dimethyldipropargylmalonate,[78] dipropargylcyanomethylacetate[79] and dipropargylacetylcloride[75] were prepared as reported in the literature.

Polymerization of DEDPM. In a representative polymerization stock solutions of DEDPM (0.406 M) and **1a** (0.00676 M) in toluene that had been distilled over sodium benzophenone ketyl, stored over molecular sieves (4 Å) and passed through alumina, were prepared. To 3007 μl of the catalyst stock solution 3 mL of toluene was added. 1000 μl of

the monomer stock solution were squirted in. Within 30 s the reaction mixture turned deep red. After 6 h 16 µl of benzaldehyde were added. After stirring for 3 more hours the solution was concentrated in vacuo to about 1.5 mL. The polymer was precipitated in 60 mL of pentane, collected on a frit and dried in vacuo yielding a red, powderous material (90 mg, 91%). All operations were carried out under dinitrogen and the polymers were only briefly exposed to air for the sample preparation for the GPC analysis. Samples for MALDI TOF mass spectroscopy were submitted as a 10^{-7} molar solution (based on the M_n determined by GPC) in acetone under dinitrogen. ^{1}H NMR ($CDCl_3$) δ 6.2 (br, 1H, =CH), 5.9 (br, 1H, =CH), 4.2 (m, 4H, CH_2CH_3), 3.2 (br, 2H, $CH_{2(ring)}$), 2.9 (br, 2H, $CH_{2(ring)}$), 1.2 (t, 4H, CH_2CH_3). ^{13}C NMR ($CDCl_3$) δ 170.7 (CO_2Et), 134.3, 133.9, 132.9, 131.7 (sp^2-C), 61.5 (CH_2CH_3), 54.5 (C_{quat}), 35.0, 32.2 ($CH_{2(ring)}$), 14.0 (CH_2CH_3). Minor additional resonances for the polymer backbone protons and carbons as well as the ring CH_2 groups can be detected in the ^{1}H and ^{13}C NMR spectra. We attribute these to cis/trans isomerism at the exocyclic double bond.

Polymerization of other heptadiyne monomers. All polymerizations were carried out in a manner similar to the polymerization of DEDPM in toluene with the exception of the polymerization of DPMCA, which was carried out in CH_2Cl_2 due to the insolubility of poly(DPMCA)$_n$ in toluene.

Polymerization of DEDPM in the presence of a base. In a representative series of polymerizations employing one initiator and several bases, stock solutions of DEDPM (0.254 M) and **2a** (0.0126 M) were prepared. All reactions involving the same initiator were run at the same time to assure identical conditions and one reaction with each catalyst was carried out in the absence of a base. To 1 mL of the catalyst stock solution 5 mL of toluene and subsequently one equivalent of the base were added. After stirring for 2 min 1 mL of the monomer solution was squirted in. Depending on the nature of the base the solution eventually turned deep red. After 20 h 12 µl of benzaldehyde were added. After stirring for one more hour the solutions were concentrated *in vacuo* to about 1.5 mL.

The polymer was precipitated in 60 mL of pentane, collected on a fritt and dried in vacuo yielding a red, fluffy material (55 to 65 mg, 82 to 96%). All operations were carried out under dinitrogen and the polymers were only briefly exposed to air for the sample preparation for the GPC analysis.

***tert*-Butylethyldipropargylmalonate (BEDPM).** *t*-Butylethylmalonate (5.0 g, 26.6 mmol) was added to a suspension of NaH (1.4 g, 58.4 mmol) in THF under ice cooling. The reaction mixture was allowed to warm up to room temperature and after the gas evolution had stopped, propargyl bromide (6.95 g, 58.4 mmol; 80% wt solution in toluene) was added at 0 °C. After the reaction mixture was stirred overnight, 100 mL of water and 100 mL of ether were added. The organic layer was separated and the water phase was washed two times with more ether. The combined organic extracts were dried over magnesium sulfate, all volatiles were removed and the resulting off-white solid was recrystallized from pentane to give white needles (4.8 g, 18.2 mmol, 68%). ^{1}H NMR ($CDCl_3$) δ 4.22 (q, 2H, C*H*$_2$CH$_3$), 2.92 (d, 4H, C*H*$_2$CCH), 2.01 (t, 2H, CCH), 1.44 (s, 9H, CMe$_3$), 1.25 (t, 3H, CH$_2$C*H*$_3$); ^{13}C NMR ($CDCl_3$) δ 168.9 (*C*O$_2$CCH$_2$CH$_3$), 167.5 (*C*O$_2$Me$_3$), 82.6 (*C*Me$_3$), 78.8 (CH$_2$*C*CH), 71.4 (CH$_2$C*C*H), 61.7 (O*C*H$_2$CH$_3$), 56.7 (C$_{quat}$), 27.7 (C*Me*$_3$), 22.5 (*C*H$_2$CCH), 14.0 (CH$_2$*C*H$_3$). Anal. Calcd. for $C_{15}H_{20}O_4$: C, 68.16; H, 7.63; N, 0. Found: C, 68.13; H, 7.79 N, -0.06.

2,2-Dipropargylneopentylacetate (DPNpA). A solution of dipropargyl acetylchloride (2.0 g, 12.94 mmol) in 15 mL diethyl ether was added at room temperature to a solution of neopentanol (1.14 g, 12.94 mmol) and pyridine (1.02 g, 12.94 mmol) in 40 mL of ether. A white precipitate formed immediately and the reaction mixture was stirred for 22 h. The precipitate was filtered off, the volatiles were removed in vacuo and the remaining oil was distilled at 115 °C at reduced pressure (10 Torr) yielding a clear oil (1.5 g, 7.3 mmol, 57%). ^{1}H NMR ($CDCl_3$) δ 3.80 (s, 2H, OCH$_2$), 2.77 (p, 1H, CHCO$_2$), 2.64 (m, 4H, CH$_2$CCH), 1.98 (t, 2H, CCH), 0.92 (s, 9H, CH$_3$); ^{13}C NMR ($CDCl_3$) δ 172.3 (CO$_2$), 80.5 (CH$_2$*C*CH), 74.3 (OCH$_2$), 70.5 (C*C*H), 43.2 (*C*HCO$_2$),

31.3 (CCH_3), 26.4 (CH_3), 19.9 (CH_2). MS (EI) m/e 206 (M^+). Anal. Calcd. for $C_{13}H_{18}O_2$: C, 75.69; H, 8.80; N, 0. Found: C, 75.30; H, 8.91 N, -0.02.

2,2-Dipropargyl-*tert*-butylacetate (DPBA). A solution of *t*-butyl alcohol (960 mg, 12.94 mmol) in 5 mL of THF was added to a suspension of NaH (311 mg, 12.94 mmol) in 15 mL THF at room temperature. The reaction mixture cleared up after stirring for 7 h and dipropargylacetylchlorid (2.0 g, 12.94 mmol) was added at 0 °C. The reaction mixture was stirred overnight, the resulting precipitate was filtered off and all volatiles were removed from the filtrate. Distillation at 85 °C at 10 Torr gave a colorless oil (1.1 g, 5.7 mmol, 44%). ^1H NMR ($CDCl_3$) δ 2.65 (m, 1H, $CHCO_2$), 2.56 (m, 4H, CH_2), 1.97 (t, 2H, CCH), 1.43 (s, 9H, CH_3); ^{13}C NMR ($CDCl_3$) δ 171.5 (CO_2), 81.4 (CCH_3), 80.7 (CH_2CCH), 70.3 (CCH), 43.7 ($CHCO_2$), 28.0 (CH_3), 20.0 (CH_2).

Dipropargylmethylcyanoacetate (DPMCA). Methylcyanoacetate (15.0 g, 151 mmol) was added to a suspension of NaH (3.0 g, 124.7 mmol) at 0 °C. After stirring for 2 h at room temperature, the reaction mixture was cooled down to 0 °C again and propargylbromide (39.6 g, 333 mmol; 80% wt solution in toluene) was added. After stirring overnight 200 mL of water and 200 mL of ether were added to the brown suspension. The organic layer was collected and the water phase was washed twice with ether. The combined organic extracts were dried over magnesium sulfate, the volatiles were removed *in vacuo* and the remaining solid was recrystallized from pentane to afford colorless cubes (12.7 g, 48%). ^1H NMR ($CDCl_3$) δ 3.88 (s, 3H, OCH_3), 2.93 (d, 4H, CH_2), 2.23 (t, 2H, CCH).

Dipropargyl-*tert*-butylcyanoacetate (DPBCA). *tert*-Butylcyanoacetate (8.0 g, 56.7 mmol) was added to a suspension of NaH (3.0 g, 124.7 mmol) at 0 °C. After stirring for 2 h at room temperature, the reaction mixture was chilled down to 0 °C again and propargylbromide (14.9 g, 124.7 mmol; 80% wt solution in toluene) was added. After stirring overnight 200 mL of water and 200 mL of ether were added. The organic layer was collected and the water phase was washed twice with ether. The combined organic

phases were dried over magnesium sulfate, the volatiles were removed in vacuo and the remaining oil was distilled at 90 °C at oil pump vacuum. The clear distillate was crystallized from pentane to afford white needles (9.2 g, 75%). ^{1}H NMR ($CDCl_3$) δ 2.88 (d, 4H, CH_2), 2.21 (t, 2H, CCH), 1.52 (s, 9H, CH_3); ^{13}C NMR ($CDCl_3$) δ 164.6 (CO_2), 117.4 (CN), 85.2 (CCH_3), 76.3 (CH_2CCH), 73.4 (CCH), 47.6 ($CHCO_2$), 27.7 (CH_3), 25.7 (CH_2). Anal. Calcd. for $C_{13}H_{15}NO_2$: C, 71.87; H, 6.96; N, 6.45. Found: C, 71.87; H, 7.04 N, 6.37.

Decarboxyethylation of poly(DEDPM)$_n$. To a solution of poly(DEDPM)$_n$ (76 mg, 0.32 mmol of monomer units) in 5 mL of DMSO, H_2O (5.8 mL, 0.32 mmol) and LiCl (27 mg, 0.64 mmol) were added under Argon. After refluxing for 3 h the solvent was removed in vacuo and the structure of the polymer was confirmed by ^{1}H NMR and ^{13}C NMR spectroscopy.

Hydrolysis of poly(DEDPM)$_n$. A solution of KOH (52 mg, 0.93 mmol) in THF/H_2O (15:1, 15 mL) was added to a solution of poly(DEDPM)$_n$ (100 mg, 0.423 mmol of monomer units) in THF (2 mL). The reaction mixture was refluxed for 12 h and resulted in a clear solution with purple precipitate. After decanting of the solvent, the product was washed with THF and dried under oil pump vacuum until almost all the solvent was removed yielding a glassy film. ^{1}H NMR (D_2O) δ 6.3 (s, 1H, =CH), 6.0 (s, 1H, =CH), 3.0 (s, 2H, CH_2), 2.9 (s, 2H, CH_2); ^{13}C NMR (D_2O) δ 181.3 (CO_2), 138-126 (=CH), 59.0 (C_{quat}), 37.2 (CH_2), 34.7 (CH_2).

Hydrolysis of poly(BEDPM)$_n$. A solution of KOH (28 mg, 0.69 mmol) in THF/H_2O (15:1, 2 mL) was added to a solution of poly(BEDPM)$_n$ (183 mg, 0.69 mmol of monomer units) in THF (3 mL). The reaction mixture was refluxed for 14 h and resulted in a clear solution with purple precipitate. After decanting of the solvent, the product was washed with THF and dried under oil pump vacuum until almost all the solvent was removed yielding a glassy film. ^{1}H NMR (D_2O) δ 7.4-5.7 (br, 2H, =CH), 2.9-2.3 (br, 4H, CH_2), 2.9 (s, 9H, CH_3); ^{13}C NMR (D_2O) δ 173 (CO_2), 167 (CO_2), 134-121 (=CH),

75 (CMe_3), 51 (C_{quat}), 30-22 (CH_2), 20 (CCH_3). The analogous reaction with NaOH gave the same result.

CHAPTER 3

Soluble, Highly Conjugated Polyenes via the Molybdenum-Catalyzed Copolymerization of Acetylene and Diethyldipropargylmalonate

Most of the material covered in this chapter has appeared in print:

Schattenmann F. S., Schrock, R. R. *Macromolecules* **1996**, *29*, 8990.

INTRODUCTION

The cyclopolymerization of diethyldipropargylmalonate (DEDPM) by **1a** and **2b** to give soluble, dark red polyenes that contain only six-membered rings in the polymer backbone as a consequence of a selective head-to-tail cyclopolymerization process was addressed in great detail in the previous chapter (eq 1).[70] The lowest energy λ_{max} was found to be 534 nm. In comparison, the absorption due to the lowest π to π^* transition in the parent polyacetylene was reported at 594 nm for all-*cis* polyacetylene and 700 nm for

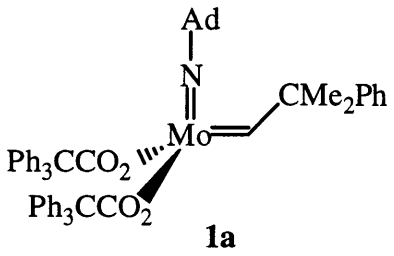

1a

Ad = adamantyl

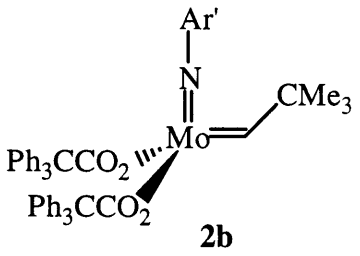

2b

Ar' = 2-*t*-butylphenyl

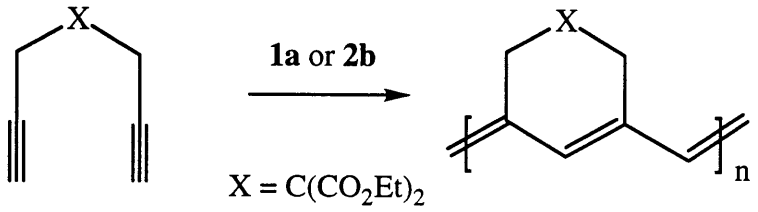

(1)

the all-*trans* polymer.[80] As pointed out before, polyacetylene is an insoluble and intractable material and many techniques were developed to tackle the processability problems such as synthesis as a free standing film from acetylene[81,82] and multi-step routes over soluble polymer precursors.[83-85] However the resulting materials are still intractable. Polyenes that approach the degree of conjugation of pure polyacetylene, yet are still soluble and processable are highly desired.

In order to increase the conjugation length, while hopefully maintaining solubility and relative air stability, we considered the preparation of random copolymers of sterically demanding DEDPM units with parent acetylene as an elegant entry to less substituted and

more conjugated polyacetylene derivatives. There is only one report of a controlled polymerization of acetylene by a well-defined catalyst,[16] as the rate of propagation is usually much greater than the rate of initiation. Synthesis of a copolymer from two monomers with homopolymerization reactivity differences as great as suspected between DEDPM and acetylene is an additional significant challenge.[86,87]

The failure of **1a** and **2b** to function as catalysts for the ring-opening of norbornenes and substituted norbornadienes suggests that "backbiting" into a polyene sequence formed by incorporation of several equivalents of acetylene is expected to be an unlikely side reaction (Scheme 3.1). We report in this chapter that it is possible to synthesize random copolymers of acetylene and DEDPM, if the rate of addition of acetylene to **1a** or **2b** in the presence of DEDPM is tightly controlled.

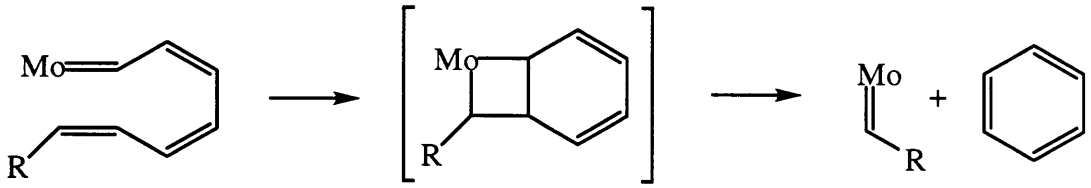

Scheme 3.1. Formation of Benzene by Subsequent Insertion of at Least Three Actylene Units into the Molybdenum Alkylidene Bond Followed by Intramolecular Metathesis.

RESULTS AND DISCUSSION

Acetylene Addition System.

Preliminary experiments involved the addition of acetylene via syringe through a rubber septum into the reaction vessel and indicated the possibility of a successful random copolymerization of DEDPM and acetylene. However reproducibility was an issue with regard to the rate of acetylene addition and leakage of acetylene. In order to yield

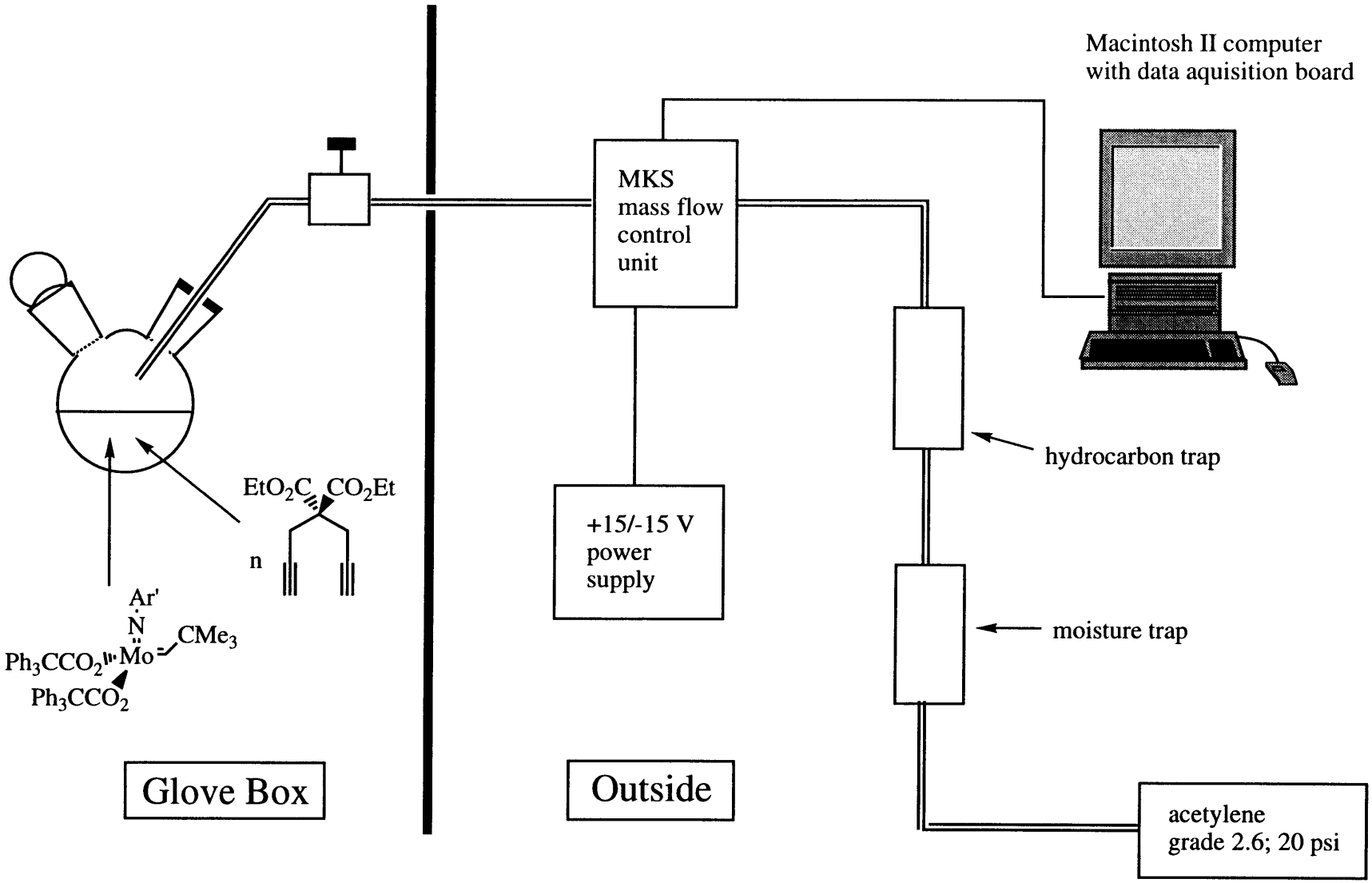

Figure 3.1. Schematic Representation of the Acetylene Addition System. Vacuum Cycles, Valves etc. Omitted for Clarity.

reproducible results, a computer controlled gas addition system had to be implemented. A schematic representation of the acetylene addition setup is pictured in Figure 3.1. Acetylene of the highest, commercially available purity (grade 2.6) was supplied with a maximal pressure of 20 psi above atmospheric pressure. Traces of moisture were removed by passing the gas through molecular sieves. Acetone, used as an acetylene stabilizer, and other impurities were removed by an activated charcoal trap. Essential to the gas addition setup was a mass flow controller unit with a flow range of 0 to 10 mL/min. The mass flow control unit was driven by a computer equipped with a data aquisition board. A two neck flask with one neck attached to the addition system served as the reaction vessel, the other neck was used to add the catalyst and DEDPM solutions. The acetylene was introduced into the head space of the reaction mixture immediately above the stirring solution in a linearly decreasing manner starting from a selected initial flow rate over a preset period of time.

Copolymerization of DEDPM and Acetylene.

In a typical experiment a solution of DEDPM in toluene was added to a solution of initiator **1a** in toluene followed by addition of purified acetylene using the described setup. The color of the reaction mixture changed from orange to red to purple, and in the cases where the polymer had a high acetylene content (>1 acetylene per DEDPM), to navy blue. The color change accelerated upon acetylene addition and the final color was usually observed within minutes of completion of acetylene addition indicating the end of the copolymerization. Insertion of an acetylene unit into the molybdenum alkylidene bond affords a propagating species with an alkylidene functional group with protons on the α, β, and γ carbon. Such an 'open' alkylidene species is presumably very reactive and will rapidly insert acetylene or DEDPM. A dependence of the reactivity on the steric demand of the alkylidene functional group in the synthesis of polyenes using alkylidene bis(alkoxide) complexes has been shown before.[16]

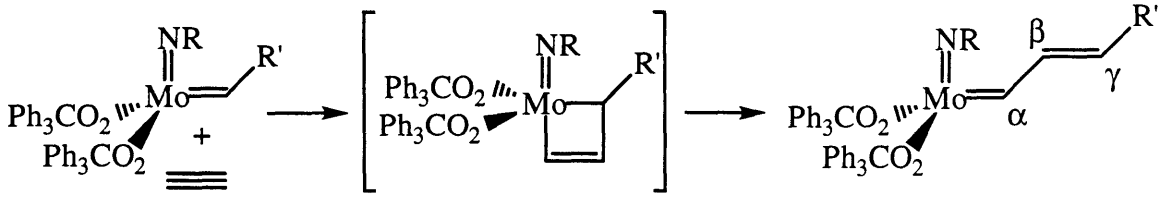

Scheme 3.2. Propagating Species with Protons on the α, β and γ Carbons from the Reaction of Acetylene with a Monosubstituted Molybdenum Alkylidene Complex.

The resulting polymers form intensely colored solutions, and upon evaporation of the solvent, films that have a copper-like luster. All such films can be redissolved readily in chloroform, THF, dichloromethane, and toluene; they are insoluble in pentane and ether. Yields of the copolymers ranged from 90 to 100%.

Acetylene Incorporation.

The ^1H NMR spectra of the copolymers were found to be similar to those of the homopolymers of DEDPM with two additional resonances in the olefinic region representing the only difference. The copolymer proton NMR spectra are generally broader than the spectra of the homopolymers of DEDPM indicating that the six-membered rings are in different chemical environments as expected for a statistical copolymer. The acetylene content in the polymer could be determined by integrating the olefinic resonances versus the methylene resonances in the ethyl groups or the six-membered ring. The peak for the ethyl CH_2 groups usually gave a higher integral value than the six-membered ring methylene signals, but in most cases the difference amounted to less than 5%. The average of the two different methylene integrals was used to calculate the % acetylene found, as shown in Table 3.1. The degree of acetylene incorporation correlates well to the amount of acetylene added (Table 3.1 and Figure 3.2).

Table 3.1. Acetylene Incorporation Determined by ^{1}H NMR and UV/Vis Data for DEDPM/Acetylene Copolymers Using **1a** as Initiator in Toluene.

entry[a]	acetylene theory (%)[b]	acetylene found (%)[c]	λ_{max} (nm)[d]	ε_{max} (cm^2/g)[d]
1	50	53	548	47300
2	75	81	562	55200
3	100	101	576	81000
4	100	96	576	69700
5	120	119	586	75700
6	120	121	584	76600
7	150	153	598	86300

[a] All runs with 20 mg (0.021 mmol) of **1a**, 12 mL of toluene and 30 equiv of DEDPM (0.63 mmol; 149 mg). [b] Mol percentage of acetylene relative to DEDPM. [c] Determined by ^{1}H NMR. [d] In CH_2Cl_2.

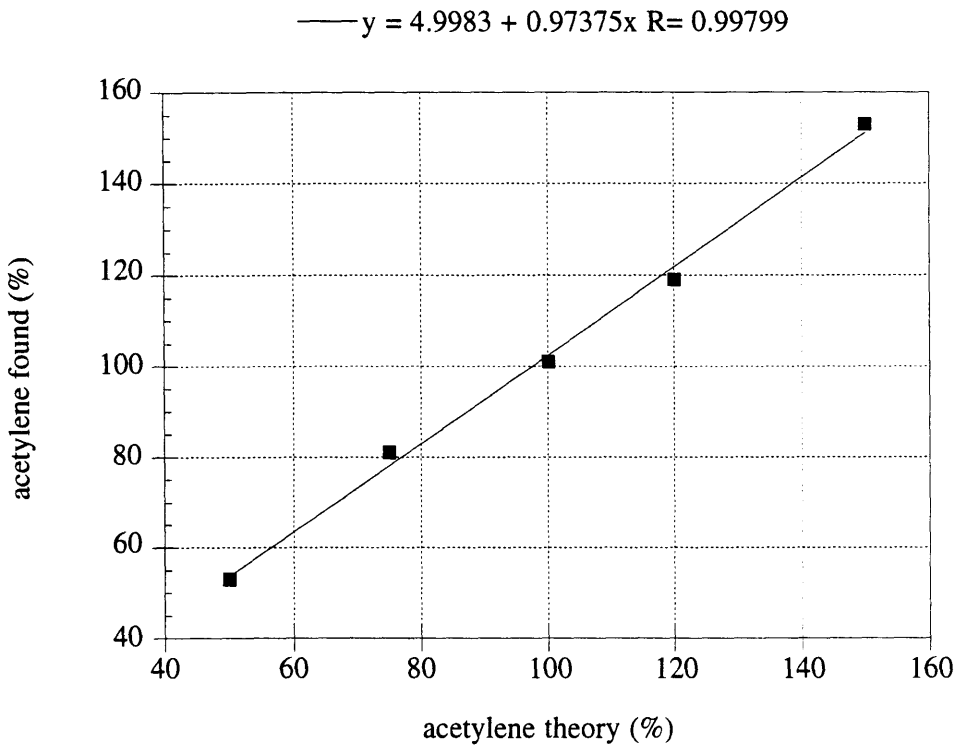

Figure 3.2. Plot Showing Acetylene Found in DEDPM/Acetylene Copolymers Using **1a** as Initiator in Toluene versus Acetylene in Theory.

Monomer Sequence of Copolymers.

A useful diagnostic resonance in ^{13}C NMR spectra is the signal due to the quaternary carbon atom in the six-membered ring.[70] The resonance for the homopolymer (i below; X = $C(CO_2Et)_2$); Figure 3.3a)[70] shows some fine structure that we ascribe to as yet undefined conformers. Three basic types of quaternary carbon resonances can be distinguished by ^{13}C NMR in the copolymers (Figure 3.3b, 3.3c, 3.3d). One is a quaternary carbon atom in a homopolymer triad (type i) at 54.5 ppm. A second is a quaternary carbon atom in a triad of type ii or iii at 54.2 or 54.1 ppm. A third is a quaternary carbon atom in a triad of type iv at 53.9 ppm. The ratio of triads ii and iii, which are inherently different as a consequence of the asymmetry of the six-membered

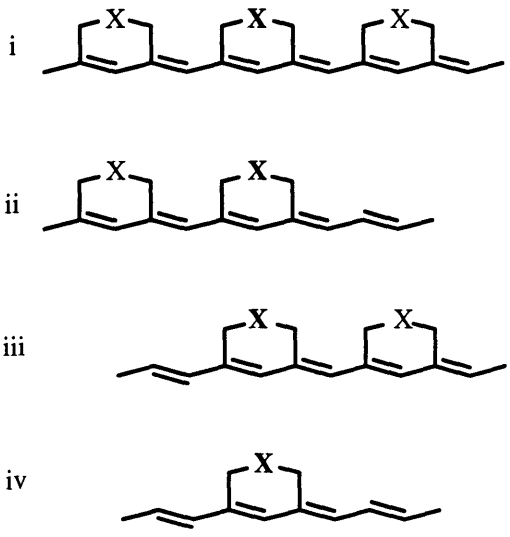

ring, is approximately 1:1, as one would expect. The fact that all four resonances have about the same intensity in the "1:1 copolymer" (Figure 3.3c) is consistent with an

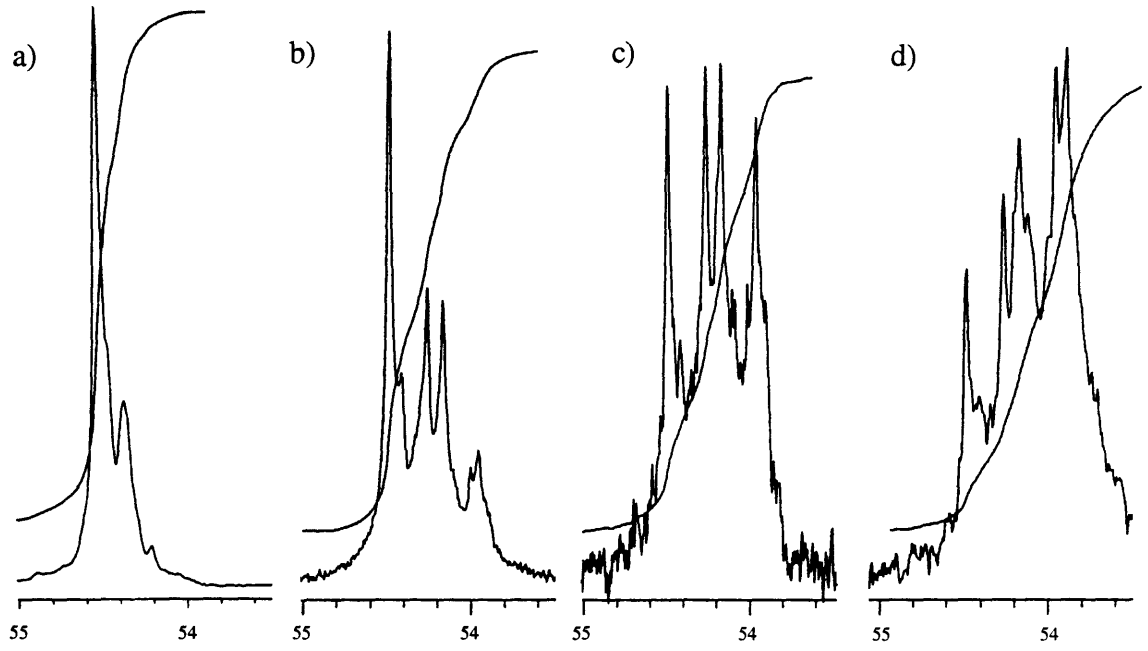

Figure 3.3. Quaternary Carbon Resonances of (a) Homopolymer (DEDPM; see Chapter 1) and Copolymers with Different Monomer Compositions (DEDPM:Acetylene): (b) 1:0.53; (c) 1:1.01; (d) 1:1.53.

essentially statistically random incorporation of acetylene and DEDPM, and the lack of any significant side reaction involving acetylene, such as trimerization. The quaternary carbon resonance characteristic of triad iv clearly increases with increasing acetylene content. The presence of more than one acetylene "spacer" between six-membered rings leads to further fine structure and overall broadening of the quaternary carbon resonances (Figure 3.3d). Presumably the quaternary carbon resonance is sensitive to pentad structure, and broadening and fine structure of the resonance in Figure 3.3d is the result. Due to the similar chemical nature of the two monomers, perfectly alternating copolymers cannot be synthesized by this method. The copolymerization of two different monomers will only afford perfectly alternating polymers if both of the homopolymerization pathways are inaccessible.

Molecular Weights and Polydispersities of Copolymers.

The molecular weights and polydispersities of several 1:1 copolymers prepared by using **1a** and **2b** are listed in Table 3.2 and Table 3.3 respectively. The molecular weights were determined by GPC using a viscometry detector versus a polystyrene calibration curve. The limitations in the determination of the molecular weights of poly(DEDPM)$_n$ using viscometry were addressed in great detail in Chapter 2. Although the molecular weights were off by a certain factor, the employed GPC setup proved to be intrinsically consistent for poly(DEDPM)$_n$. For the copolymers, however, an additional problem could arise from varying monomer composition of the copolymers. Copolymers with different monomer compositions are different types of polymers and can well exhibit substantially different solution behavior. Therefore the values for the molecular weights listed in Table 3.2 and Table 3.3 have to be judged with caution.

Some dependence of molecular weights and polydispersities on the type of initiator, the concentration of initiator and DEDPM, the rate of addition of acetylene and the diffusion of acetylene from the head space into the reaction mixture can be observed, although the

Table 3.2. GPC Data for DEDPM/Acetylene Copolymers Prepared Using **1a** in Toluene as a Function of Concentration, Stirring Rate and Acetylene Addition Mode.

entry	**1a** (μmol/mL)	ratio[a]	stirring[b]	t_{add} (min)[c]	$(m/t)_o$[d]	M_n[e]	M_w/M_n[e]
1[f]	1.75	1/1	slow	10	3.12	91000	5.7 (m)
2[g]	1.75	1/1	slow	4	7.70	134000	1.97 (u)
3	1.75	1/0.5	slow	4	3.90	55000	2.01 (bi)
4	1.75	1/0.75	slow	4	5.85	35000	1.39 (u)
5	1.75	1/1	slow	4	7.80	147000	1.82 (u)
6	1.75	1/1.2	medium	6	6.20	11100	1.58 (u)
7	1.75	1/1.2	medium	6	6.20	14650	1.58 (u)
8	1.75	1/1.5	medium	6	7.73	60000	1.71 (bi)
9	1.40	1/0.5	fast	2	6.60	16800	1.65 (bi)
10	1.40	1/1	fast	4	6.20	8900	1.69 (u)
11	0.93	1/0.5	fast	2	6.16	13200	1.58 (bi)
12	0.93	1/1	fast	3	8.27	15000	1.54 (bi)
13	0.70	1/0.5	fast	1	9.30	16000	1.44 (bi)
14	1.58	1/1	medium	3	6.20	69000	1.75 (u)
15	1.58	1/1	slow	3	6.20	insoluble	

[a] Ratio of DEDPM to acetylene (mol/mol) with always 30 equiv of DEDPM to 1 equiv of initiator. [b] slow = small stirring bar, medium = large stirring bar with slow stirring, fast = large stirring bar under vigorous stirring. [c] Acetylene addition time. [d] Initial mass flow in mL/min. [e] Determined by GPC on-line viscometry versus a polystyrene universal calibration curve (Viscotek); (u) = unimodal (possibly with a shoulder), (bi) bimodal and (m) = multimodal distribution (PDI determined over entire peak area in all cases). [f] λ_{max} = 578 nm; ε_{max} = 75200 cm^2/g; acetylene found = 92%. [g] See entry 4 in Table 3.1.

Table 3.3. GPC Data for DEDPM/Acetylene Copolymers Prepared Using **2b** in Toluene as a Function of Concentration, Stirring Rate and Acetylene Addition Mode.

entry	**2b** (μmol/mL)	ratio[a]	diffusion[b]	t_{add} (min)[c]	$(m/t)_o$[d]	M_n[e]	M_w/M_n[e]
1	1.69	1/0.5	fast	4	3.80	4950	1.91 (bi)
2	1.69	1/1	fast	4	7.55	4800	1.78 (bi)
3	1.13	1/0.5	fast	4	3.80	5300	1.42 (bi)
4	1.13	1/1	fast	4	7.55	19900	2.05 (bi)
5[f]	1.13	1/1	fast	3	6.67	6700	1.46 (bi)
6	0.75	1/1	fast	3	6.67	15600	1.72 (u)[g]
7	0.75	1/1	fast	3	6.67	24500	1.70 (u)[g]
8	0.61	1/1	fast	3	6.67	3400	1.71 (bi)
9	0.61	1/1	fast	3	6.67	7400	1.47 (bi)
10	1.69	1/1	medium	3	6.67	24500	1.99 (m)
11	1.69	1/0.5	slow	2	5.00	29700	2.00 (m)
12[h]	1.69	1/0.5	slow	2	5.00	solid byproducts	
13[i]	1.69	1/1	medium	2	10.00	32500	1.74 (bi)
14[h]	1.69	1/1	medium	2	10.00	17000	1.68 (u)

[a] Ratio of DEDPM to acetylene (mol/mol) with always 30 equiv of DEDPM to 1 equiv of initiator. [b] slow = small stirring bar, medium = large stirring bar with slow stirring, fast = large stirring bar under vigorous stirring. [c] Acetylene addition time. [d] Initial mass flow in mL/min. [e] Determined by GPC on-line viscometry versus a polystyrene universal calibration curve (Viscotek); (u) = unimodal (possibly with a shoulder), (bi) bimodal and (m) = multimodal distribution (PDI determined over entire peak area in all cases). [f] 1 min delay of acetylene addition after addition of DEDPM. [g] Low molecular weight shoulder present. [h] 2 minute delay. [i] 1.25 min delay.

trends are not clear cut. Acetylene addition was controlled by two parameters, the initial mass flow [$(m/t)_o$] and the total addition time (t_{add}). Three different rates of diffusion were employed by varying stirring bar size and stirring intensity as indicated in Table 3.2 and Table 3.3. Unimodal distributions were observed more often when employing initiator **1a** than **2b**. Polydispersities are typically higher (1.4 to 2.0) than in the homopolymer of DEDPM, most likely since the copolymerization is a complex process that could involve as many as eight chain propagation steps (two homopolymerization and two cross polymerization rates for two different alkylidene rotamers[32,33]). Additional complications arise from the diffusion of acetylene from the head space into the reaction mixture. As in the case of the homopolymerization, initiator **2b** leads generally to polymers with smaller molecular weights and polydispersities than **1a**. Bimodal distributions were expected since two different types of initiators with very different reactivities (uninitiated and already initiated catalysts) are present in solution at the time when the acetylene diffuses into the reaction mixture. However unimodal distributions with broader polydispersities were obtained by slow diffusion (especially with initiator **1a**). Presumably the acetylene is mainly consumed by the more reactive propagating species also resulting in significantly higher molecular weights. Unimodal distribution were also observed when the acetylene addition was started with a delay consistent with the presence of mainly propagating species. Addition times of 10 min or longer led to the formation of insoluble material. Presumably after all DEDPM is used up, excess acetylene forms sequences of polyacetylene which drive the polymer out of solution. Fast addition, fast diffusion and a low initiator concentration usually led to a bimodal but relatively narrow distribution. Some degree of control over molecular weights and polydispersities could be demonstrated by systematic variation of the reaction conditions.

Optical Data.

UV/Vis spectra reveal that λ_{max} and ε_{max} (Table 3.1) correlate smoothly with the amount of acetylene incorporated (Figure 3.4). Due to the uncertainty of the molecular weight determination, λ_{max} and ε_{max} per double bond could not reliably be determined. In an ideal 1 to 1 copolymer of DEDPM and acetylene only one third of the double bonds stem from acetylene, since the polymerization of one DEDPM monomer results in a unit with two conjugated double bonds. The λ_{max} values for the DEDPM homopolymers have been found to not exceed 534 nm (Chapter 2). In a polymer with 50% acetylene incorporation λ_{max} increases to 548 nm, but only 20% of the double bonds come from acetylene units. Incorporation of 1.5 equivalents of acetylene per DEDPM yields a completely soluble, blue polymer with a λ_{max} value close to 600 nm and ε_{max} of almost 90,000 cm^2/g,

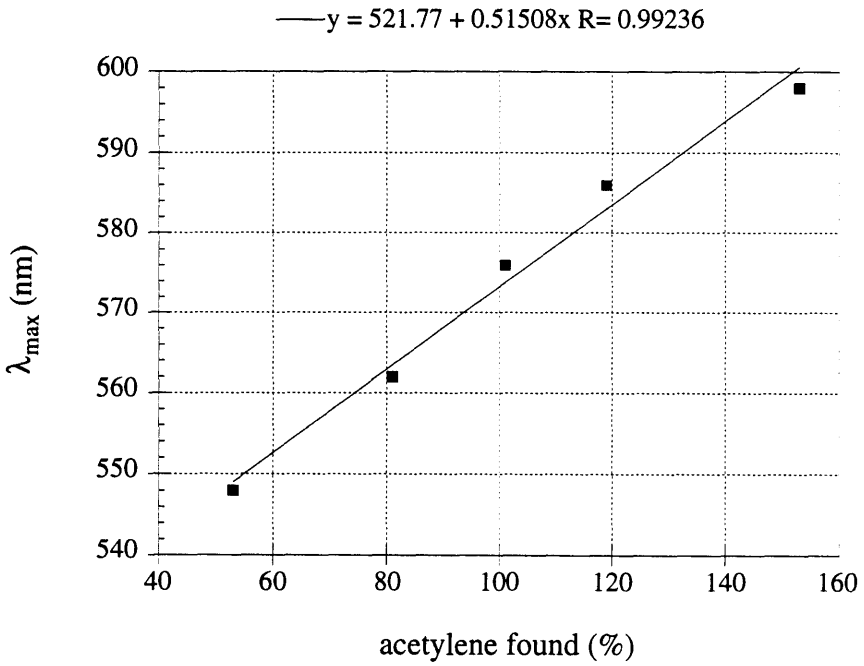

Figure 3.4. Dependence of the Optical Absorption Maximum (λ_{max}) in CH_2Cl_2 versus the Portion of Acetylene Found in DEDPM/Acetylene Copolymers Prepared Using **1a**.

consistent with a very high degree of conjugation. In comparison the λ_{max} for all-*cis* polyacetylene, an intractable and insoluble material, was reported to be 600 nm as stated above.[80] Polymers containing more than 1.5 equivalents of acetylene per equivalent of DEDPM were found to be increasingly insoluble in chloroform, THF, dichloromethane, or toluene. All copolymers were found to be unstable to air.

CONCLUSIONS

In the past copolymers that contain unsubstituted polyene sequences usually have been prepared by ring-opening of 7,8-bis(trifluoromethyl)tricyclo[4.2.2.$0^{2,5}$]deca-3,7.9-triene (TCDT); poly(TCDT) sequences are then transformed into polyacetylene by heating.[14,83,88,89] The results reported in this chapter show that it is possible to employ acetylene itself as a comonomer. Benefits as well as limitations of the copolymerization of acetylene with DEDPM have been revealed. The reproducibility of the synthesis and a high degree of control over the acetylene incorporation and the polymer properties could be achieved. The uncomplicated NMR properties of regioregular poly(DEDPM)$_n$ prepared using bis(carboxylate) initiators **1a** and **2b** enabled the determination of the acetylene content as well as the monomer sequence of these copolymers. Polymers with a highly statistical monomer sequence were prepared with no insoluble side products. A disadvantage is that the polydispersity of such polymers is considerably larger than is typical for ring-opening metathesis polymerizations involving well-defined alkylidene catalysts. λ_{max} values approaching 600 nm and ε_{max} approaching 90,000 cm^2/g were found for copolymers containing the highest fraction of acetylene consistent with a strongly increased degree of conjugation over that of the poly(DEDPM)$_n$ homopolymer.

EXPERIMENTAL

General details. All experiments were performed under a nitrogen atmosphere in a Vacuum Atmospheres drybox or by standard Schlenk techniques under an argon atmosphere unless otherwise specified. Celite and alumina were dried at ~130 °C for at least a week. Pentane was washed with sulfuric/nitric acid (95/5 v/v), sodium bicarbonate and water, stored over calcium chloride, and distilled from sodium benzophenone ketyl under nitrogen. Reagent grade diethyl ether, tetrahydrofuran, toluene, benzene and 1,2-dimethoxyethane were distilled from sodium benzophenone ketyl under nitrogen. Reagent grade dichloromethane was distilled from calcium hydride under nitrogen. Toluene used for polymerizations was stored over 4Å molecular sieves and passed through alumina prior to use. Benzaldehyde was distilled and passed through alumina before use.

All gel permeation chromatography (GPC) experiments were carried out using two Jordi-Gel DVB Mixed Bed columns in series and a Viscotek Differential Refractometer/Viscometer H-500 on samples 0.1-0.2% w/v in THF, which were filtered through a Millex-SR 0.5 μm filter in order to remove particulates. GPC columns were calibrated versus polystyrene standards (Polymer Laboratories Ltd.) which ranged from 1206 to 1.03x106 MW. The GPC data were analyzed using Unical 4.03 (Viscotek). NMR data were obtained at 300 MHz (^{1}H) and 75.43 MHz (^{13}C) on a Varian XL 300 and a Varian Unity 300 NMR spectrometer or at 500 MHz (^{1}H) and 125 MHz (^{13}C) on a Varian 500 NMR spectrometer and are listed in parts per million downfield from tetramethylsilane. Spectra were obtained at room temperature unless otherwise noted. UV/Vis spectra were obtained using a Hewlett Packard 8452 A Diode Array Spectrometer.

The gas addition apparatus consisted of a MKS Instruments Inc. 1179 Mass Flow controller (valve closed: no flow; valve open: flow range 0.2 to 10 mL/min; flow rate error: 1% of maximum flow) powered by a +15/-15 V power supply, a Macintosh II computer equipped with a National Instruments Lab-NB data aquisition board and Lab View data aquisition software (National Instruments), a Hydro-purge moisture in line trap and a

hydrocarbon in line trap (both Alltech Associates) and a sealed, stainless steel tubing system with all valves, quick connects from Swagelock.

Copolymerization of DEDPM and Acetylene. In a representative polymerization a stock solution of **1a** (0.0105 M) in toluene that had been distilled over sodium benzophenone ketyl, stored over 4Å molecular sieves and passed through alumina, was prepared. Prior to every polymerization attempt the gas line between the mass flow controller and the quick connector was three times evacuated and purged with acetylene. To 2000 μl of the catalyst stock solution 9 mL of toluene were added into the reaction flask. 149 mg (0.63 mmol) DEDPM was dissolved in 1 mL toluene. The DEDPM solution was squirted into the initiator solution and after sealing the system, the acetylene (15.4 mL, 0.63 mmol) addition was started within a few seconds. The gas was added with a linearly decaying addition mode over 4 min with an initial mass flow of 7.7 mL/min. Within 30 s the reaction mixture turned deep red and after 2 min purple. After 6 h the polymers were capped with 16 μl of benzaldehyde. The solution was stirred for another hour, passed through alumina and all volatiles were removed *in vacuo* yielding a dark purple film with a copper like luster. Yields were always close to 100% using this method and no major impurities could be detected by NMR; in order to justify this workup method the polymer was precipitated from solution in pentane and collected in a fritt in a control experiment (yield: 92%). All operations were carried out under dinitrogen and the polymers were only briefly exposed to air for the sample preparation for the GPC analysis and the UV/vis measurements.

CHAPTER 4

The Synthesis of Zirconium Complexes Containing Tridentate Diamido Ligands and the Polymerization of 1-Hexene

INTRODUCTION

The group 4 metal catalyzed polymerization of α-olefins has emerged as one of the most important industrial processes since its discovery by Ziegler and Natta more than 40 years ago. In the early 1980's the first homogeneous polymerizations using single-site group 4 metal catalysts were reported and over the last 15 years enormous progress has been made in the further development and design of such catalysts.[90] The vast majority of catalysts are metallocene-based, but complexes containing bridged monocyclopentadienyl-amide ligand systems have also been implemented.[91-93] Some of the metallocene and monocyclopentadienyl-amide complexes have distinguished themselves by extraordinary activity and are currently used in large scale industrial applications. A common feature of such catalysts is the loss of olefin by β hydride elimination resulting in chain transfer.

Complexes with chelating bis(amide) ligand systems[94-105] have recently received attention as potential Ziegler-Natta type polymerization catalyst precursors, in particular since 1996, when McConville et al.[106] reported the first living polymerization of neat α-olefins using arylsubstituted propylene bridged diamido complexes of titanium. More recently Baumann and Schrock[107] discovered a zirconium complex containing the [(*t*-Bu-d_6-N-*o*-C_6H_4)$_2$O]$^{2-}$ ([NON]$^{2-}$) ligand that can be activated to form a living catalyst at 0 °C. These results indicated that group 4 Ziegler-Natta type catalysts containing bridged diamido ligands can be designed that are significantly more stable towards loss of olefin via β hydride elimination than metallocene based catalysts. An important goal included therefore to explore the correlation of the coordination sphere and ligand structure of a specific catalyst with the polymerization behavior by designing and employing catalysts containing other polydentate bis(amide) ligands.

In this chapter the synthesis, characterization and polymerization behavior of complexes that contain tridentate bridged diamido ligands are addressed. Focus was directed towards the development of catalysts containing ligand systems that are synthetically accessible in few high yield steps.

One ligand consists of a silicon bridged diamide system [*t*-$BuNHSiMe_2NHCH_2CH_2NMe_2$] ($H_2[NSiN_2]$) with a pendant tertiary amino donor to enhance stability towards degradation and deactivation of the activated, cationic species. The expected geometry around the metal center is a trigonal bipyramidal arrangement with the *t*-butylamide and the NMe_2 group in apical positions, a coordination sphere similar to that of complexes containing tridentate cyclopentadienyl-amido-donor ligands.[108]

The other ligands, $(RNHCH_2CH_2)_2O$ (R = 2,6-*i*-Pr_2-C_6H_3 , 2,6-Me_2-C_6H_3 and phenyl), are based on a $[RN_2O]^{2-}$ framework similar to the $[NON]^{2-}$ ligand. Although electronically comparable to the $[NON]^{2-}$ ligand,[107] the flexible, saturated ligand backbone and different steric properties of the arylamido compared to the *t*-butylamido group of the $[NON]^{2-}$ ligand promised possible differences in the coordination environment.

RESULTS AND DISCUSSION

Zirconium Complexes Containing the $[NSiN_2]^{2-}$ Ligand.

t-$BuNHSiMe_2NHCH_2CH_2NMe_2$ (**1**) was synthesized in one step from $LiNHCH_2CH_2NMe_2$ and *t*-$BuNHSiMe_2Cl$[109] (eq 1). **1** was afforded as a colorless oil after

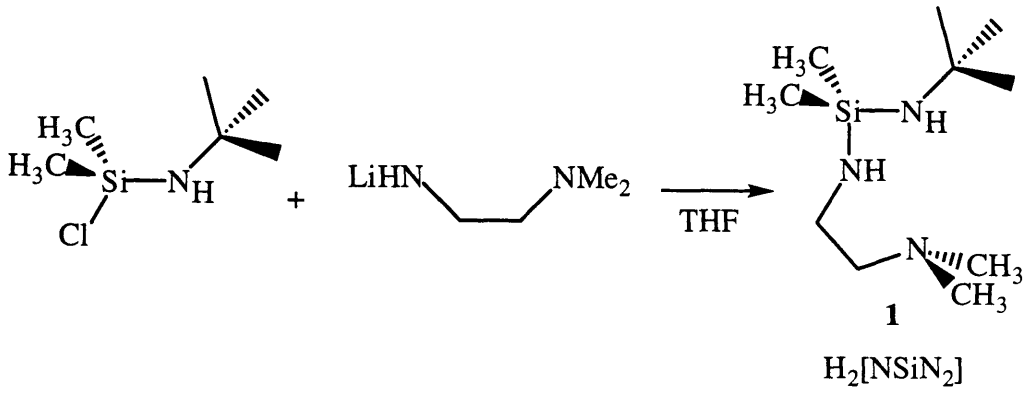

(1)

pentane extraction (at least 95% pure by NMR) and was used for the subsequent metallation reactions without further purification.

$[NSiN_2]Zr(NMe_2)_2$ (**2**) was prepared in 79% yield by the reaction of **1** with $Zr(NMe_2)_4$. ^1H NMR suggests almost quantitative conversion, but the high solubility of **2** prevented a higher, isolated yield. Reaction of **2** with excess trimethylsilylchloride gave $[NSiN_2]ZrCl_2$ (**3**) in 98% isolated yield (eq 2). Alternatively **3** can be obtained in excellent overall yield (88%) directly from **1** in a one-pot synthesis without isolation of **2**. ^1H and ^{13}C NMR spectra of **2** and **3** are consistent with C_s symmetry.

$$\mathbf{1} + Zr(NMe_2)_4 \xrightarrow[\text{pentane}]{} \underset{\mathbf{2}}{[NSiN_2]Zr(NMe_2)_2} \xrightarrow[\text{pentane}]{\text{xs TMSCl}} \underset{\mathbf{3}}{[NSiN_2]ZrCl_2} \qquad (2)$$

Alkylation of **3** with 2 equiv of MeLi or MeMgBr did not provide a clean product, however a series of extremely soluble dialkyl complexes can be easily prepared from **3** (Scheme 4.1). Reaction of **3** with solid $LiCH_2SiMe_3$ afforded $[NSiN_2]Zr(CH_2SiMe_3)_2$

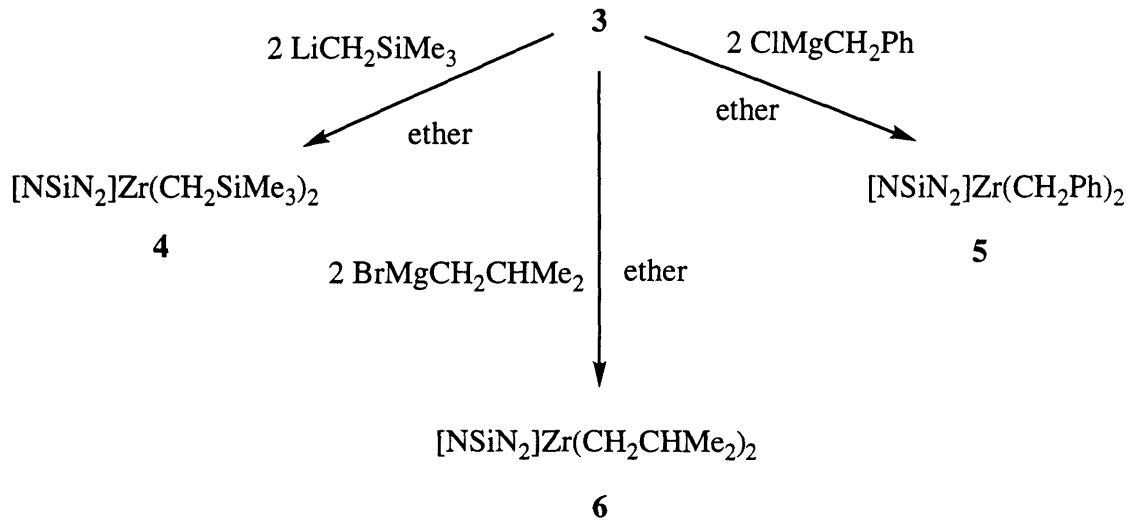

Scheme 4.1. Dialkyl Complexes Prepared from **3**.

(**4**) as a colorless oil. Although clean by NMR, all attempts to crystallize **4** failed. $[NSiN_2]Zr(CH_2Ph)_2$ (**5**) was obtained from the reaction of **3** with 2 equiv of $ClMgCH_2Ph$ in 76% yield as a yellow, crystalline solid. Alkylation of **3** with isobutylmagnesium bromide gave colorless crystals of $[NSiN_2]Zr(CH_2CHMe_2)_2$ (**6**) in 78% yield. This compound is unusual since it contains β hydrogen atoms. Compounds of this type usually decompose by β hydride elimination and only few other diamide complexes of group 4 metals with β hydrogen atoms have appeared in the literature.[110-113]

When the addition of dioxane was omitted from the synthetic procedure of the preparation of **6**, a small amount of crystals was obtained which proved to be insoluble in pentane at room temperature in contrast to crystals of **6**. An X-ray diffraction study of those crystals depicted a magnesium chloride bridged dimeric structure (Figure 4.1, Table 4.1) for this compound (**7**).

The structure represents a rare example of a stable zirconium alkyl complex with β-hydrogens. To our knowledge this is the first X-ray crystallographically characterized zirconium isobutyl complex. The Zr-C(α)-C(β) bond angles range between 106.7° and 130.2°, where one Zr center possesses isobutyl goups with larger Zr-C(α)-C(β) bond angles (128.3(4)° and 130.2(3)°) than the other (106.7(7)° and 120.7(3)°). The larger Zr-C(α)-C(β) bond angles suggest α agostic interactions. The *t*-butylamide nitrogens are trigonal planar as expected, while the bridging amide nitrogen of the chelating ligand system, surprisingly, is tetrahedral due to coordination to magnesium. Consistently the *t*-butyl amide N-Zr distances (2.074(4)Å) are shorter than the bridging N-Zr bond lengths (2.212(3) and 2.228(5)Å) as a result of additional π interactions. A trigonal bipyramidal coordination sphere was found for magnesium where one coordination site is occupied by the bridging amide nitrogen. This represents a rather important piece of information about

Table 4.1. Crystallographic Data, Collection Parameters, and Refinement Parameters for $\{[NSiN_2]Zr(CH_2CHMe_2)_2MgCl_2\}_2$ (**7**).

Empirical Formula	$C_{18}H_{43}Cl_2MgN_3SiZr$
Formula Weight	516.07
Crystal Color	colorless
Crystal Dimensions (mm)	0.39 x 0.28 x 0.22
Crystal System	Triclinic
a	12.082(3) Å
b	13.395(3) Å
c	18.240(5) Å
α	107.304(13)°
β	104.22(2)°
γ	93.31(2)°
V	2704.5(12) $Å^3$
Space Group	$P\bar{1}$
Z	4
D_{calc}	1.267 g/cm^3
F_{000}	1088
Diffractometer	Siemens SMART/CCD
$\lambda(MoK_\alpha)$	0.71073 Å
Scan Type	ω scans
Temperature	183(2) K
Total No. Unique Reflections	7003
No. Variables	479
R	0.0399
R_w	0.1040
GoF	1.206

Figure 4.1. X-ray Crystal Structure of $\{[NSiN_2]Zr(CH_2CHMe_2)_2MgCl_2\}_2$ (**7**).

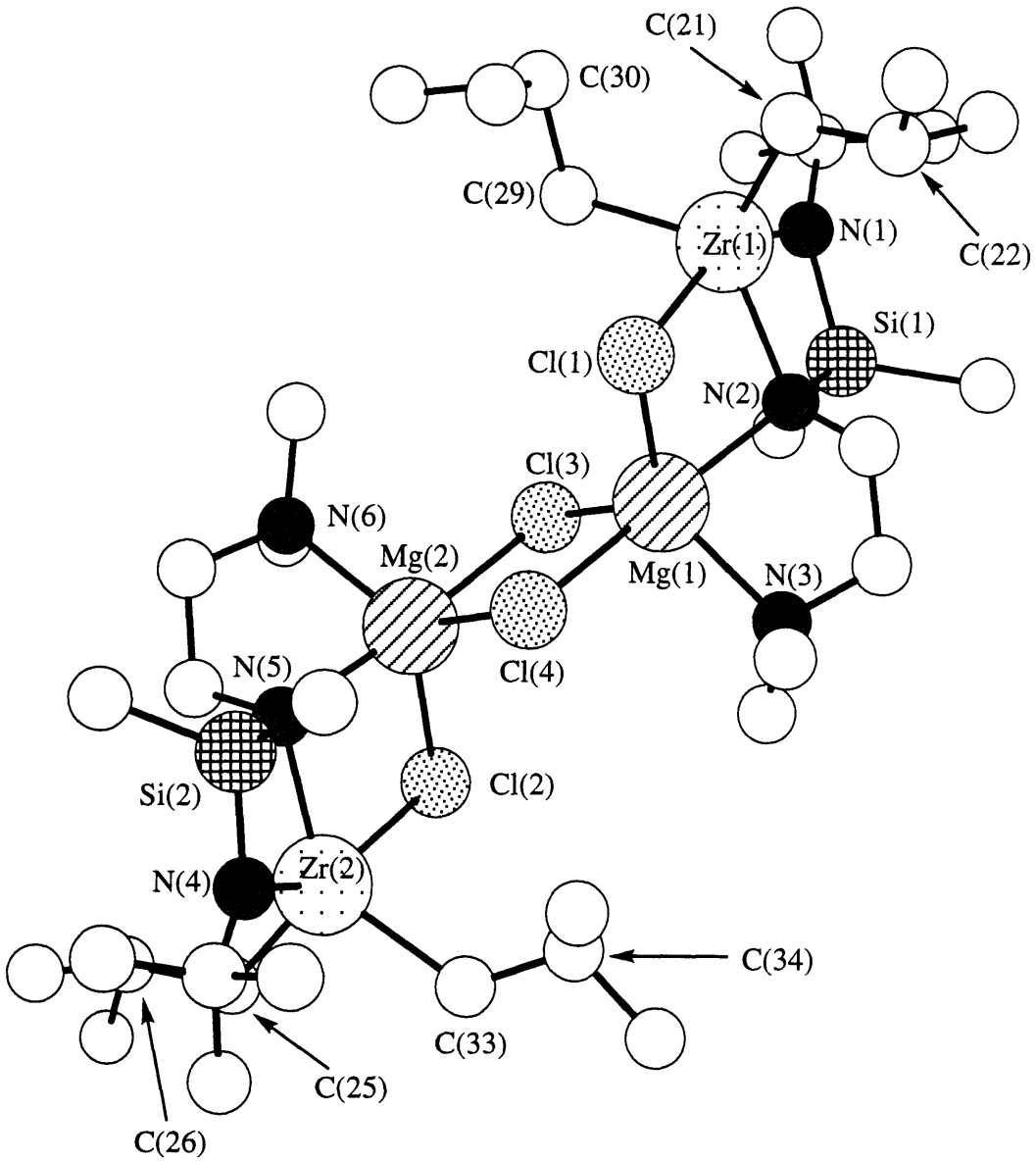

Table 4.2. Selected Interatomic Distances (Å) and Angles (deg) for the Non-Hydrogen Atoms of $\{[NSiN_2]Zr(CH_2CHMe_2)_2MgCl_2\}_2$ (**7**).

Bond Lengths

Zr(1)-N(1)	2.074(4)	Zr(2)-N(4)	2.074(4)
Zr(1)-N(2)	2.212(3)	Zr(2)-N(5)	2.228(5)
Zr(1)-Cl(1)	2.600(3)	Zr(2)-Cl(2)	2.615(3)
Zr(1)-C(21)	2.235(5)	Zr(2)-C(25)	2.228(5)
Zr(1)-C(29)	2.250(5)	Zr(2)-C(33)	2.237(5)
Mg(1)-N(2)	2.195(4)	Mg(2)-N(5)	2.159(4)
Mg(1)-N(3)	2.174(4)	Mg(2)-N(6)	2.178(4)
Mg(1)-Cl(1)	2.442(2)	Mg(2)-Cl(2)	2.430(2)
Mg(1)-Cl(3)	2.359(2)	Mg(2)-Cl(3)	2.547(2)
Mg(1)-Cl(4)	2.512(2)	Mg(2)-Cl(4)	2.358(2)

Bond Angles

N(1)-Zr(1)-N(2)	139.1(2)	N(4)-Zr(2)-N(5)	129.7(2)
Zr(1)-C(21)-C(22)	120.7(3)	Zr(2)-C(25)-C(26)	130.2(3)
Zr(1)-C(29)-C(30)	106.7(6)	Zr(2)-C(33)-C(34)	128.3(4)

the strength of π bonding of the nitrogen lone pair to the d^0 Zr center. Apparently an already four coordinate Mg center competes favorably with Zr for the N lone pair. The fact that the ligand system binds to a Lewis acid like $MgCl_2$ questions the ability of the $[NSiN_2]^{2-}$ ligand to behave as an innocent ligand during catalysis.

$[RN_2O]^{2-}$ Ligand Syntheses.

(2,6-*i*-Pr_2-$C_6H_3NHCH_2CH_2)_2O$ (**8**) ($H_2[ArN_2O]$) can be prepared in one step from $(TsOCH_2CH_2)_2O$ and 2,6-*i*-Pr_2-C_6H_3NHLi in 82% yield (eq 3). The orange oil obtained after extraction with pentane was used without further purification. Upon standing for several days the oil would crystallize in some cases.

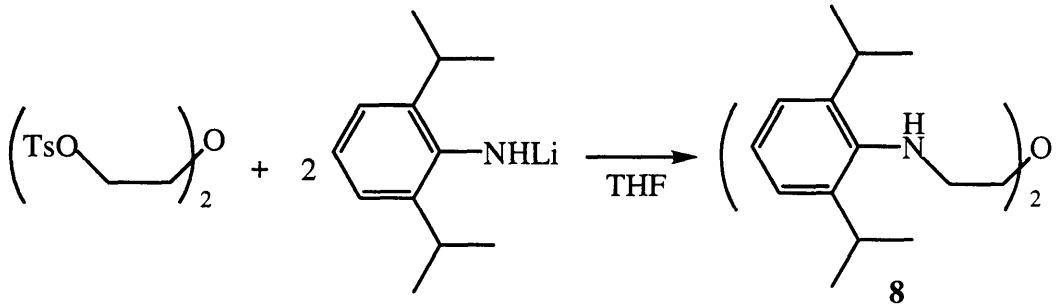

(3)

8

$H_2[ArN_2O]$

Similar to the preparation of **8** reaction of 2 equiv of 2,6-Me_2-C_6H_3NHLi with $(TsOCH_2CH_2)_2O$ yields (2,6-Me_2-$C_6H_3NHCH_2CH_2)_2O$ (**9**) ($H_2[Ar'N_2O]$) as colorless crystals in 62% isolated yield.

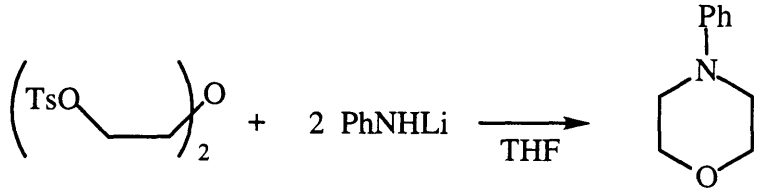

(4)

In contrast to the synthesis of **8** and **9**, reaction of 2 equiv of PhNHLi with $(TsOCH_2CH_2)_2O$ cleanly afforded a heterocyclic compound via intramolecular cyclization (eq 4). The corresponding heterocycle was already observed as a minor side product in the synthesis of **9**. Presumably the first PhNHLi reacts with $(TsOCH_2CH_2)_2O$ in a S_N2 type reaction and the second PhNHLi deprotonates the generated secondary amine, catalyzing

the intramolecular cyclization. The two *ortho* substituents on the aryl ring protect the NH group sufficiently from a similar attack of ArNHLi and Ar'NHLi in the formation of **8** and **9**. Substituents in both *ortho* positions are required as evidenced by the reaction of 2 equiv of 2-*t*-Bu-C_6H_4NHLi with $(TsOCH_2CH_2)_2O$ which afforded the analogous heterocyclic compound.

The unsubstituted ligand $(PhNHCH_2CH_2)_2O$ (**11**) ($H_2[PhN_2O]$), however, can be synthesized from $(TsOCH_2CH_2)_2O$ when trimethylsilyl protecting groups are employed (eqs 5 and 6). The formation of **10** does not proceed cleanly; the product mixture contains about 35-40% $PhNH(SiMe_3)$, most likely from a competing E_2 type reaction, keeping the isolated yield of **10** at around 40%. The deprotection reaction (eq 6) yields **11** quantitatively as a light brown oil, which was used without further purification.

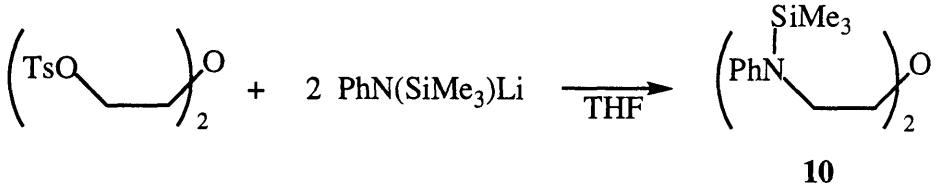

(5)

10

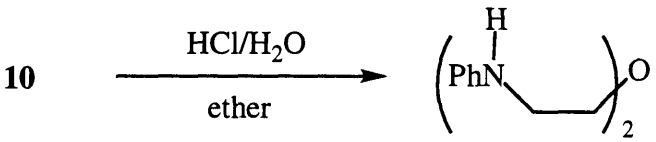

(6)

11

$H_2[PhN_2O]$

Zirconium Dichloride Complexes Containing the $[ArN_2O]^{2-}$ and $[Ar'N_2O]^{2-}$ Ligands.

The reaction of a protonated ligand with $Zr(NR_2)_4$ has been employed recently for the synthesis of zirconium bis(cyclopentadienyl) complexes[114-117] and has been shown in many cases to be a more elegant, high-yield entry into zirconium chemistry than the traditional metathesis reaction of zirconium tetrachloride with the lithium salt of the ligand.

The $Zr(NR_2)_4$ route works also well with amide based ligand systems.[98,107] An example was already introduced earlier in this chapter by the synthesis of **2**.

Addition of $Zr(NMe_2)_4$ to **8** in pentane yields $[ArN_2O]Zr(NMe_2)_2$ (**12**) in 68% yield (eq 7). The product crystallizes out of the reaction mixture at room temperature. Reaction of **12** with excess trimethylsilylchloride in ether gives $[ArN_2O]ZrCl_2$ (**13**) in good yield (73%) (eq 7).

$$\mathbf{8} + Zr(NMe_2)_4 \xrightarrow[\text{pentane}]{} \underset{\mathbf{12}}{[ArN_2O]Zr(NMe_2)_2} \xrightarrow[\text{ether}]{\text{xs TMSCl}} \underset{\mathbf{13}}{[ArN_2O]ZrCl_2} \qquad (7)$$

$[Ar'N_2O]ZrCl_2$ (**17**) is accessible from **9** in two straightforward steps analogous to the synthesis of **13** (eq 8). The higher crystallinity of complexes containing the $[Ar'N_2O]^{2-}$ ligand compared to those containing the $[ArN_2O]^{2-}$ ligand leads to higher isolated yields for the former. $[Ar'N_2O]Zr(NMe_2)_2$ (**16**) crystallizes within minutes during addition of $Zr(NMe_2)_4$ to **9** and can be obtained in excellent isolated yield (97%). Reaction

$$\mathbf{9} + Zr(NMe_2)_4 \xrightarrow[\text{pentane}]{} \underset{\mathbf{16}}{[Ar'N_2O]Zr(NMe_2)_2} \xrightarrow[\text{ether}]{\text{xs TMSCl}} \underset{\mathbf{17}}{[Ar'N_2O]ZrCl_2} \qquad (8)$$

of **16** with excess trimethylsilylchloride in ether gives $[Ar'N_2O]ZrCl_2$ (**17**) in high yield (88%). It is important to note that the reaction mixtures in the syntheses of the zirconium dichloride compounds **13** and **17** have to be kept sufficiently dilute, otherwise $[ArN_2O]Zr(NMe_2)Cl$ and $[Ar'N_2O]Zr(NMe_2)Cl$ cocrystallize with **13** and **17**, respectively.

Synthesis of Zirconium Complexes Containing the $[PhN_2O]^{2-}$ Ligand.

All attempts to synthesize $[PhN_2O]ZrCl_2$ directly by metathesis of the trimethylsilyl substituted ligand **10** with $ZrCl_4$ or $ZrCl_4(THF)_2$ failed,[97] whereas the aminolysis reaction between $Zr(NMe_2)_4$ and **11** provided $[PhN_2O]Zr(NMe_2)_2(HNMe_2)$ (**21**) in 78% yield as colorless crystals (eq 9). Coordination of the generated dimethylamine to the metal center is an indication for the small, steric demand of the $[PhN_2O]^{2-}$ ligand.

$$\mathbf{11} \quad + \quad Zr(NMe_2)_4 \xrightarrow[\text{pentane}]{} \underset{\mathbf{21}}{[PhN_2O]Zr(NMe_2)_2(HNMe_2)} \qquad (9)$$

In contrast to the syntheses of **13** and **17**, the trimethylsilyl substituted ligand **10** is recovered from the reaction of **21** with excess Me_3SiCl. All attempts to produce the zirconium dihalide complex by reaction of **21** with Me_3SiCl or CH_3I at various temperatures and concentrations failed, suggesting that the phenylamides are more susceptible towards electrophilic attack than the NMe_2 groups. These results suggest that lack of protection of the amide nitrogens by substituents in the *ortho* positions of the phenyl ring prohibit the role of the $[PhN_2O]^{2-}$ ligand as an innocent ligand.

Synthesis of Zirconium Dialkyl Complexes.

The readily available dichlorides **13** and **17** are excellent precursors for the preparation of a variety of alkyl complexes. $[ArN_2O]ZrMe_2$ (**14**) can be obtained by reaction of two equivalents of BrMgMe with **13** as colorless cubes in 72% yield (eq 10). Alkylation of **13** with $BrMgCH_2CHMe_2$ in diethyl ether produces $[ArN_2O]Zr(CH_2CHMe_2)_2$ (**15**) as colorless crystals (eq 10).

$$\mathbf{13} \xrightarrow[\text{ether}]{\text{2 BrMgR}} [ArN_2O]ZrR_2 \qquad (10)$$

R = Me (**14**), CH_2CHMe_2 (**15**)

^1H and ^{13}C NMR spectra of **14** exhibit only one sharp resonance for the Me groups and are indicative of a compound with C_{2v} symmetry. Interestingly, two signals are observed for the isopropylmethyl groups in complex **14**. The diastereotopic methyl groups can only be explained with a hindered rotation around the N-C_{ipso} bond. C_{2v} symmetry on the NMR time scale and rotation around the N-C_{ipso} bond would render all isopropylmethyl groups indistinguishable. Analogous NMR characteristics were found for all complexes containing the $[ArN_2O]^{2-}$ ligand.

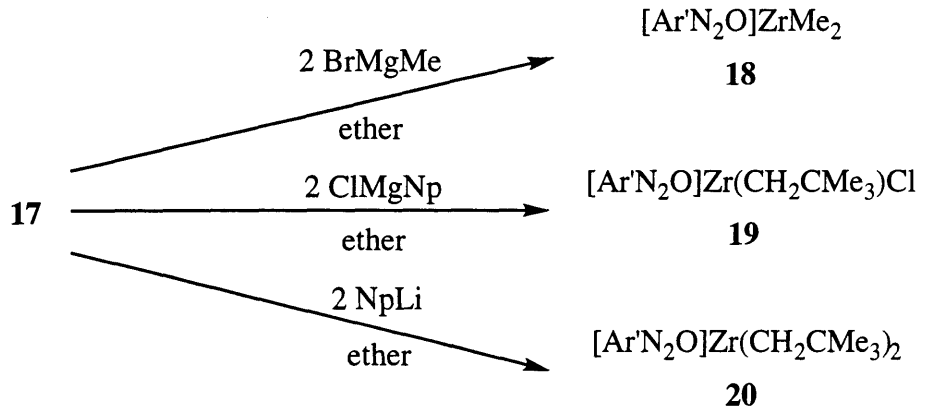

Scheme 4.2. Alkyl Derivatives Available from Dichloride Complex **17**.

Alkylation of **17** with 2 equiv of BrMgMe gives $[Ar'N_2O]ZrMe_2$ (**18**) in 69% yield (Scheme 4.2). Reaction of **17** with 2.2 equiv of $BrMgCH_2CMe_3$ does not yield the corresponding bis(neopentyl) complex, but instead produces the mono alkylated compound **19** (Scheme 4.2) in low isolated yield (24%). However the bis(neopentyl) complex **20** is accessible through the reaction of **17** with 2 equiv of neopentyllithium (Scheme 4.2). **20** is stable in the solid state, but decomposes in solution at room temperature within few hours. We assume a similar restricted rotation for the N-C_{ipso} bond in the 2,6-

dimethylphenyl substituted complexes, although we have no spectroscopic handle to prove it.

An important question has remained unanswered so far: Which type of coordination geometry around the metal center is favored by the $[ArN_2O]^{2-}$ and $[Ar'N_2O]^{2-}$ ligands in the solid state? At this stage we expected a trigonal bipyramidal coordination environment similar to the structures of $[NON]TiMe_2$ and $\{[NON]ZrMe\}[MeB(C_6F_5)_3]$, where the ligand amides and one methyl group are positioned in the plane and the O and the remaining methyl group in the apical positions. Analogous to the complexes containing the $[ArN_2O]^{2-}$ and $[Ar'N_2O]^{2-}$ ligand, NMR spectra of $[NON]TiMe_2$ also revealed C_{2v} symmetry in solution. An equilibrating process via a planar intermediate of the $[NON]^{2-}$ ligand was proposed for the observed C_{2v} symmetry on the NMR time scale. A trigonal bipyramidal coordination sphere was also reported for the related structures of $[(Me_3SiNCH_2CH_2)_2N(SiMe_3)]TiMe_2$[104] and $[(Me_3SiNCH_2CH_2)_2N(SiMe_3)]ZrCl[CH(SiMe_3)_2]$.[94]

An X-ray structural study of **18** showed a distorted trigonal bipyramidal environment at the zirconium center (Table 4.3; Figure 4.3 and 4.4; relevant bond lengths and angles are listed in Table 4.4.). The Zr-N bond distances of 2.084(3) Å each are slightly longer than in $\{[NON]ZrMe\}[MeB(C_6F_5)_3]$ (2.049(10) and 2.065(10) Å) and well in the range found for other zirconium-amido complexes. A Zr-O(2) bond length of 2.336(3) Å suggests a $Zr\text{-}O_{donor}$ bond. The structure has a crystallographic mirror plane defined by Zr, O(2), C(5) and C(6). In sharp contrast to the $[NON]^{2-}$ complexes mentioned above, however, the N atoms occupy the apical and the methyl groups the equatorial positions. Zr, O(2), N(3) and N(4) lie approximately in a plane and as a consequence the aryl rings are symmetrically positioned above and below the two coordination sites. The planes of the aryl rings are perpendicular to the Zr-O(2)-N(3)-N(4) plane. Although the C-O-C angles in the structures of $[NON]TiMe_2$ (115.5(4)°) and

Table 4.3. Crystallographic Data, Collection Parameters, and Refinement Parameters for [Ar'N_2O]ZrMe_2 (**18**).

Empirical Formula	$C_{22}H_{32}N_2OZr$
Formula Weight	431.72
Diffractometer	Enraf-Nonius CAD-4
Crystal Color	colorless
Crystal Dimensions (mm)	0.20 x 0.20 x 0.12
Crystal System	orthorhombic
a	12.741(3) Å
b	22.663(5) Å
c	7.518(2) Å
α	90°
β	90°
γ	90°
V	2170.9(8) $Å^3$
Space Group	Pnma
Z	4
D_{calc}	1.321 g/cm^3
F_{000}	904
Diffractometer	Siemens SMART/CCD
$\lambda(MoK_\alpha)$	0.71073 Å
Scan Type	ω scans
Temperature	183(2) K
Total No. Unique Reflections	1607
No. Variables	125
R	0.0368
R_w	0.1009
GoF	1.179

Figure 4.2. X-ray Crystal Structure of [Ar'N_2O]ZrMe_2 (**18**) with View Perpendicular to the ZrN_2O Plane.

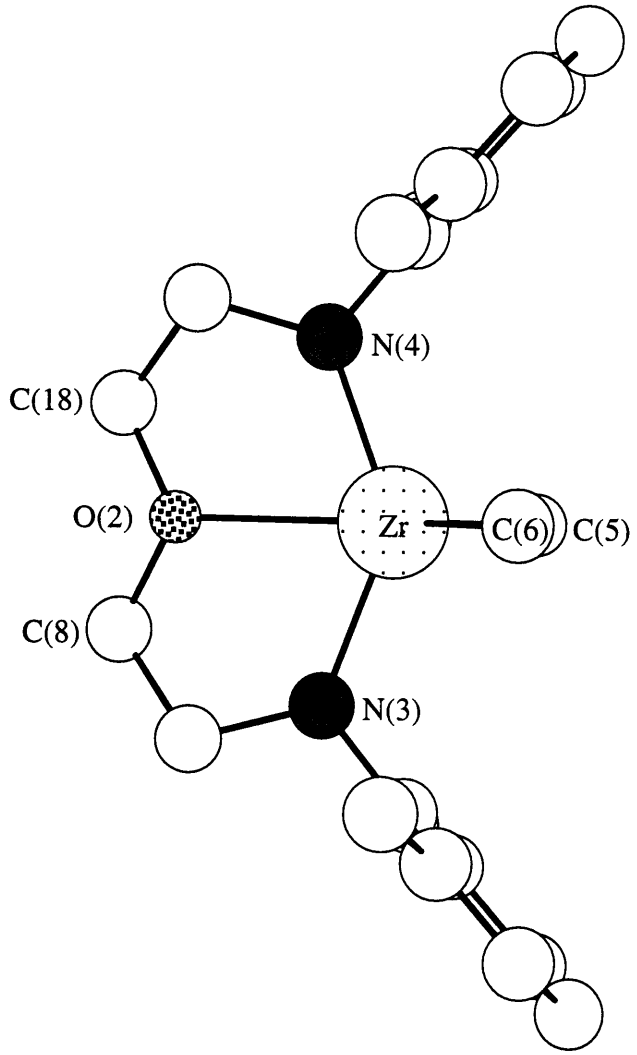

Figure 4.3. X-ray Crystal Structure of [Ar'N_2O]ZrMe_2 (**18**) with View along the Zr-O Bond.

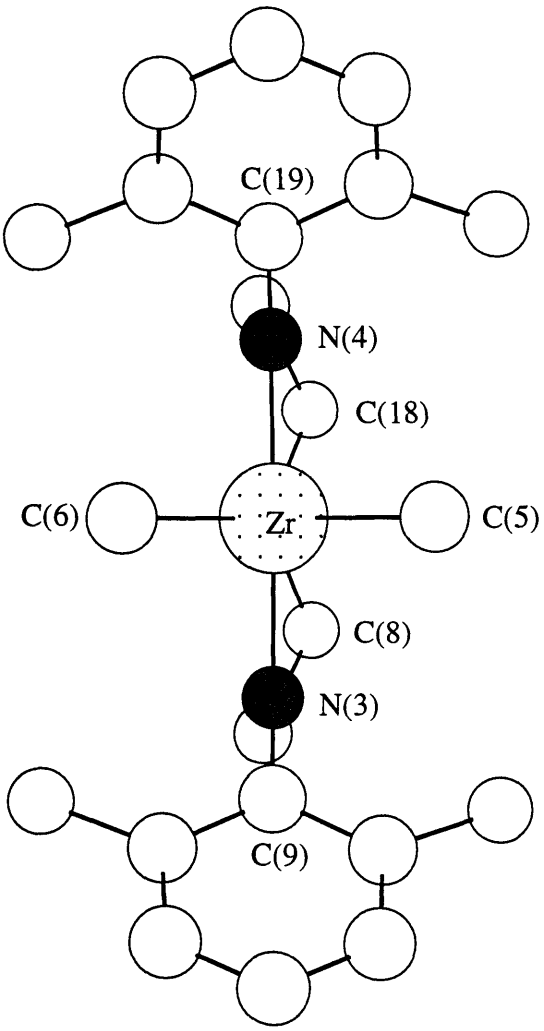

Table 4.4. Selected Interatomic Distances (Å) and Angles (deg) for the Non-Hydrogen Atoms of [Ar'N_2O]ZrMe_2 (**18**).

Bond Lengths

Zr-N(3)	2.084(3)	Zr-C(5)	2.255(6)
Zr-N(4)	2.084(3)	Zr-C(6)	2.253(6)
Zr-O(2)	2.336(3)		

Bond Angles

N(3)-Zr-N(4)	139.1(2)	O(2)-Zr-C(5)	129.7(2)
N(3)-Zr-C(5)	102.9(1)	O(2)-Zr-C(6)	130.2(2)
N(3)-Zr-C(6)	103.1(1)	C(5)-Zr-C(6)	100.0(2)
N(4)-Zr-C(5)	102.9(1)	C(8)-O(2)-C(18)	113.7(4)
N(4)-Zr-C(6)	103.1(1)	C(9)-N(3)-Zr	120.2(2)
N(3)-Zr-O(2)	69.54(9)	C(19)-N(4)-Zr	120.2(2)
N(4)-Zr-O(2)	69.54(9)		

{[NON]ZrMe}[Me$B(C_6F_5)_3$] (116.4(9)°) are in the same range as for **18** (C(8)-O(2)-C(18) = 113.7(4)°), only in the compounds with the rigid phenylene backbone is this angle translated into the coordination geometry. The 'flexible' ligand backbone apparently permits the bulky aryl groups to be as far apart as possible. The structure is closely related to the structure of [(2,6-Et_2-$C_6H_3NCH_2)_2NC_5H_3$]ZrMe_2 ([BDEP]ZrMe_2) (Figure 4.4).[98]

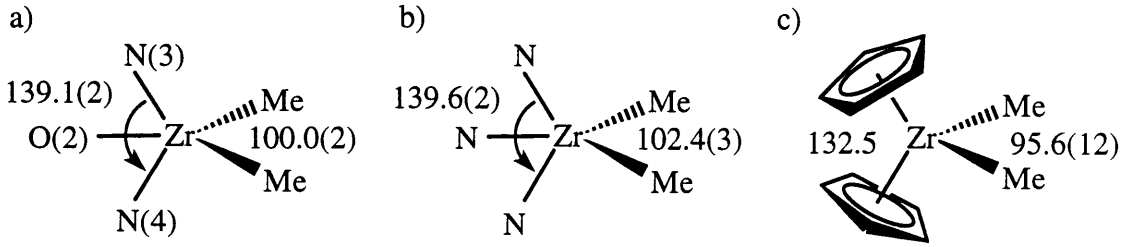

Figure 4.4. Coordination Sphere of (a) **18**, (b) [BDEP]$ZrMe_2$ and (c) Cp_2ZrMe_2.

The coordination spheres of **18** and [BDEP]$ZrMe_2$ closely resemble that of Cp_2ZrMe_2. Frontier orbitals very similar to those of Cp_2ZrMe_2 can be expected for **18** as were reported for [BDEP]$ZrMe_2$. An important difference between [BDEP]$ZrMe_2$ and **18** is the rigidity of the $[BDEP]^{2-}$ ligand. The flexibility of the $[Ar'N_2O]^{2-}$ ligand backbone could permit a different coordination sphere for a cationic species.

The analogy between the coordination spheres of [BDEP]$ZrMe_2$ and **18** offers an explanation for the observed, high susceptibilty towards electrophilic attack on the amides of the $[PhN_2O]^{2-}$ ligand assuming that the $[PhN_2O]^{2-}$ ligand occupies essentially the same geometry as found for the $[BDEP]^{2-}$ ligand in [BDEP]$ZrMe_2$ and the $[Ar'N_2O]$ ligand in **18**. Frontier orbital calculations[98] for [BDEP]$ZrMe_2$ showed that only the asymmetrical combination of the p-orbitals of the amides can sufficiently overlap with a zirconium based orbital resulting in a ligand centered nonbonding orbital on the amides. In complexes containing the $[ArN_2O]^{2-}$ and the $[Ar'N_2O]^{2-}$ ligand this orbital is protected by the *ortho* substituents.

Generation and Observation of Zirconium Alkyl Cations.

Addition of $[PhNMe_2H][B(C_6F_5)_4]$ to **14** in chlorobenzene-d_5 at -30 °C cleanly generates $\{[ArN_2O]ZrMe(PhNMe_2\}[B(C_6F_5)_4]$ (**22**). **22** is stable at room temperature for at least 1 h. Reaction under various conditions of bis(isobutyl) complex **15** with either $[PhNMe_2H][B(C_6F_5)_4]$ (**I**) or $[Ph_3C][B(C_6F_5)_4]$ (**II**) in C_6D_5Cl did not yield a single product.

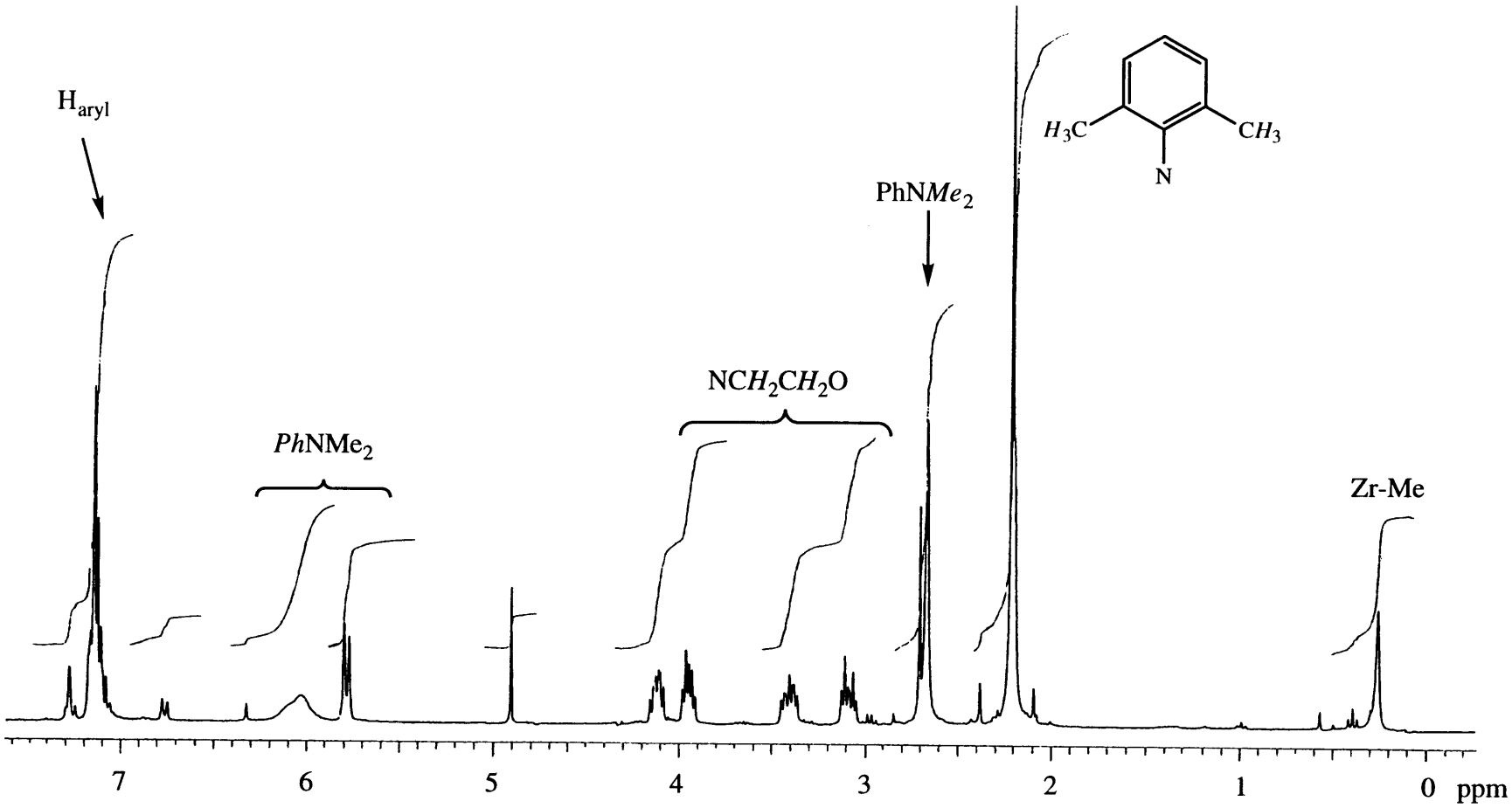

Figure 4.5. ^{1}H NMR Spectrum of the Reaction of [PhNMe$_2$H][B(C$_6$F$_5$)$_4$] with **18**.

Addition of **I** to **18** forms {[Ar'N_2O]ZrMe($PhNMe_2$}[$B(C_6F_5)_4$] (**23**) at -30 °C in chlorobenzene-d_5. The proton NMR spectrum at room temperature is shown in Figure 4.5. Aryl resonances at approximately 6 ppm and a broad signal at 2.67 ppm for the methyl groups suggest that dimethylaniline is coordinated (sharp singlet at 2.70 ppm for free $PhNMe_2$). Four multiplets between 3.0 and 4.2 ppm represent the AA'BB' pattern for each ligand arm. A coordination sphere similar to that of **18** with one methyl group replaced by $PhNMe_2$ is most likely for **22** and **23**, but a coordination geometry analogous to that of {[NON]ZrMe}[$MeB(C_6F_5)_3$] can not be excluded at this stage. **23** starts to decompose within minutes at room temperature and is considerably less stable in solution than **22** consistent with better steric protection against decomposition for the complex containing the bulkier 2,6-diisopropylphenyl substituted ligand.

Polymerization of 1-Hexene.

Complex **6** containing the $[NSiN_2]^{2-}$ ligand proved to be inactive towards the polymerization of 1-hexene. No polymer could be obtained from the addition of 1-hexene to the reaction mixture of **6** and either [$PhNMe_2H$][$B(C_6F_5)_4$] (**I**) or [Ph_3C][$B(C_6F_5)_4$] (**II**) in chlorobenzene at 0 °C. The X-ray structural study of $MgCl_2$-bridged dimer **7** already showed a high susceptible of the bridging amide towards electrophilic attack. In view of the activation involving **I**, protonation could alternatively happen at the bridging amide, as was found for related tantalum complexes.

Alkyl complexes **14** and **15** containing the $[ArN_2O]^{2-}$ ligand can be activated by either **I** or **II** for the polymerization of 1-hexene in chlorobenzene at 0 °C. Polymerization results are summarized in Table 4.5.

Quantitative polymerization yields prove 100% conversion, however the molecular weights of the polymers were found to be significantly smaller than expected. These results suggest that chain termination competes significantly with propagation. The approximately quantitative yields indicate that the catalytic center remains active after the

chain termination step. The carbon NMR spectrum of the polymer in entry 1 (Table 4.5) shows resonances in the olefinic region and resonances between 28 and 35 ppm typical for branching supporting the assumption that β-hydride elimination is the chain termination step. The smaller than expected polymer molecular weights suggest that already formed polymer chains insert with a slower rate than the monomer.

Table 4.5. GPC and Yield Data for Poly(1-hexene)$_n$ Prepared Using Catalysts **14** and **15** and Cocatalysts $[PhNMe_2H][B(C_6F_5)_4]$ (**I**) and $[Ph_3C][B(C_6F_5)_4]$ (**II**) at 0 °C.[a]

entry	catalyst	cocatalyst	M_n(theory)	M_n[b]	M_w[b]	M_w/M_n[b]	yield (%)
1	**14**	**I**	13440	2670	3560	1.33	96
2	**14**	**II**	16800	2460	4220	1.72	96
3	**15**	**I**	16800	2650	8550	3.23	94
4[c]	**15**	**II**	16800	1010	2640	2.62	[d]

[a] Catalyst (44 μmol), cocatalyst (40 μmol), 200 equiv (entry 1: 160 equiv) 1-hexene, 10 mL chlorobenzene (for details see experimental section). [b] Determined by GPC on-line light scattering (Wyatt Technology). [c] In the presence of N,N-dimethylaniline. [d] Not available.

Bis(isobutyl) complexes such as **15** are interesting precursors for the polymerization of α olefins. Provided that the transformation to the corresponding cation proceeds cleanly, the cationic monoisobutyl zirconium species can be viewed as the first insertion product with 1,2-regioselectivity of propene into a Zr-Me unit. Therefore the rate of initiation and the rate of propagation should be in a comparable range for an initiator of that type and k_p/k_i problems could possibly be avoided. Polymerizations employing **15** at 0 °C produced polymers with relatively broad polymer distributions (entries 3 and 4, Table 4.5). Polymerization activity is shut down in the presence of 2,4-lutidine.

The lowest polydispersity (PDI = 1.33) was found in the polymer generated using **14** activated with **I**. The considerably lower polydispersities employing initiator **14** compared to **15** are probably a consequence of the extent of cation formation as addressed in the preceding section.

The steric bulk of the $[ArN_2O]^{2-}$ ligand offers a possible explanation for the observed loss of olefin via β elimination. Bimolecular propagation and monomolecular β-hydride elimination are competing reactions in Ziegler-Natta type olefin polymerization. A crowded coordination site not only hinders approach of the monomer, thereby slowing down the propagation rate, but also favors the small hydride (product of β hydride elimination) over the growing alkyl chain. The bulky ligand sphere apparently stabilizes the hydride sufficiently as indicated by the quantitative polymer yields.

In view of these considerations we were interested in how the substantially less crowded complexes containing the $[Ar'N_2O]^{2-}$ ligand would perform as catalysts for the polymerization of 1-hexene. In Chapter 2 we discussed that a smaller alkylidene ligand generally results in a smaller k_p/k_i. The reasoning was that the monomer triple bond simply can access the alkylidene double bond better leading to a faster rate of initiation. Qualitatively the situation is quite the contrary for the zirconium alkyl cation in Ziegler-Natta type polymerization of α olefins as was mentioned already for bis(isobutyl) complex **15**. Since the metal alkyl cation usually is low coordinate and extremely electron deficient, the olefin has to compete with solvent molecules or other electron donors such as the generated dimethylaniline in reactions involving **I** for the vacant coordination site. If the alkyl ligand is considerably smaller than the growing polymer chain at the metal center, the electron donor will bind tighter to the metal center deactivating the initiator species. The result is an increased k_p/k_i. Bis(neopentyl) complex **20** qualifies as a suitable candidate in view of a large alkyl group. GPC and yield data for polymers prepared using **18** and **20** are listed in Table 4.6.

The average number molecular weights of polymers prepared by using **18** and **I** or **II** as cocatalysts are still lower than expected, but significantly higher than those prepared by employing **14** or **15**. Polymer polydispersities of approximately 1.5 are in the same range as found for **14**. Surprisingly the yield for all polymerizations involving **18** and **I** was found to be between 65 and 70%. Polymers synthesized by using bis(neopentyl) complex **20** exhibited larger than expected molecular weights and a high molecular weight peak in the GPC trace.

Table 4.6. GPC and Yield Data for Poly(1-hexene)$_{200}$ Prepared Using Catalysts **18** and **20** and Cocatalysts $[PhNMe_2H][B(C_6F_5)_4]$ (**I**) and $[Ph_3C][B(C_6F_5)_4]$ (**II**) at 0 °C.[a]

entry	catalyst	cocatalyst	M_n(theory)	M_n[b]	M_w[b]	M_w/M_n[b]	yield (%)
1	**18**	**I**	16800	9000	13000	1.44	70[c]
2	**18**	**II**	16800	11700	18000	1.55	100
3	**20**	**I**	16800	25400	83500	3.3	90
4	**20**	**II**	16800	27500	77300	2.8	93

[a] Catalyst (44 μmol), cocatalyst (40 μmol), 200 equiv 1-hexene, 10 mL chlorobenzene (for details see experimental section). [b] Determined by GPC on-line light scattering (Wyatt Technology). [c] The experiment was repeated several times and polymer yields always were found between 65 and 70%.

The carbon NMR spectrum of the polymer prepared using **18** and **I** (entry 1, Table 4.6) exhibits no olefinic resonances and no peaks attributable to polymer branching or cross linking, in contrast to the polymer prepared using **14** containing the bulkier $[ArN_2O]^{2-}$ ligand and **I** (entry 3, Table 4.5). The ^{13}C NMR spectrum is consistent with a regioregular polymer structure.[118]

CONCLUSIONS

Recent reports of the living Ziegler-Natta type polymerization of 1-hexene using catalysts containing chelating diamide ligands motivated us to explore related catalysts based on tridentate diamide ligands with focus on short, low cost ligand syntheses. A family of zirconium dialkyl complexes containing the $[NSiN_2]^{2-}$ ligand can easily be prepared. Unfortunately $[NSiN_2]Zr(CH_2CHMe_2)_2$ could not be activated by $[PhNMe_2H][B(C_6F_5)_4]$ or $[Ph_3C][B(C_6F_5)_4]$ to polymerize 1-hexene. An X-ray structural study of the $MgCl_2$-bridged dimer of $[NSiN_2]Zr(CH_2CHMe_2)_2$ indicated the susceptibility of the $[NSiN_2]^{2-}$ ligand towards electrophilic attack.

A class of ligand systems of the type $(RNHCH_2CH_2)O$ (R = 2,6-*i*-Pr_2-C_6H_3 and 2,6-Me_2-C_6H_3) related to the H_2[NON] ligand can be conveniently prepared in one step. Although electronically comparable to the $[NON]^{2-}$ ligand, the different steric demand of the aryl substituents and a flexible, saturated ligand backbone led to substantial differences in the coordination environment and polymerization behavior. An X-ray structural study of $[Ar'N_2O]ZrMe_2$ revealed a coordination sphere more similar to that of Cp_2ZrMe_2 than that of $[NON]^{2-}$ complexes. Clean generation of cations was only observed for the dimethyl complexes. As a result polymerizations of 1-hexene involving dimethyl complexes were generally found to be better behaved than those involving complexes containing larger alkyls (i.e. neopentyl). Evidence for β hydride elimination was found for catalysts containing the bulky $[ArN_2O]^{2-}$ ligand, although the β hydrogen containing complex $[ArN_2O]Zr(CH_2CHMe_2)_2$ was isolated and fully characterized. A regioregular structure was found for polymers synthesized by employing $[Ar'N_2O]ZrMe_2$.

EXPERIMENTAL

General details. All experiments were performed in a Vacuum Atmospheres dry box under a nitrogen atmosphere or by standard Schlenk techniques under an argon atmosphere unless specified otherwise. Celite and alumina were dried at ~130 °C for several days.

Pentane was washed with sulfuric/nitric acid (95/5 v/v), sodium bicarbonate and water, stored over calcium chloride, and distilled from sodium benzophenone ketyl under nitrogen. Reagent grade diethyl ether, tetrahydrofuran, toluene, benzene and 1,2-dimethoxyethane were distilled from sodium benzophenone ketyl under nitrogen. Reagent grade dichloromethane was distilled from calcium hydride under nitrogen. Chlorobenzene was distilled from calcium hydride and stored over activated alumina.

All gel permeation chromatography (GPC) experiments were carried out using two Jordi-Gel DVB Mixed Bed columns in series and a Wyatt Mini Dawn light scattering detector and a Knauer Refractometer on samples 0.5-0.6% w/v in CH_2Cl_2, which were filtered through a Millex-SR 0.5 μm filter in order to remove particulates. The GPC data were analyzed using Astrette 1.2 (Wyatt Technology). NMR data were obtained at 300 MHz (^1H) and 75.43 MHz (^{13}C) on a Varian XL 300 or a Varian Unity 300 NMR spectrometer or at 500 MHz (^1H) and 125 MHz (^{13}C) on a Varian 500 NMR spectrometer and are listed in parts per million downfield from tetramethylsilane for proton and carbon. Spectra were obtained at room temperature unless otherwise noted. Benzene-d_6 and dichloromethane-d_2 were sparged with argon and stored over molecular sieves (4Å). Chlorobenzene-d_5 and bromobenzene-d_5 were sparged with argon, stored over alumina and passed through alumina prior to use.

Elemental analyses (C, H, N) were performed using a Perkin-Elmer 2400 CHN analyzer in our laboratories. X-ray data were collected on a Siemens platform goniometer with a CCD detector.

All chemicals used were reagent grade (Aldrich) and used without further purification unless specified otherwise. $ClMe_2SiNH(t\text{-Bu})$[109] was prepared as reported in the literature.

***t*-BuNHSiMe$_2$NHCH$_2$CH$_2$NMe$_2$ (1) (= H$_2$[NSiN$_2$]).** Solid $LiNHCH_2CH_2NMe_2$ (5.67 g, 60.3 mmol) was added over 10 min to a solution of $ClMe_2SiNH(t\text{-Bu})$ (10 g, 60.3 mmol) in THF at -30 °C. The reaction mixture was stirred

overnight at room temperature. All volatiles were removed under vacuum and the residue was extracted with pentane. Removal of solvents under vacuum gave **1** as a colorless oil (12.3 g, 93%) which could be used without further purification: ^{1}H NMR ($CDCl_3$) δ 2.79 (q, 2H, NHCH_2), 2.26 (t, 2H, CH_2NMe_2), 2.19 (s, 6H, NMe_2), 1.13 (s, 9H, CMe_3), 0.81 (br t, 1H, CH_2NH), 0.68 (br, 1H, *t*-BuNH), 0.00 (s, 6H, SiMe_2); ^{13}C NMR ($CDCl_3$) δ 63.2 (NHCH_2), 49.0 (*C*Me_3), 45.6 (NMe_2), 39.0 (*C*H_2NMe_2), 33.6 (CMe_3), 0.6 (SiMe_2).

[*t*-BuNSiMe$_2$NCH$_2$CH$_2$NMe$_2$]Zr(NMe$_2$)$_2$ (2). A solution of **1** (3.89 g, 17.9 mmol) in pentane (5 mL) was added over 10 min to a solution of Zr(NMe_2)$_4$ (4.25 g, 17.9 mmol) in pentane (10 mL) at room temperature. The reaction mixture was mixed well by vigorous shaking and after standing at room temperature for 5 h, it was concentrated to about 6 mL and allowed to crystallize at -30 °C. Analytically pure crystals were isolated and upon further concentration of the mother liquor a second crop was obtained. Total yield was 5.6 g (79%): ^{1}H NMR (C_6D_6) δ 3.40 (t, 2H, SiNCH_2), 2.92 (s, 12H, ZrNMe_2), 2.15 (t, 2H, CH_2NMe_2), 1.87 (s, 6H, NMe_2), 1.47 (s, 9H, CMe_3), 0.51 (s, 6H, SiMe_2); ^{13}C NMR (C_6D_6) δ 65.3 (SiNCH_2), 54.9 (*C*Me_3), 46.7 (*C*H_2NMe_2), 46.1 (NMe_2), 43.0 (ZrNMe_2), 36.4 (CMe_3), 4.8 (SiMe_2). Anal. Calcd. for $C_{14}H_{37}N_5SiZr$: C, 42.59; H, 9.45; N, 17.74. Found: C, 42.68; H, 9.74; N, 18.03.

[*t*-BuNSiMe$_2$NCH$_2$CH$_2$NMe$_2$]ZrCl$_2$ (3). Neat TMSCl (1.87 g, 17.2 mmol) was added to a solution of **2** (1.7 g, 4.3 mmol) in 10 mL pentane at room temperature. After thorough mixing by vigorous shaking the reaction mixture was allowed to stand overnight at room temperature. Colorless crystals (1.6 g) were obtained after 2 h at -30 °C in 98% yield. ^{1}H NMR (C_6D_6) δ 3.22 (t, 2H, SiNCH_2), 2.41 (t, 2H, CH_2NMe_2), 2.24 (s, 6H, NMe_2), 1.50 (s, 9H, CMe_3), 0.34 (s, 6H, SiMe_2); ^{13}C NMR (C_6D_6) δ 65.4 (SiNCH_2), 57.5 (*C*Me_3), 48.1 (*C*H_2NMe_2), 47.2 (NMe_2), 34.3 (CMe_3), 3.2 (SiMe_2). Anal. Calcd. for $C_{10}H_{25}Cl_2N_3SiZr$: C, 31.81; H, 6.67; N, 11.13. Found: C, 31.98; H, 6.75; N, 10.98.

Alternative one-pot synthesis of 3. A solution of **1** (4.80 g, 22.0 mmol) in pentane (10 mL) was added over 10 min to a solution of $Zr(NMe_2)_4$ (5.90 g, 22.0 mmol) in pentane (20 mL) at room temperature. The reaction mixture was mixed well by vigorous shaking and after standing at room temperature for 6 h neat TMSCl (9.6 g, 88.0 mmol) was added. After shaking the flask several times, the reaction mixture was allowed to stand overnight at room temperature. Colorless crystals (7.3 g) were obtained at -30 °C in 88% overall yield.

[*t*-BuNSiMe$_2$NCH$_2$CH$_2$NMe$_2$]Zr(CH$_2$SiMe$_3$)$_2$ (4). A solution of $LiCH_2SiMe_3$ (205 mg, 2.17 mmol) in diethyl ether (3 mL) was added within 1 min to a solution of **3** (400 mg, 1.06 mmol) in ether (5 mL) at -30 °C. Within seconds a fine precipitate appeared. Allowing the reaction mixture to warm to room temperature, it was stirred for 20 min followed by fitration through Celite. Removal of solvents under vacuum gave a colorless oil in quantitative yield. Although at least 95% pure by NMR, **4** failed to crystallize: ^{1}H NMR (C_6D_6) δ 3.30 (t, 2H, $SiNCH_2$), 2.32 (t, 2H, CH_2NMe_2), 2.06 (s, 6H, NMe_2), 1.51 (s, 9H, CMe_3), 0.41 (s, 6H, $SiMe_2$), 0.18 (d, 2H, $ZrCH_2$), -0.01 (d, 2H, $ZrCH_2$); ^{13}C NMR (C_6D_6) δ 66.1 ($SiNCH_2$), 56.0 (CMe_3), 49.1 ($ZrCH_2$), 47.1 (NMe_2), 46.8 (CH_2NMe_2), 35.9 (CMe_3), 4.9 ($SiMe_2$), 4.5 ($SiMe_3$).

[*t*-BuNSiMe$_2$NCH$_2$CH$_2$NMe$_2$]Zr(CH$_2$Ph)$_2$ (5). A solution of $ClMgCH_2Ph$ (1.0 M in ether, 6.5 mL, 6.5 mmol) was added to a solution of **3** (1.2 g, 3.18 mmol) in diethyl ether (10 mL) at -30 °C. Almost immediately a fine precipitate formed and after 15 min of stirring and warming to room temperature, the reaction mixture was filtered through Celite. All volatiles were removed under vacuum and the residue was extracted with pentane. Recrystallization at -30 °C from pentane yielded yellow crystals (1.18 g) in 76% yield: ^{1}H NMR (C_6D_6) δ 7.11 (t, 4H, H_m), 6.98 (d, 4H, H_o), 6.83 (t, 2H, H_p), 3.14 (t, 2H, $SiNCH_2$), 2.18 (d, 2H, $ZrCH_2$), 2.07 (d, 2H, $ZrCH_2$), 1.94 (t, 2H, CH_2NMe_2), 1.66 (s, 6H, NMe_2), 1.33 (s, 9H, CMe_3), 0.36 (s, 6H, $SiMe_2$); ^{13}C NMR (C_6D_6) δ 147.5 (C_{ipso}), 129.5 (C_o), 127.3 (C_m), 121.7 (C_p), 65.7 ($SiNCH_2$), 59.9

($ZrCH_2$), 56.6 (CMe_3), 46.9 (CH_2NMe_2), 45.5 (NMe_2), 35.5 (CMe_3), 4.4 ($SiMe_2$). Anal. Calcd. for $C_{24}H_{39}N_3SiZr$: C, 58.96; H, 8.04; N, 8.59. Found: C, 58.66; H, 8.23; N, 8.58.

[*t*-BuNSiMe$_2$NCH$_2$CH$_2$NMe$_2$]Zr(CH$_2$CHMe$_2$)$_2$ (6). A solution of $BrMgCH_2CHMe_2$ (2.51 M in ether, 3.0 mL, 7.55 mmol) was added to a solution of **3** (1.39 g, 3.67 mmol) in diethyl ether (15 mL) at -30 °C. A fine precipitate formed upon addition and after 15 min of stirring under warming to room temperature, dioxane (663 mg, 7.55 mmol) was added. After 20 min of additional stirring all volatiles were removed under vacuum and the residue was extracted with pentane. Recrystallization at -30 °C from only 2 mL pentane yielded yellow crystals (1.2 g) in 78% yield: ^{1}H NMR (C_6D_6) δ 3.35 (t, 2H, $SiNCH_2$), 2.29 (t, 2H, CH_2NMe_2), 2.24 (m, 2H, CH_2CHMe_2), 2.03 (s, 6H, NMe_2), 1.55 (s, 9H, CMe_3), 1.18 (d, 6H, CH_2CHMe_2), 1.15 (d, 6H, CH_2CHMe_2), 0.78 (d, 2H, $ZrCH_2$), 0.54 (d, 2H, $ZrCH_2$), 0.43 (s, 6H, $SiMe_2$); ^{13}C NMR (C_6D_6) δ 72.1 ($ZrCH_2$), 65.9 ($SiNCH_2$), 55.9 (CMe_3), 46.8 (CH_2NMe_2), 46.5 (NMe_2), 35.9 (CMe_3), 30.5 (CH_2CHMe_2), 29.9 (CH_2CHMe_2), 29.7 (CH_2CHMe_2), 4.4 ($SiMe_2$). Anal. Calcd. for $C_{18}H_{43}N_3SiZr$: C, 51.37; H, 10.30; N, 9.98. Found: C, 51.45; H, 10.53; N, 9.94.

X-ray structure of {[*t*-BuNSiMe$_2$NCH$_2$CH$_2$NMe$_2$]Zr(CH$_2$CHMe$_2$)$_2$ MgCl$_2$}$_2$ (7). In a similar preparation of **6**, where the addition of dioxane was omitted from the synthetic procedure, a small amount of crystals was obtained which proved to be insoluble in pentane at room temperature in contrast to crystals of **6**. X-ray structure analysis exhibited a magnesium chloride bridged dimeric structure for compound **7**.

General synthesis of lithium anilides. In a representative synthesis 2,6-Me_2-$C_6H_3NH_2$ (6 g, 49.5 mmol) was dissolved in 100 mL of pentane and chilled to -30 °C. Butyllithium (52.0 mol, 20.8 mL, 2.5 M in hexanes) was added over 10 min. Almost immediately precipitation of the lithium salt occured. The suspension was allowed to stir

for 3 h and was filtered through a medium frit. The collected solid was washed twice with pentane and dried in vacuo.

(2,6-*i*-Pr$_2$-C$_6$H$_3$NHCH$_2$CH$_2$)$_2$O (8) (= H$_2$[ArN$_2$O]). Solid (TsOCH$_2$CH$_2$)$_2$O (5 g, 12.0 mmol) was added to a chilled (-30 °C) solution of 2,6-*i*-Pr$_2$-C$_6$H$_3$NHLi (4.53 g, 24.8 mmol) in THF (30 mL). After stirring at room temperature for 24 h all volatiles were removed under vacuum. The residue was extracted with pentane. Removal of all volatiles under vacuum gave an orange oil (4.2 g, 82%), which was used without further purification. Upon standing the oil would crystallize in some cases. An analytically pure sample was obtained by recrystallization from a concentrated pentane solution at -30 °C: ^{1}H NMR (C$_6$D$_6$) δ 7.18 - 7.14 (m, 6H, H$_{aryl}$), 3.60 (t, 2H, NH), 3.48 (sep, 4H, C*H*Me$_2$), 3.35 (t, 4H, OCH$_2$), 3.07 (q, 4H, CH$_2$N), 1.06 (d, 24H, CH*Me*$_2$); (CDCl$_3$) δ 7.18 - 7.05 (m, 6H, H$_{aryl}$), 3.70 (t, 4H, OCH$_2$), 3.57 (br, 2H, NH), 3.36 (sep, 4H, C*H*Me$_2$), 3.14 (br t, 4H, CH$_2$N), 1.27 (d, 24H, CH*Me*$_2$). ^{13}C NMR (CDCl$_3$) δ 142.9 (C$_{ipso}$), 142.5 (C$_o$), 123.7 (C$_p$), 123.6 (C$_m$), 70.7 (OCH$_2$), 51.3 (CH$_2$N), 27.6 (*C*HMe$_2$), 24.3 (CH*Me*$_2$). Anal. Calcd. for C$_{28}$H$_{44}$N$_2$O: C, 79.19; H, 10.44; N, 6.60. Found: C, 79.14; H, 10.23; N, 6.30.

(2,6-Me$_2$-C$_6$H$_3$NHCH$_2$CH$_2$)$_2$O (9) (= H$_2$[Ar'N$_2$O]). Solid (TsOCH$_2$CH$_2$)$_2$O (6.47 g, 15.6 mmol) was added to a chilled (-30 °C) solution of 2,6-Me$_2$-C$_6$H$_3$NHLi (4.0 g, 31.5 mmol) in THF (40 mL). After stirring at room temperature for 72 h all volatiles were removed *in vacuo*. The residue was extracted with pentane. The solution was concentrated *in vacuo* until white crystals appeared. Recrystallization at -30 °C from pentane afforded colorless crystals (3.0 g, 9.6 mmol, 62%): ^{1}H NMR (C$_6$D$_6$) δ 6.99 (d, 4H, H$_m$), 6.88 (dd, 2H, H$_p$), 3.50 (t, 2H, NH), 3.15 (t, 4H, OCH$_2$), 2.95 (dt, 4H, CH$_2$N), 2.24 (s, 12H, Ar*Me*). ^{13}C NMR (C$_6$D$_6$) δ 146.8 (C$_{ipso}$), 130.2 (C$_o$), 129.6 (C$_m$), 122.7 (C$_p$), 70.8 (OCH$_2$), 48.6 (CH$_2$N), 18.9 (Ar*Me*). Anal. Calcd. for C$_{20}$H$_{28}$N$_2$O: C, 76.88; H, 9.03; N, 8.97. Found: C, 76.93; H, 8.96; N, 8.83.

$[C_6H_5N(SiMe_3)CH_2CH_2]_2O$ (10). A solution of n-butyllithium (30.3 mL, 48.4 mmol, 1.6 M in hexane) was added to a chilled (-30 °C) solution of $HNPh(SiMe_3)$ (8.0 g, 48.4 mmol) in DME (80 mL). The solution was stirred for 2 h at room temperature. Solid $(TsOCH_2CH_2)_2O$ (9.86 g, 23.8 mmol) was added and the resulting green solution was refluxed for 1.5 h. After 20 min during the reflux period, a precipitate appeared. The solution was allowed to cool to room temperature and all volatiles were removed under vacuum. The residue was extracted with pentane and the solvents were removed under vacuum. Distillation of the resulting yellow oil under reduced pressure (200 mTorr) allowed the separation of $HNPh(SiMe_3)$ (bp = 40 °C) from **10** (3.8 g, 40%; bp = 148 - 155 °C) as colorless oils: ^1H NMR (C_6D_6) δ 7.15 (t, 4H, H_m), 6.98 (d, 4H, H_o), 6.86 (t, 2H, H_p), 3.44 (t, 4H, OCH_2), 3.25 (t, 4H, CH_2N), 0.21 (d, 24H, $SiMe_3$). ^{13}C NMR (C_6D_6) δ 149.6 (C_{ipso}), 129.5 (C_m), 122.6 (C_o), 121.2 (C_p), 70.7 (OCH_2), 48.4 (CH_2N), 1.4 ($SiMe_3$).

$(C_6H_5NHCH_2CH_2)_2O$ (11). An aqueous solution of hydrogen chloride was added at room temperature to a solution of **10** in diethyl ether (30 mL). The solution was stirred overnight at 45 °C. The reaction mixture was treated with aqueous NaOH until basic. The organic phase was collected and the aqueous phase was washed twice with ether. The combined organic extracts were washed with water and dried over magnesium sulfate. Removal of solvents gave a brownish oil in quantitative yield. The oil was dissolved in pentane and passed through alumina. The oil obtained after removal of volatiles was at least 98% pure by NMR and was used for organometallic reactions without further purification: ^1H NMR ($CDCl_3$) δ 7.19 (t, 4H, H_m), 6.73 (t, 2H, H_p), 6.64 (d, 4H, H_o), 3.94 (br, 2H, NH), 3.71 (t, 4H, OCH_2), 3.33 (t, 4H, CH_2N). ^{13}C NMR (C_6D_6) δ 149.0 (C_{ipso}), 129.9 (C_m), 118.2 (C_p), 113.7 (C_o), 69.9 (OCH_2), 44.0 (CH_2N).

$[(2,6\text{-}i\text{-}Pr_2\text{-}C_6H_3NCH_2CH_2)_2O]Zr(NMe_2)_2$ (12). A solution of $Zr(NMe_2)_4$ (2.5 g, 9.4 mmol) in pentane (4 mL) was added to a solution of **8** (4.0 g, 9.4

mmol) in pentane (14 mL) at room temperature. Almost instantaneous crystallization occurred. After standing overnight the crystals were collected and the mother liquor was cooled to -30 °C yielding a second crop of crystals. Total yield was 3.85 g (68%): ^{1}H NMR (C_6D_6) δ 7.18 - 7.05 (m, 6H, H_{aryl}), 3.71 (sep, 4H, C*H*Me$_2$), 3.56 (t, 4H, OCH_2), 3.33 (t, 4H, CH_2N), 2.56 (s, 12H, $ZrNMe_2$), 1.31 (d, 12H, CH*Me*$_2$), 1.28 (d, 12H, CH*Me*$_2$). ^{13}C NMR (C_6D_6) δ 150.2 (C_{ipso}), 146.2 (C_o), 125.2 (C_p), 124.2 (C_m), 72.8 (OCH_2), 57.7 (CH_2N), 42.7 ($ZrNMe_2$), 28.6 (*C*HMe$_2$), 27.0 (CH*Me*$_2$), 25.0 (CH*Me*$_2$). Anal. Calcd. for $C_{32}H_{54}N_4OZr$: C, 63.84; H, 9.04; N, 9.31. Found: C, 63.96; H, 9.16; N, 9.20.

[(2,6-*i*-Pr$_2$-C$_6$H$_3$NCH$_2$CH$_2$)$_2$O]ZrCl$_2$ (13). Neat TMSCl (578 mg, 5.3 mmol) was added to a solution of **12** (400 mg, 0.664 mmol) in 10 mL diethyl ether at room temperature. After thorough mixing by vigorous shaking, the reaction mixture was allowed to stand overnight at room temperature yielding colorless crystals (285 mg) in 73% yield. If the reaction mixture is too concentrated, [ArN_2O]Zr(NMe_2)Cl cocrystallized with **13**: ^{1}H NMR (C_6D_6) δ 7.17 (br, 6H, H_{aryl}), 3.73 (sep, 4H, C*H*Me$_2$), 3.66 (t, 4H, OCH_2), 3.35 (t, 4H, CH_2N), 1.51 (d, 12H, CH*Me*$_2$), 1.26 (d, 12H, CH*Me*$_2$). ^{13}C NMR (C_6D_6) δ 146.4 (C_{ipso}), 145.1 (C_o), 127.6 (C_p), 125.1 (C_m), 73.6 (OCH_2), 59.3 (CH_2N), 29.0 (*C*HMe$_2$), 26.9 (CH*Me*$_2$), 25.4 (CH*Me*$_2$). Anal. Calcd. for $C_{28}H_{42}Cl_2N_2OZr$: C, 57.51; H, 7.24; N, 4.79. Found: C, 57.10; H, 7.28; N, 4.46.

[(2,6-*i*-Pr$_2$-C$_6$H$_3$NCH$_2$CH$_2$)$_2$O]ZrMe$_2$ (14). A chilled (-30 °C) solution of BrMgMe (4.1 M in ether, 428 mL, 1.75 mmol) was added to a suspension of **13** (500 mg, 0.85 mmol) in diethyl ether (20 mL) at -30 °C. A fine precipitate slowly replaced the suspension of crystals and after stirring for 2 h at room temperature, dioxane (154 mg, 1.75 mmol) was added. After 20 min of additional stirring all volatiles were removed and the residue was extracted with pentane. Recrystallization from pentane yielded 280 mg (61%) of colorless crystals: ^{1}H NMR (C_6D_6) δ 7.12 (br, 6H, H_{aryl}), 3.84 (sep, 4H, C*H*Me$_2$), 3.41 (br, 8H, OC*H*$_2$C*H*$_2$N), 1.38 (d, 12H, CH*Me*$_2$), 1.23 (d, 12 H, CH*Me*$_2$),

0.30 (s, 6H, ZrMe). ^{13}C NMR (C_6D_6) δ 147.1 (C_{ipso}), 146.5 (C_o), 126.5 (C_p), 124.7 (C_m), 73.6 (OCH_2), 58.6 (CH_2N), 43.6 (ZrMe), 28.9 ($CHMe_2$), 27.3 ($CHMe_2$), 24.9 ($CHMe_2$). Anal. Calcd. for $C_{30}H_{48}N_2OZr$: C, 66.24; H, 8.89; N, 5.15. Found: C, 66.32; H, 8.87; N, 5.12.

[(2,6-*i*-Pr$_2$-C$_6$H$_3$NCH$_2$CH$_2$)$_2$O]Zr(CH$_2$CHMe$_2$)$_2$ (15). A chilled (-30 °C) solution of $BrMgCH_2CHMe_2$ (2.51 M in ether, 286 mL, 0.72 mmol) was added to a suspension of **13** (205 mg, 0.35 mmol) in diethyl ether (10 mL) at -30 °C. A fine precipitate slowly replaced the suspension of crystals and after stirring for 1.5 h at room temperature, dioxane (63 mg, 0.72 mmol) was added. After 20 min of additional stirring all volatiles were removed and the residue was extracted with pentane. Recrystallization from pentane yielded 158 mg (72%) of colorless crystals: ^1H NMR (C_6D_6) δ 7.15 - 7.12 (br, 6H, H_{aryl}), 3.91 (sep, 4H, $CHMe_2$), 3.42 (br, 8H, OCH_2CH_2N), 1.92 (sep, 2H, CH_2CHMe_2), 1.45 (d, 12H, $CHMe_2$), 1.23 (d, 12H, $CHMe_2$), 0.85 (d, 12H, CH_2CHMe_2), 0.70 (d, 4H, CH_2CHMe_2). ^{13}C NMR (C_6D_6) δ 149.2 (C_{ipso}), 146.0 (C_o), 126.2 (C_p), 124.6 (C_m), 78.1 (CH_2CHMe_2), 74.5 (OCH_2), 58.3 (CH_2N), 29.7 (CH_2CHMe_2), 28.9 ($CHMe_2$), 28.4 (CH_2CHMe_2), 27.4 ($CHMe_2$), 24.6 ($CHMe_2$). Anal. Calcd. for $C_{36}H_{60}N_2OZr$: C, 68.84; H, 9.63; N, 4.46. Found: C, 68.96; H, 9.59; N, 4.40.

[(2,6-Me$_2$-C$_6$H$_3$NCH$_2$CH$_2$)$_2$O]Zr(NMe$_2$)$_2$ (16). A solution of $Zr(NMe_2)_4$ (1.07 g, 4.0 mmol) in pentane (4 mL) was added to a solution of **9** (1.26 g, 4.05 mmol) in pentane (14 mL) at room temperature. Instantaneous crystallization occurred during the course of addition. After standing overnight the crystals were collected and the mother liquor was cooled to -30 °C yielding a second crop of crystals. Total yield was 1.90 g (97%): ^1H NMR (C_6D_6) δ 7.11 (d, 4H, H_m), 6.92 (t, 2H, H_p), 3.55 (t, 4H, OCH_2), 3.21 (t, 4H, CH_2N), 2.65 (s, 12H, $ZrNMe_2$), 2.43 (s, 12H, Ar*Me*). ^{13}C NMR (C_6D_6) δ 152.7 (C_{ipso}), 134.9 (C_o), 128.9 (C_m), 123.7 (C_p), 72.8 (OCH_2), 54.1

(CH_2N), 42.1 ($ZrNMe_2$), 19.6 (Ar*Me*). Anal. Calcd. for $C_{32}H_{54}N_4OZr$: C, 58.85; H, 7.82; N, 11.44. Found: C, 59.16; H, 7.95; N, 11.46.

[(2,6-Me_2-$C_6H_3NCH_2CH_2)_2O$]$ZrCl_2$ (17). Neat TMSCl (5.2 g, 48 mmol) was added to a solution of **16** (1.17 g, 2.39 mmol) in 80 mL diethyl ether at room temperature. After thorough mixing by vigorous shaking the reaction mixture was allowed to stand for 46 h at room temperature yielding colorless needles (0.99 g) in 88% yield. Using less solvent led to cocrystallization of **17** and [Ar'N_2O]$Zr(NMe_2)Cl$: ^1H NMR (C_6D_6) δ 7.01 (d, 4H, H_m), 6.94 (dd, 2H, H_p, 3.49 (t, 4H, OCH_2), 3.09 (t, 4H, CH_2N), 2.43 (s, 12H, Ar*Me*); (CD_2Cl_2) δ 7.10 (d, 4H, H_m), 7.01 (dd, 2H, H_p), 4.62 (t, 4H, OCH_2), 3.77 (t, 4H, CH_2N), 2.43 (s, 12H, Ar*Me*). ^{13}C NMR (C_6D_6) δ 148.5 (C_{ipso}), 134.6 (C_o), 129.7 (C_m), 126.7 (C_p), 73.8 (OCH_2), 55.8 (CH_2N), 19.4 (Ar*Me*). Anal. Calcd. for $C_{20}H_{26}Cl_2N_2OZr$: C, 50.83; H, 5.55; N, 5.93. Found: C, 50.83; H, 5.57; N, 5.84.

[(2,6-Me_2-$C_6H_3NCH_2CH_2)_2O$]$ZrMe_2$ (18). A chilled (-30 °C) solution of BrMgMe (3.0 M in ether, 580 mL, 1.74 mmol) was added to a suspension of **17** (400 mg, 0.85 mmol) in CH_2Cl_2 (10 mL) at -30 °C. A fine precipitate formed and after stirring for 20 min at room temperature, dioxane (159 mg, 1.80 mmol) was added. After 20 min of additional stirring, the reaction mixture was filtered. Upon addition of pentane (5 mL) the filtrate turned slightly cloudy and was filtered again. All volatiles were removed and the residue was dissolved in ether. Crystallization at -30 °C yielded 252 mg (69%) of colorless cubes in two crops. Crystals suitable for X-ray crystallography were obtained by crystallization from ether at -30 °C: ^1H NMR (C_6D_6) δ 7.14 (d, 4H, H_m), 7.01 (dd, 2H, H_p), 3.27 (m, 8H, OCH_2CH_2N), 2.44 (s, 12H, Ar*Me*), 0.27 (s, 6H, ZrMe). ^{13}C NMR (C_6D_6) δ 148.7 (C_{ipso}), 136.5 (C_o), 129.4 (C_m), 125.7 (C_p), 74.7 (OCH_2), 55.5 (CH_2N), 43.4 (ZrMe), 19.3 (Ar*Me*). Anal. Calcd. for $C_{22}H_{32}N_2OZr$: C, 61.21; H, 7.47; N, 6.49. Found: C, 61.31; H, 7.56; N, 6.46.

[(2,6-Me_2-$C_6H_3NCH_2CH_2)_2O$]Zr(CH_2CMe_3)Cl (19). A chilled (-30 °C) solution of $BrMgCH_2CMe_3$ (3.16 M in ether, 236 mL, 0.74 mmol) was added to a suspension of **17** (160 mg, 0.34 mmol) in CH_2Cl_2 (8 mL) at -30 °C. A fine precipitate formed and after stirring for 30 min at room temperature, dioxane (70 mg, 1.80 mmol) was added. After 20 min of additional stirring the reaction mixture was filtered. All volatiles were removed and the residue was dissolved in ether and filtered again. Crystallization at -30 °C yielded 42 mg (24%) of colorless crystals in two crops: ^{1}H NMR (C_6D_6) δ 7.08 (d, 4H, H_m), 6.97 (t, 2H, H_p), 3.50 (m, 2H, OCH_2C), 3.37 (m, 2H, OCH_2C), 3.16 (m, 4H, CH_2N), 2.50 (s, 6H, Ar*Me*), 2.46 (s, 6H, Ar*Me*), 1.23 (s, 2H, $ZrCH_2$), 1.11 (s, 9H, CH_2CMe_3). ^{13}C NMR (C_6D_6) δ 149.8 (C_{ipso}), 135.14, 135.05 (C_o), 129.55, 129.52 (C_m), 126.1 (C_p), 81.4 ($ZrCH_2$), 73.4 (OCH_2), 55.5 (CH_2N), 35.8 (CH_2CMe_3), 35.0 (CH_2CMe_3), 20.0, 19.8 (Ar*Me*). Anal. Calcd. for $C_{25}H_{37}ClN_2OZr$: C, 59.08; H, 7.34; N, 5.51. Found: C, 59.14; H, 7.42; N, 5.46.

[(2,6-Me_2-$C_6H_3NCH_2CH_2)_2O$]Zr($CH_2CMe_3)_2$ (20). A solution of $LiCH_2CMe_3$ (68 mg, 0.87 mmol) in ether (2 mL) was added to a suspension of **17** (200 mg, 0.42 mmol) in ether (6 mL) at -30 °C. Everything dissolved immediately and a fine precipitate formed rapidly. After stirring for 15 min, the reaction mixture was filtered. All volatiles were removed and the residue was dissolved in ether and filtered again. Crystallization at -30 °C yielded 146 mg (63%) of colorless crystals in two crops: ^{1}H NMR (C_6D_6) δ 7.11 (d, 4H, H_m), 6.96 (t, 2H, H_p), 3.43 (t, 4H, OCH_2C), 3.26 (t, 4H, CH_2N), 2.53 (s, 12H, Ar*Me*), 0.99 (s, 18H, $ZrCH_2CMe_3$), 0.91 (s, 4H, $ZrCH_2CMe_3$). ^{13}C NMR (C_6D_6) δ 152.3 (C_{ipso}), 135.1 (C_o), 129.5 (C_m), 125.4 (C_p), 89.1 ($ZrCH_2$), 73.4 (OCH_2), 55.7 (CH_2N), 36.5 (CH_2CMe_3), 35.0 (CH_2CMe_3), 20.3 (Ar*Me*). Anal. Calcd. for $C_{30}H_{48}N_2OZr$: C, 66.24; H, 8.89; N, 5.15. Found: C, 66.17; H, 8.55; N, 4.98.

[($C_6H_5NCH_2CH_2)_2O$]Zr($NMe_2)_2$($HNMe_2$) (21). A solution of $Zr(NMe_2)_4$ (0.59 g, 2.22 mmol) in a mixture of ether (1.5 mL) and pentane (3 mL) was

added to a solution of **20** (0.57 g, 2.22 mmol) in ether (8 mL) at room temperature. The reaction mixture was thoroughly mixed and upon standing overnight, crystals formed. The mother liquor was cooled to -30 °C yielding a second crop of crystals. The combined yield was 0.83 g (78%): ^{1}H NMR (C_6D_6) δ 7.39 (t, 4H, H_m), 7.03 (d, 4H, H_o), 6.64 (t, 2H, H_p), 3.37 (t, 4H, OCH_2), 3.17 (t, 4H, CH_2N), 3.06 (s, 12H, $ZrNMe_2$), 1.65 (d, 6H, $HNMe_2$), 0.79 (sep, 1H, $HNMe_2$). ^{13}C NMR (C_6D_6) δ 156.5 (C_{ipso}), 129.5 (C_m), 117.3 (C_p), 116.2 (C_o), 74.3 (OCH_2), 52.6 (CH_2N), 45.6 ($ZrNMe_2$), 39.2 ($HNMe_2$). Anal. Calcd. for $C_{22}H_{37}N_5OZr$: C, 55.19; H, 7.79; N, 14.63. Found: C, 55.36; H, 7.96; N, 14.49.

{[ArN$_2$O]ZrMe(PhNMe$_2$}[B(C$_6$F$_5$)$_4$] (22). Solid [ArN_2O]$ZrMe_2$ (20 mg, 37 μmol) was added to a chilled (-30 °C) suspension of [$PhNHMe_2$][$B(C_6F_5)_4$] (29 mg, 37 μmol) in C_6D_5Cl. The reaction mixture was stirred for 5 min under warming to room temperature and then chilled to 0 °C: ^{1}H NMR (C_6D_5Cl) δ 7.27-7.11 (m, 6H, H_{aryl}), 6.33 (br t, 1H, H_p of $PhNMe_2$), 5.85 (m, 4H, H_m and H_o of $PhNMe_2$), 4.22 (m, 2H, OCH_2C), 3.98 (m, 2H, OCH_2C), 3.73 (m, 2H, CH_2N), 3.33 (m, 2H, CH_2N), 3.23 (sep, 4H, $CHMe_2$), 2.80 (s, 6H, $PhNMe_2$), 1.45 (d, 6H, $CHMe_2$), 1.35 (d, 6H, $CHMe_2$) 1.24 (d, 6H, $CHMe_2$), 1.16 (d, 6H, $CHMe_2$), 0.22 (s, 3H, ZrMe).

{[Ar'N$_2$O]ZrMe(PhNMe$_2$}[B(C$_6$F$_5$)$_4$] (23). Solid [Ar'N_2O]$ZrMe_2$ (13 mg, 30 μmol) was added to a chilled (-30 °C) suspension of [$PhNHMe_2$][$B(C_6F_5)_4$] (24 mg, 30 μmol) in C_6D_5Cl. The reaction mixture was stirred for 5 min under warming to room temperature and then chilled to 0 °C. ^{1}H NMR (C_6D_5Cl) δ 7.13 (m, 6H, H_{aryl}), 6.03 (br, 3H, H_m and H_p of $PhNMe_2$), 5.79 (d, 2H, H_o of $PhNMe_2$), 4.12 (m, 2H, OCH_2C), 3.95 (m, 2H, OCH_2C), 3.41 (m, 2H, CH_2N), 3.10 (m, 2H, CH_2N), 2.67 (s, 6H, $PhNMe_2$), 2.22 (s, 12H, Ar*Me*), 0.26 (s, 3H, ZrMe).

Polymerization of 1-hexene using cocatalyst [PhNMe$_2$H][B(C$_6$F$_5$)$_4$]. In a typical experiment a chilled (-30 °C) solution of **18** (19 mg, 44 μmol) in chlorobenzene (3 mL) was added to a suspension of [$PhNMe_2H$][$B(C_6F_5)_4$] (32 mg, 40

μmol) in chlorobenzene (6 mL) at -30 °C and allowing the reaction mixture to warm to room temperature, it was stirred for 15 min. The reaction mixture was cooled to 0 °C and 1-hexene (1.0 mL, 8.0 mmol) was added in one shot. After stirring for 1 h at 0 °C the reaction was quenched with HCl (1.0 M in ether, 4 mL). All volatiles were removed under vacuum (100 mTorr) at 120 °C. For the GPC with light scattering detector the dn/dc was determined for each polymer; an average value of 0.050 mL/g was found. A 10% excess of catalyst was employed to ensure complete conversion of the limiting reagent $[PhNMe_2H][B(C_6F_5)_4]$: ^{13}C NMR ($CDCl_3$) δ 40.2, 34.5, 34.4, 32.3, 28.7, 28.3, 23.3.

Polymerization of 1-hexene using cocatalyst $[Ph_3C][B(C_6F_5)_4]$. In a typical experiment a chilled (-30 °C) solution of **18** (19 mg, 44 μmol) in chlorobenzene (3 mL) was added to a suspension of $[Ph_3C][B(C_6F_5)_4]$ (37 mg, 40 μmol) in chlorobenzene (6 mL) at -30 °C and the reaction mixture was stirred for 2 min. The reaction mixture was allowed to equilibrate at 0 °C and 1-hexene (1.0 mL, 8.0 mmol) was added in one shot. After stirring for 1 h at 0 °C the reaction was quenched with HCl (1.0 M in ether, 4 mL). All volatiles were removed under vacuum (100 mTorr) at 120 °C.

REFERENCES

(1) Grubbs, R. H. in "Comprehensive Organometallic Chemistry"; G. Wilkinson, F. G. A. Stone and E. W. Abel, Ed.; Pergamon: New York, 1982; Vol. 8.

(2) Ivin, K. J. "Olefin Metathesis"; Academic Press: London, 1983.

(3) Schrock, R. R.; Murdzek, J. S.; Bazan, G. C.; Robbins, J.; DiMare, M.; O'Regan, M. *J. Am. Chem. Soc.* **1990**, *112*, 3875.

(4) Fox, H. H.; Yap, K. B.; Robbins, J.; Cai, S.; Schrock, R. R. *Inorg. Chem.* **1992**, *31*, 2287.

(5) Oskam, J. H.; Fox, H. H.; Yap, K. B.; McConville, D. H.; O'Dell, R.; Lichtenstein, B. J.; Schrock, R. R. *J. Organometal. Chem.* **1993**, *459*, 185.

(6) Schrock, R. R. *Pure Appl. Chem.* **1994**, *66*, 1447.

(7) Fox, H. H.; Lee, J.-K.; Park, L. Y.; Schrock, R. R. *Organometallics* **1993**, *12*, 759.

(8) Fox, H. H.; Schrock, R. R.; O'Dell, R. *Organometallics* **1994**, *13*, 635.

(9) McConville, D. H.; Wolf, J. R.; Schrock, R. R. *J. Am. Chem. Soc.* **1993**, *115*, 4413.

(10) Park, L. Y.; Stieglitz, S. G.; Crowe, W. M.; Schrock, R. R. *Macromolecules* **1991**, *24*, 3489.

(11) Schrock, R. R. *Acc. Chem. Res.* **1990**, *23*, 158.

(12) Schrock, R. R. in "Ring-Opening Polymerization"; D. J. Brunelle, Ed.; Hanser: Munich, 1993; pp 129.

(13) Nomura, K.; Schrock, R. R. *Macromolecules* **1996**, *29*, 540.

(14) Knoll, K.; Schrock, R. R. *J. Am. Chem. Soc.* **1989**, *111*, 7989.

(15) Fox, H. H.; Schrock, R. S. *Organometallics* **1992**, *11*, 2763.

(16) Schlund, R.; Schrock, R. R.; Crowe, W. E. *J. Am. Chem. Soc.* **1989**, *111*, 8004.

(17) Schrock, R. R.; Luo, S.; Zanetti, N.; Fox, H. H. *Organometallics* **1994**, *13*, 3396.

(18) Schrock, R. R.; Luo, S.; Lee, J. C. J.; Zanetti, N. C.; Davis, W. M. *J. Am. Chem. Soc.* **1996**, *118*, 3883.

(19) Buchmeiser, M.; Schrock, R. R. *Macromolecules* **1995**, *28*, 6642.

(20) Bazan, G.; Khosravi, E.; Schrock, R. R.; Feast, W. J.; Gibson, V. C.; O'Regan, M. B.; Thomas, J. K.; Davis, W. M. *J. Am. Chem. Soc.* **1990**, *112*, 8378.

(21) Bazan, G. C.; Schrock, R. R.; Cho, H.-N.; Gibson, V. C. *Macromolecules* **1991**, *24*, 4495.

(22) Mitchell, J. P.; Gibson, V. C.; Schrock, R. R. *Macromolecules* **1991**, *24*, 1220.

(23) Bazan, G. C.; Schrock, R. R.; O'Regan, M. B. *Organometallics* **1991**, *10*, 1062.

(24) Feast, W. J.; Gibson, V. C.; Marshall, E. L. *J. Chem. Soc., Chem. Commun.* **1992**, 1157.

(25) O'Dell, R.; McConville, D. H.; Hofmeister, G. E.; Schrock, R. R. *J. Am. Chem. Soc.* **1994**, *116*, 3414.

(26) Schrock, R. R.; Lee, J.-K.; O'Dell, R.; Oskam, J. H. *Macromolecules* **1995**, *28*, 5933.

(27) Totland, K. M.; Boyd, T. J.; Lavoie, G. G.; Davis, W. M.; Schrock, R. R. *Macromolecules* **1996**, *29*, 6114.

(28) Bazan, G.; Schrock, R. R.; Khosravi, E.; Feast, W. J.; Gibson, V. C. *Polymer Commun.* **1989**, *30*, 258.

(29) Bazan, G. C.; Oskam, J. H.; Cho, H.-N.; Park, L. Y.; Schrock, R. R. *J. Am. Chem. Soc.* **1991**, *113*, 6899.

(30) Schrock, R. R. *Polyhedron* **1995**, *14*, 3177.

(31) Fox, H. H.; Wolf, M. O.; O'Dell, R.; Lin, B. L.; Schrock, R. R.; Wrighton, M. S. *J. Am. Chem. Soc.* **1994**, *116*, 2827.

(32) Oskam, J. H.; Schrock, R. R. *J. Am. Chem. Soc.* **1992**, *114*, 7588.

(33) Oskam, J. H.; Schrock, R. R. *J. Am. Chem. Soc.* **1993**, *115*, 11831.

(34) Schrock, R. R.; Crowe, W. E.; Bazan, G. C.; DiMare, M.; O'Regan, M. B.; Schofield, M. H. *Organometallics* **1991**, *10*, 1832.

(35) Schrock, R. R.; Messerle, L. W.; Wood, C. D.; Guggerberger, L. J. *J. Am. Chem. Soc.* **1978**, *100*, 3793.

(36) Kress, J.; Osborn, J. A. *J. Am. Chem. Soc.* **1987**, *109*, 3953.

(37) Toreki, R.; Schrock, R. R. *J. Am. Chem. Soc.* **1992**, *114*, 3367.

(38) Schrock, R. R. in "Reactions of Coordinated Ligands"; P. R. Braterman, Ed.; Plenum: New York, 1986.

(39) Brook, A. G.; Yau, L. *J. Organomet. Chem.* **1984**, *271*, 9.

(40) Eglinton, G.; Galbraith, A. R. *J. Chem. Soc.* **1959**, 889.

(41) Prasad, P. N. in "Nonlinear Optical and Electroactive Polymers"; P. N. Prasad and D. R. Ulrich, Ed.; Plenum Press: New York City, 1987; pp 41.

(42) Prasad, P. N. *Polymer* **1991**, *32*, 1746.

(43) Lytel, R.; Lipscomb, G. F.; Thackara, J.; Altman, J.; Elizondo, P.; Stiller, M.; Sullivan, B. in "Nonlinear Optical and Electroactive Polymers"; P. N. Prasad and D. R. Ulrich, Ed.; Plenum Press: New York, 1987; pp 415.

(44) Zyss, J.; Chemla, D. S. in "Nonlinear Optical Properties of Organic Molecules and Crystals"; D. S. Chemla and J. Zyss, Ed.; Academic Press: Orlando, Florida, 1987; Vol. 1; pp 23.

(45) *Conjugated Polymers*; Brédas, J. L.; Silbey, R., Ed.; Kluwer: Boston, 1991.

(46) Shirikawa, H.; Louis, E. J.; MacDiarmid, A. G.; Chiang, C. K.; Heeger, A. J. *J. Chem. Soc. Chem. Commun.* **1977**, 578.

(47) Naarmann, H. *Synth. Met.* **1987**, *17*, 223.

(48) Kajzar, F.; Etemad, S.; Baker, G. L.; Messier, J. *Solid State Commun.* **1987**, *63*, 1113.

(49) Drury, M. R. *Solid State Commun.* **1988**, *68*, 417.

(50) Shirakawa, H.; Masuda, T.; Takeda, K. in "Supplement C2: The chemistry of triple-bonded functional groups"; S. Patai, Ed.; Wiley: 1994.

(51) Stille, J. K.; Frey, D. A. *J. Am. Chem. Soc.* **1961**, *83*, 1697.

(52) Gibson, H. W.; Bailey, F. C.; Epstein, A. J.; Rommelmann, H.; Kaplan, S.; Harbour, J.; Yang, X. Q.; Tanner, D. B.; Pochan, J. M. *J. Am. Chem. Soc.* **1983**, *105*, 4417.

(53) Gibson, H. W.; Epstein, A. J.; Rommelmann, H.; Tanner, D. B.; Yang, X. Q.; Pochan, J. M. *J. Phys., Colloq.* **1983**, *C3*, 651.

(54) Akopyan, L. A.; Ambartsumyan, G. V.; Matsoyan, M. S.; Ovakimyan, E. V.; Matsoyan, S. G. *Arm. Khim. Zh.* **1977**, *30*, 771.

(55) Akopyan, L. A.; Ambartsumyan, G. V.; Grigoryan, S. G.; Matsoyan, S. G. *Vysokomol. Soedin., Ser. A* **1977**, *19*, 1068.

(56) Akyopan, L. A.; Ambartsumyan, G. V.; Ovakimyan, E. V.; Matsoyan, S. G. *Vysokomol. Soedin., Ser. A* **1977**, *19*, 271.

(57) Ambartsumyan, G. V.; Gevorkyan, S. B.; Kharatyan, V. G.; Gavalyan, V. B.; Saakyan, A. A.; Grigoryan, S. G.; Akopyan, L. A. *Arm. Khim. Zh.* **1984**, *37*, 188.

(58) Cho, O. K.; Kim, Y. H.; Choi, K. Y.; Choi, S. K. *Macromolecules* **1990**, *23*, 12.

(59) Choi, S. K. *Makromol. Chem., Macromol. Symp.* **1990**, *33*, 145.

(60) Gal, Y. S.; Choi, S. K. *Pollimo* **1987**, *11*, 563.

(61) Gal, Y. S.; Choi, S. K. *J. Polym. Sci., Part C* **1988**, *26*, 115.

(62) Gal, Y. S.; Jung, B.; Cho, H. N.; Lee, W. C.; Choi, S. K. *J. Polym. Sci., Part C* **1990**, *28*, 259.

(63) Gal, Y. S.; Choi, S. K. *J. Polym. Sci., Part A* **1993**, *31*, 345.

(64) Han, S. H.; Kim, U. Y.; Kang, Y. S.; Choi, S. K. *Macromolecules* **1991**, *24*, 973.

(65) Jin, S. H.; Kim, S. H.; Cho, H. N.; Choi, S. K. *Macromolecules* **1991**, *24*, 6050.

(66) Jin, S. H.; Cho, H. N.; Choi, S. K. *J Polym Sci A-Polym Chem* **1993**, *31*, 69.

(67) Kim, Y. H.; Gal, Y. S.; Kim, U. Y.; Choi, S. K. *Macromolecules* **1988**, *21*, 1991.

(68) Kim, Y. H.; Choi, K. Y.; Choi, S. K. *J. Polym. Sci., Part C* **1989**, *27*, 443.

(69) Kim, Y. H.; Kwon, S. K.; Choi, S. K. *Bull. Kor. Chem. Soc.* **1992**, *13*, 459.

(70) Schattenmann, F. J.; Schrock, R. R.; Davis, W. M. *J. Am. Chem. Soc.* **1996**, *118*, 3295.

(71) Danis, P. O.; Karr, D. E.; Simonsick, W. J., Jr.; Wu, D. T. *Macromolecules* **1995**, *28*, 1229.

(72) Maloney, D. R.; Hunt, K. H.; Lloyd, P. M.; Muir, A. V. G.; Richards, S. N.; Derrick, P. J.; Haddleton, D. M. *J. Chem. Soc., Chem. Commun.* **1995**, 561.

(73) Pasch, H.; Gores, F. *Polymer* **1995**, *36*, 1999.

(74) Jin, S. H.; Choi, S. J.; Ahn, W.; Cho, H. N.; Choi, S. K. *Macromolecules* **1993**, *26*, 1487.

(75) Krapcho, A. P.; Weimaster, J. F.; Eldridge, J. M.; Jr., E. G. E. J.; Lovey, A. J.; Stephens, W. P. *J. Org. Chem.* **1978**, *43*, 138.

(76) Chemla, D. S.; Zyss, J. "Nonlinear Optical Properties of Organic Molecules and Crystals"; Academic Press: Boston, MA, 1987; Vol. 1.

(77) Samuel, I. D. W.; Ledoux, I.; Dhenaut, C.; Zyss, J.; Fox, H.; Schrock, R. R.; Silbey, R. J. *Science* **1994**, *265*, 1070.

(78) Kuehne, M. E.; Parsons, W. H. *J. Org. Chem.* **1977**, *42*, 3408.

(79) Oediger, H.; Möller, F. *Ann. Chem.* **1976**, 348.

(80) Shirakawa, H.; Ito, T.; Ikeda, S. *Polym. J.* **1973**, *4*, 460.

(81) Ito, T.; Shirakawa, H.; Ikeda, S. *J. Polym. Sci., Polym. Chem. Ed.* **1974**, *12*, 11.

(82) Shirakawa, H.; Ikeda, S. *Polym. J.* **1971**, *2*, 231.

(83) Edwards, J. H.; Feast, W. J. *Polymer* **1980**, *21*, 595.

(84) Swager, T. M.; Dougherty, D. A.; Grubbs, R. H. *J. Am. Chem. Soc.* **1988**, *110*, 2973.

(85) Swager, T. M.; Grubbs, R. H. *J. Am. Chem. Soc.* **1989**, *111*, 4413.

(86) Deits, W.; Cukor, P.; Rubner, M.; Jopson, H. *Synth. Met.* **1982**, *4*, 199.

(87) Chien, J. C. W.; Wnek, G. E.; Karasz, F. E.; Hirsch, J. A. *Macromolecules* **1981**, *14*, 479.

(88) Park, L. Y.; Ofer, D.; Schrock, R. R.; Wrighton, M. S. *Chem. Mater.* **1992**, *4*, 1388.

(89) Saunders, R. S.; Cohen, R. E.; Schrock, R. R. *Acta Polymerica* **1994**, *45*, 301.

(90) Brintzinger, H. H.; Fischer, D.; Mulhaupt, R.; Rieger, B.; Waymouth, R. M. *Angew. Chem. Int. Ed.* **1995**, *34*, 1143.

(91) Okuda, J. *Chem. Ber.* **1990**, *123*, 1649.

(92) Okuda, J.; Schattenmann, F. J.; Wocadlo, S.; Massa, W. *Organometallics* **1995**, *14*, 789.

(93) Shapiro, P. J.; Bunel, E.; Schaefer, W. P.; Bercaw, J. E. *Organometallics* **1990**, *9*, 867.

(94) Cloke, F. G. N.; Hitchcock, P. B.; Love, J. B. *J. Chem. Soc., Dalton Trans.* **1995**, 25.

(95) Cloke, F. G. N.; Geldbach, T. J.; Hitchcock, P. B.; Love, J. B. *J. Organomet. Chem.* **1996**, *506*, 343.

(96) Guérin, F.; McConville, D. H.; Vittal, J. J. *Organometallics* **1995**, *14*, 3154.

(97) Guérin, F.; McConville, D. H.; Payne, N. C. *Organometallics* **1996**, *15*, 5085.

(98) Guérin, F.; McConville, D. H.; Vittal, J. J. *Organometallics* **1996**, *15*, 5586.

(99) Horton, A. D.; de With, J.; van der Linden, A. J.; van de Weg, H. *Organometallics* **1996**, *15*, 2672.

(100) Horton, A. D.; de With, J. *Chem. Commun.* **1996**, 1375.

(101) Scollard, J. D.; McConville, D. H.; Vittal, J. J. *Organometallics* **1995**, *14*, 5478.

(102) Scollard, J. D.; McConville, D. H.; Payne, N. C.; Vittal, J. J. *Macromolecules* **1996**, *29*, 5241.

(103) Aoyagi, K.; Gantzel, P. K.; Kalai, K.; Tilley, T. D. *Organometallics* **1996**, *15*, 923.

(104) Clark, H. C. S.; Cloke, F. G. N.; Hitchcock, P. B.; Love, J. B.; Wainwright, A. P. *J. Organometal. Chem.* **1995**, *501*, 333.

(105) Warren, T. H.; Schrock, R. R.; Davis, W. M. *Organometallics* **1996**, *15*, 562.

(106) Scollard, J. D.; McConville, D. H. *J. Am. Chem. Soc.* **1996**, *118*, 10008.

(107) Baumann, R.; Davis, W. M.; Schrock, R. R. *J. Am. Chem. Soc.* **1997**, *119*, 3830.

(108) du Plooy, K. E.; Moll, U.; Wocadlo, S.; Massa, W.; Okuda, J. *Organometallics* **1995**, *14*, 3129.

(109) Wannagat, U.; Schreiner, G. *Monatsh. Chem.* **1965**, *96*, 1889.

(110) Guo, Z.; Swenson, D. C.; Jordan, R. F. *Organometallics* **1994**, *13*, 1424.

(111) Andersen, R. *Inorg. Chem.* **1979**, *18*, 2928.

(112) Planalp, R. P.; Andersen, R. A.; Zalkin, A. *Organometallics* **1983**, *2*, 16.

(113) Erker, G.; Schlund, R.; Krüger, C. *Organometallics* **1989**, *8*, 2349.

(114) Diamond, G. M.; Rodewald, S.; Jordan, R. F. *Organometallics* **1995**, *14*, 5.

(115) Diamond, G. M.; Jordan, R. F.; Petersen, J. L. *J. Am. Chem. Soc.* **1996**, *118*, 8024.

(116) Diamond, G. M.; Jordan, R. F.; Petersen, J. L. *Organometallics* **1996**, *15*, 4045.

(117) Diamond, G. M.; Jordan, R. F.; Petersen, J. L. *Organometallics* **1996**, *15*, 4030.

(118) van der Linden, A.; Schaverien, C. J.; Meijboom, N.; Ganter, C.; Orpen, A. G. *J. Am. Chem. Soc.* **1995**, *117*, 3008.

ACKNOWLEDGMENTS

It is most appropriate to start the acknowledgment section by thanking my research advisor, Professor Richard R. Schrock, for giving me this tremendous opportunity to work in his group. I'll never forget the non-bureaucratic manner in which he enabled my fast transfer to MIT, when I was "stuck" in Albany. I am very grateful for the freedom he gave me to pursue all my ideas, his excitement when things worked out and the advice he provided when I requested it. Much of my knowledge and experience in inorganic and polymer chemistry I gained under his supervision. Outside of chemistry, I thank Dick for accepting the "draft" into our intramural basketball team and for partying hard (until 1 am) at my 30th birthday party.

Next, Peter Kuhn and Vibha Rao (now Subramanian), my "roomies" back in Albany, deserve credit for strongly encouraging me to go to MIT, although my personal situation suggested to stay in the Albany area. How everything in my life fell into place since then is testimony for the goodness of this decision and I am grateful that we are able to continue our friendship.

Of course, many thanks go to all the members of the Schrock group I overlapped with over the past years; all of them contributed in their own way and also helped making these years at MIT a fun experience. Thanking everybody individually would fill pages and I certainly would run the risk to leave somebody out. Thus I will only mention a few and thank the rest collectively again. Special thanks go to Nadia Zanetti (now Zanetti-Moesch) for helping to get me started and showing me a "Swiss angle" on the world; my classmates Scott Seidel and Steve "the bone" Reid; Shifang(us) Luo for valuable polyene discussions and an impressive, continuous demonstration of pure energy; Robert Baumann for many "coffee-talks" about chemistry and more often about non-chemistry stuff and of course my one and only labmate, Tim. Joel Freundlich, Tim and Sheree deserve credit for proofreading this thesis.

I thank Bill Davis for obtaining and solving all the X-ray structures presented in this thesis. Our discussions about NBA action will not be forgotten.

Heinz Köchling deserves a great deal of appreciation for running all the MALDI TOF MS samples reported in Chapter 2 and especially for his help in setting up the gas addition system presented in Chapter 3. Not only did he supply much of the hardware and all the know how, but he also took the time to teach me with unbelievable patience everything I needed to know and was always available when I ran into problems. His incredible pool of knowledge concerning electronics and anything mechanical has been a source of continual amazement.

If you are one of those people that believe that everything happens for a reason, then the next two paragraphs will provide some support for this hypothesis. When I first occupied my new laboratory, Rm 6-427, in January 1994, and was introduced to my new labmate, Tim Warren, I couldn't foresee the tremendous friendship that would develop over the years. Aside from almost perfectly matched areas of interest, parallels in our personal lives brought us close early on. Sports played an important role in my graduate career and Tim was a teammate on almost every team I played on (football, volleyball, basketball, soccer, etc.). Certainly the true highlight was winning the chemistry volleyball championship with a perfect 13-0 season. I also thank Tim for introducing me to Dennis Hall and John Gross. Although I will miss our discussions inside and all our activities outside the lab (singing beach, Wally's cafe, "beer and funk nite" and so much more), I am also looking forward to a long lasting friendship.

Although this thesis is partly dedicated to her, I will take this opportunity to thank my fiancee, Sheree Stokes, for her unbelievable love and support over the last three and a half years. I had to end up at MIT to meet her. The fact that I want to spend the rest of my life with her, speaks volumes. There is simply nothing else to say than: she is a f-i-n-e lady.

Finally, this thesis would never have happened without the constant support of my family. I thank my brother Wolfgang for his continuous interest in my chemistry and many

valuable discussions, especially since he ended up in the same field of chemistry. More importantly, however, is the friendship that connects us and I am grateful for his opinion and support in difficult decisions. There are no means to fully acknowledge the influence of my parents on my career in a few sentences and I can only try by deeply thanking them for always supporting and encouraging me to strive for the big goals.